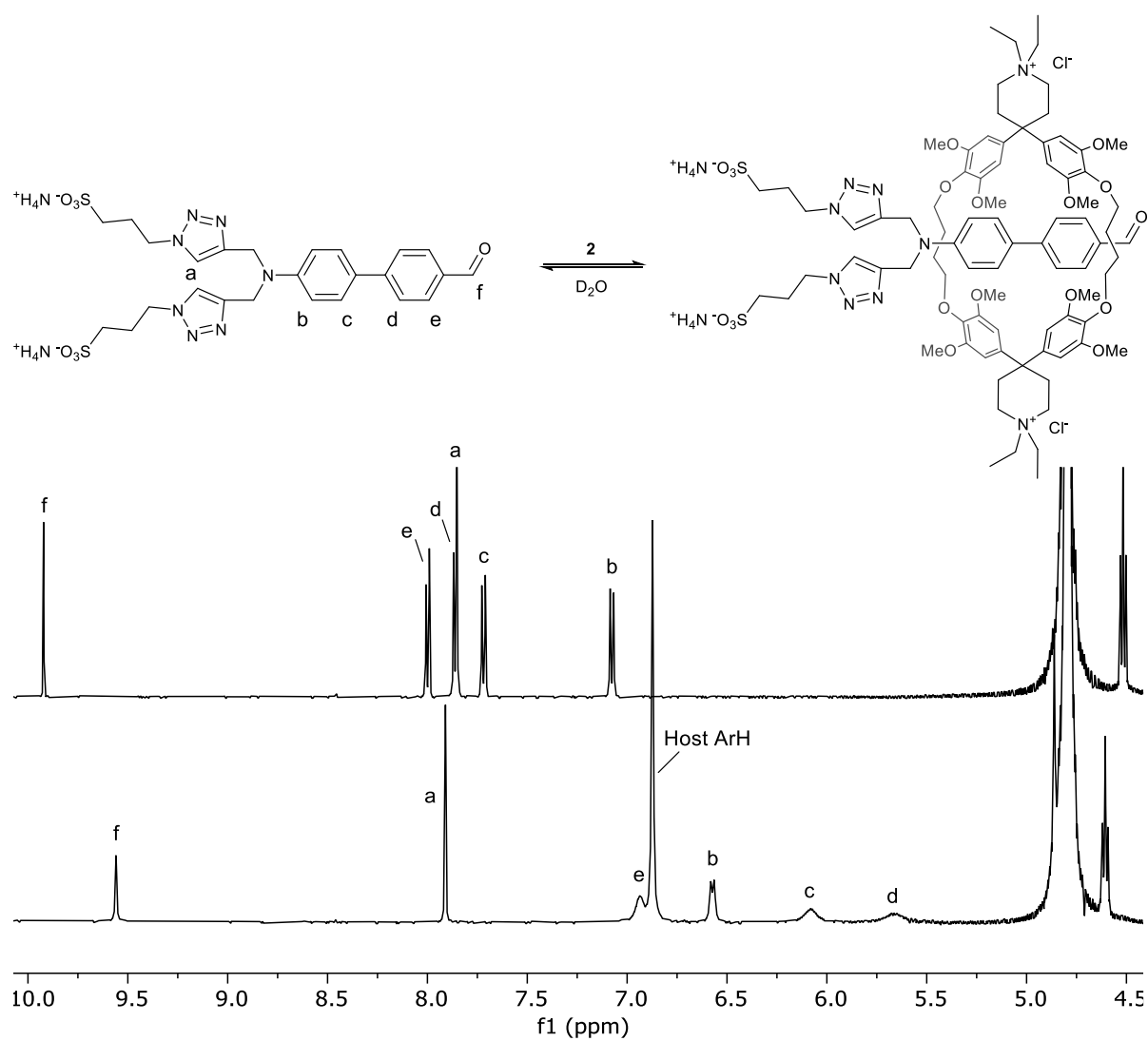


Electronic Supporting Information

¹ H-NMR spectra of pseudorotaxane 3c2	2
¹ H-NMR spectra of pseudorotaxane 1fc2	4
¹ H-NMR spectra of pseudorotaxane 9c2	7
¹ H-NMR competition experiment of 1f , 9 , and 2	9
Determination of the association constant of 1fc2	10
NOE showing <i>E</i> -selective formation of 1f	12
Optical Spectra of 1a , 1f , 1e , and 1ec2	13
Quantum Yield Determination for 1e and 1ec2	15
Unedited Photographs of Solid-State Emission and Emission Spectra	18
Deslipping Experiments of 1ec2	20
Reversibility of the Knoevenagel Condensation	21
Supplementary Reaction Schemes	23
Experimental Procedures	24
References	31
NMR Spectra	32
HR-MS Spectra	52

¹H-NMR spectra of pseudorotaxane 3⊂2



Scheme S1: Equilibrium of free guest **3** and host **2**, and the pseudorotaxane **3⊂2** in D₂O (top). Assignment of the aromatic ¹H signals to the free guest (1 mM in D₂O) and **3⊂2** (1:1 mixture, 1 mM in D₂O) in the respective ¹H-NMR spectra (bottom, 500 MHz).

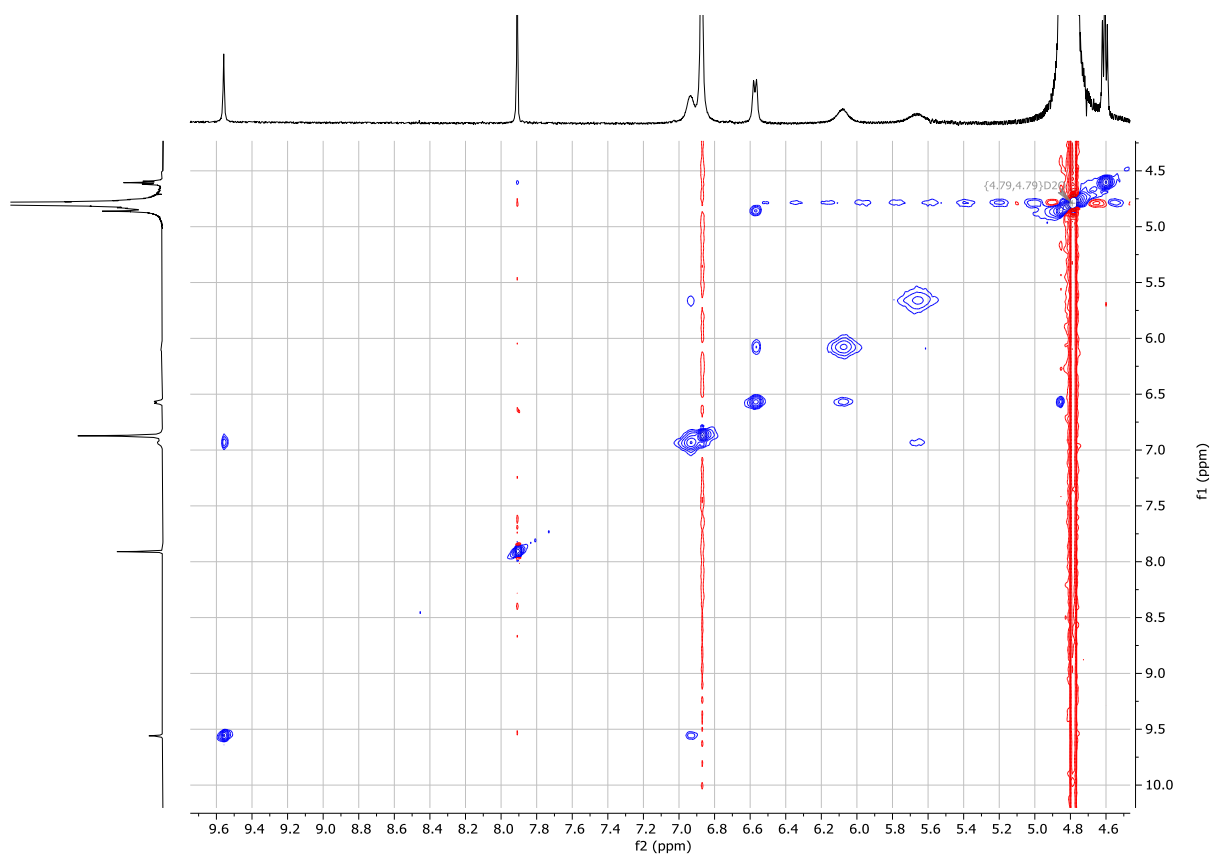


Figure S1: Excerpt of the ^1H -NOESY 2D-NMR spectrum (500 MHz) of the pseudorotaxane **3C2** at 1 mM concentration in D_2O .

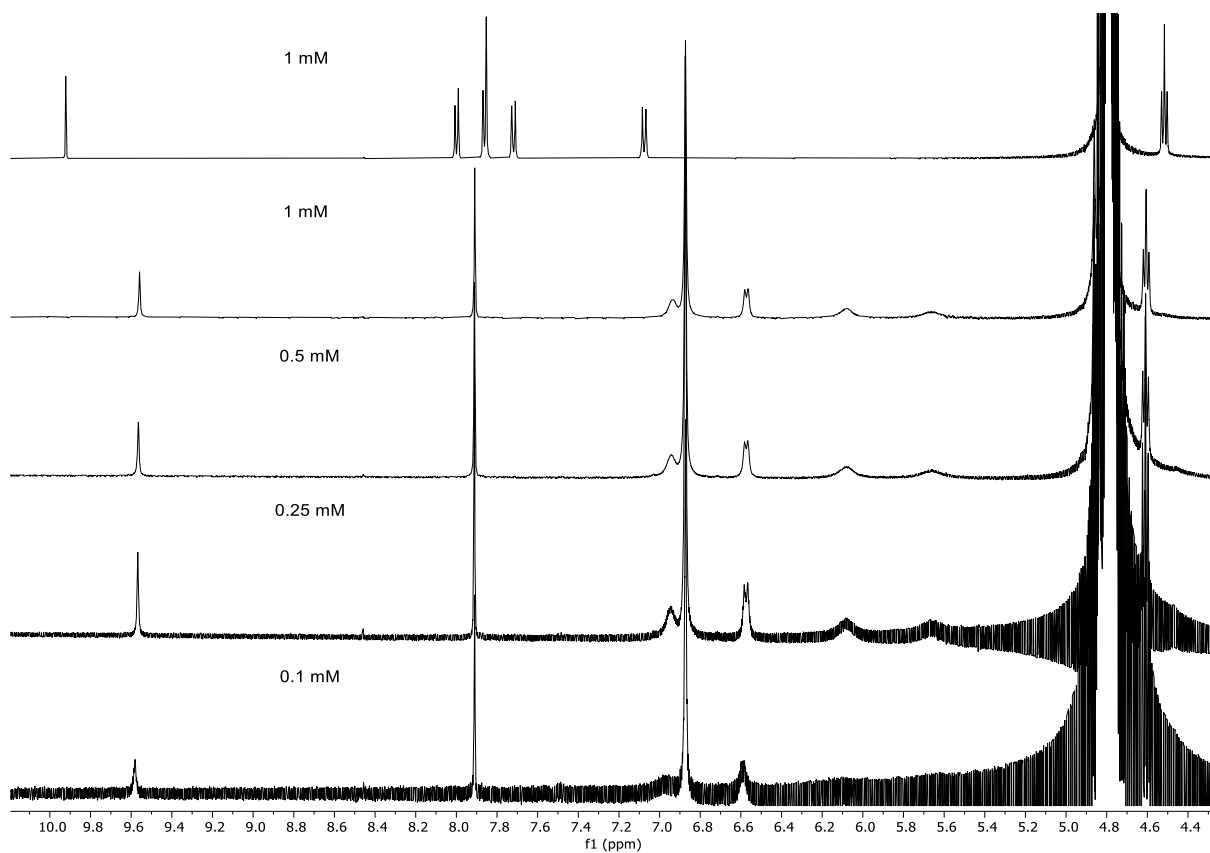
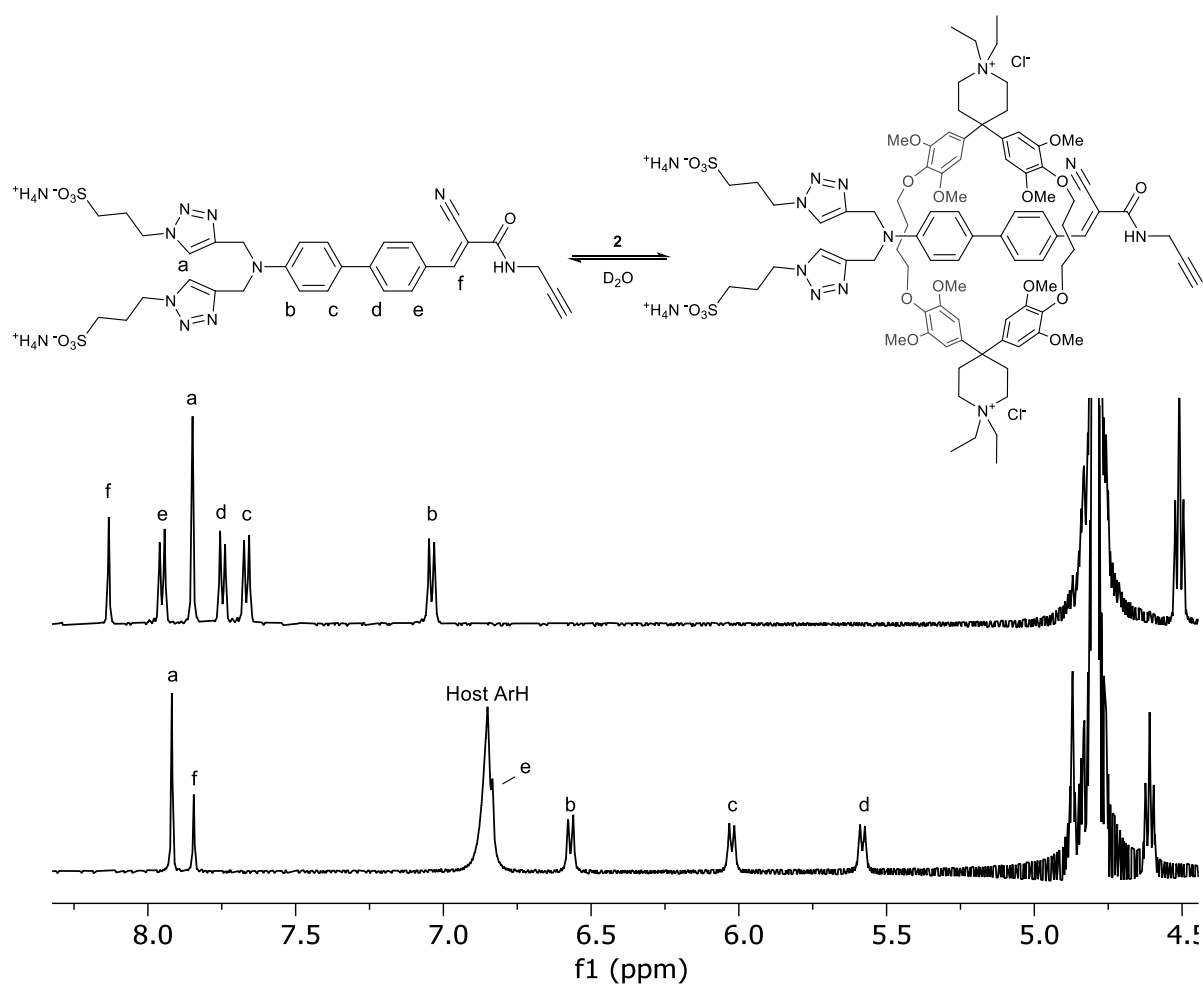


Figure S2: ^1H -NMR spectra (500 MHz) of guest **3** at 1 mM concentration in D_2O (top) and equimolar mixtures with the host **2** at decreasing concentrations.

¹H-NMR spectra of pseudorotaxane **1f**⊂**2**



Scheme S2: Equilibrium of free guest **1f** and host **2**, and the pseudorotaxane **1f**⊂**2** in D₂O (top). Assignment of the aromatic ¹H signals to the free guest (1 mM in D₂O) and **1f**⊂**2** (1:1 mixture, 1 mM in D₂O) in the respective ¹H-NMR spectra (bottom, 500 MHz).

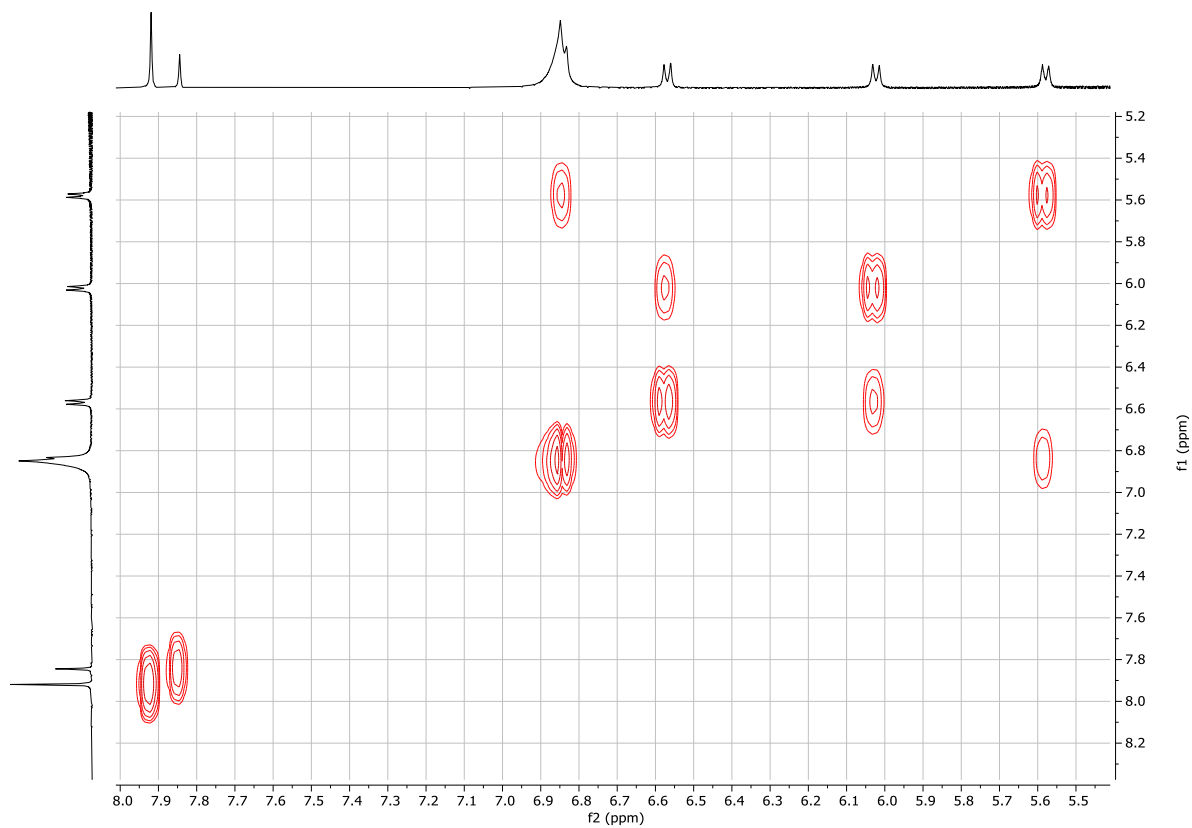


Figure S3: ^1H -COSY 2D-NMR spectrum (500 MHz) of the pseudorotaxane **1fc2** at 1 mM concentration in D_2O .

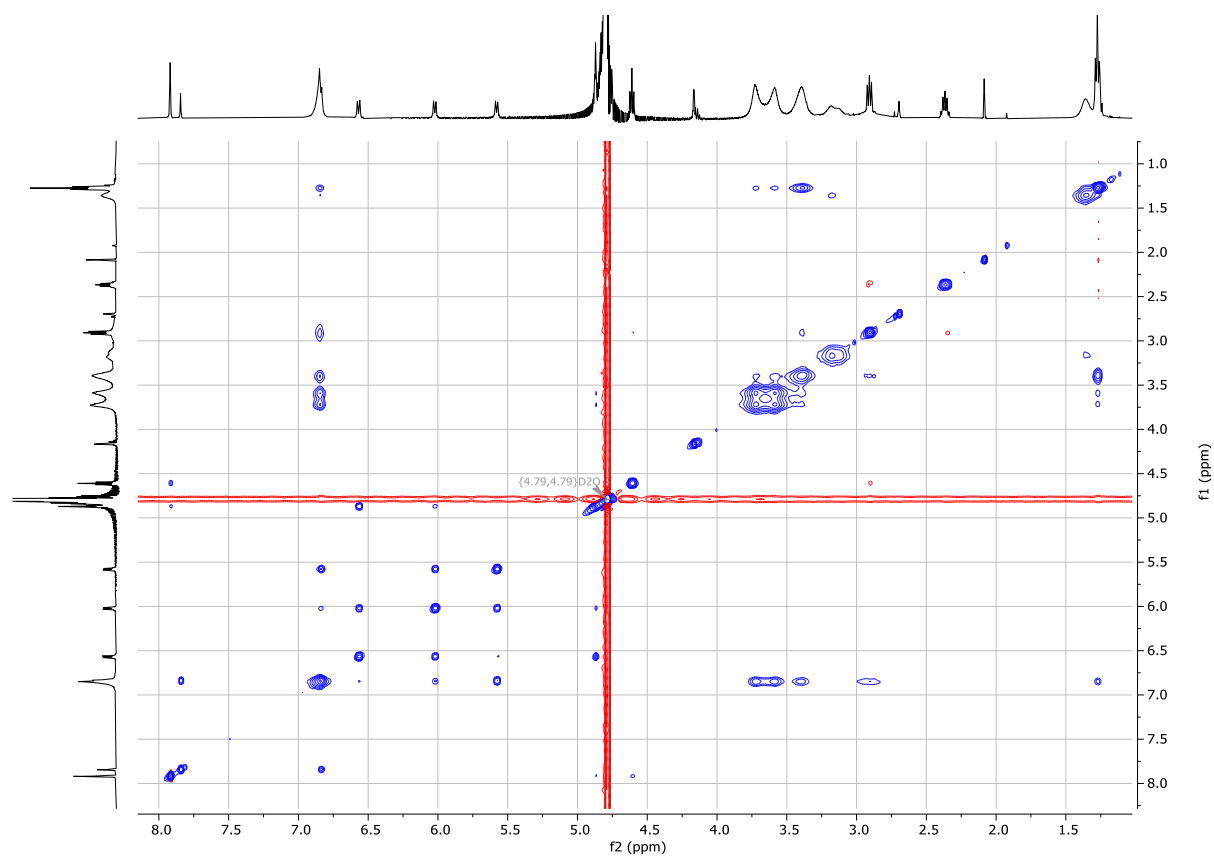


Figure S4: ^1H -NOESY 2D-NMR spectrum (500 MHz) of the pseudorotaxane **1fc2** at 1 mM concentration in D_2O .

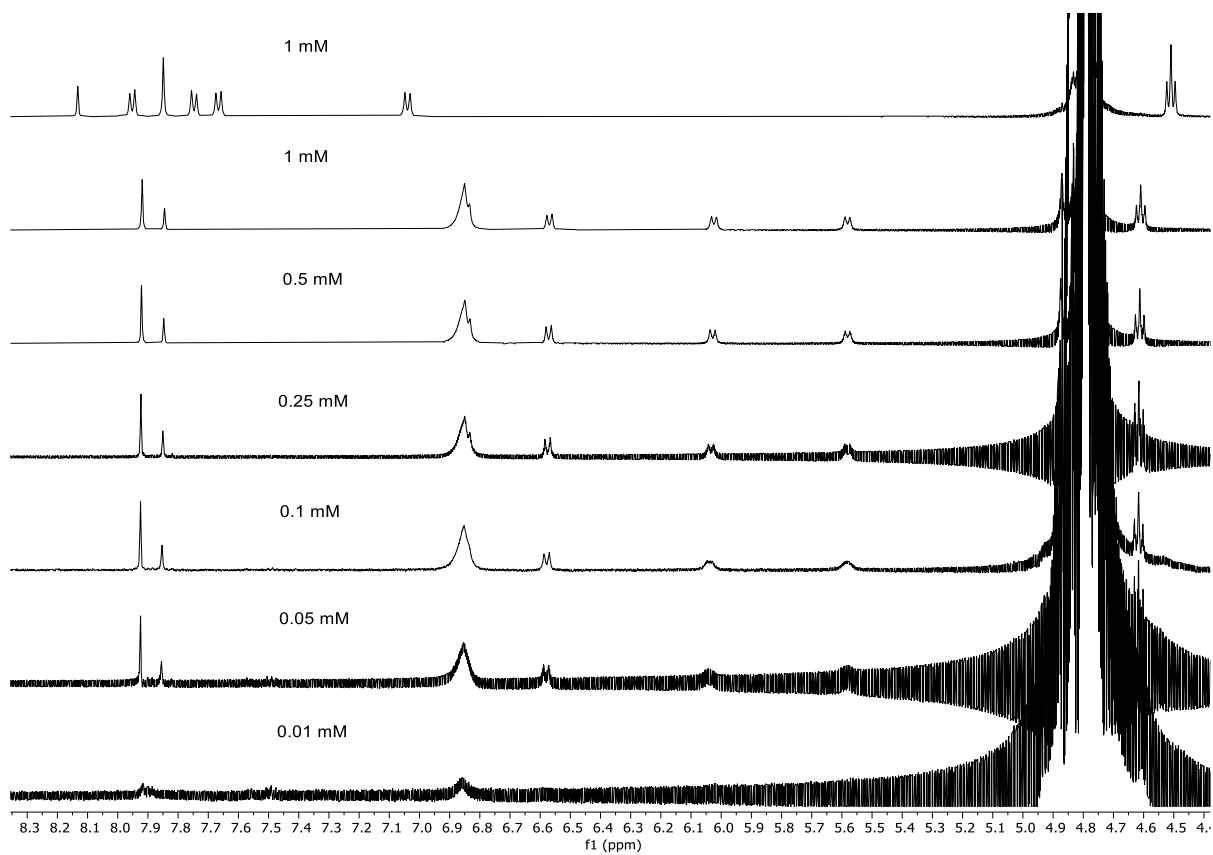


Figure S5: ¹H-NMR spectra (500 MHz) of guest **1f** at 1 mM concentration in D₂O (top) and equimolar mixtures with the host **2** at decreasing concentrations.

¹H-NMR spectra of pseudorotaxane **9**⊂**2**

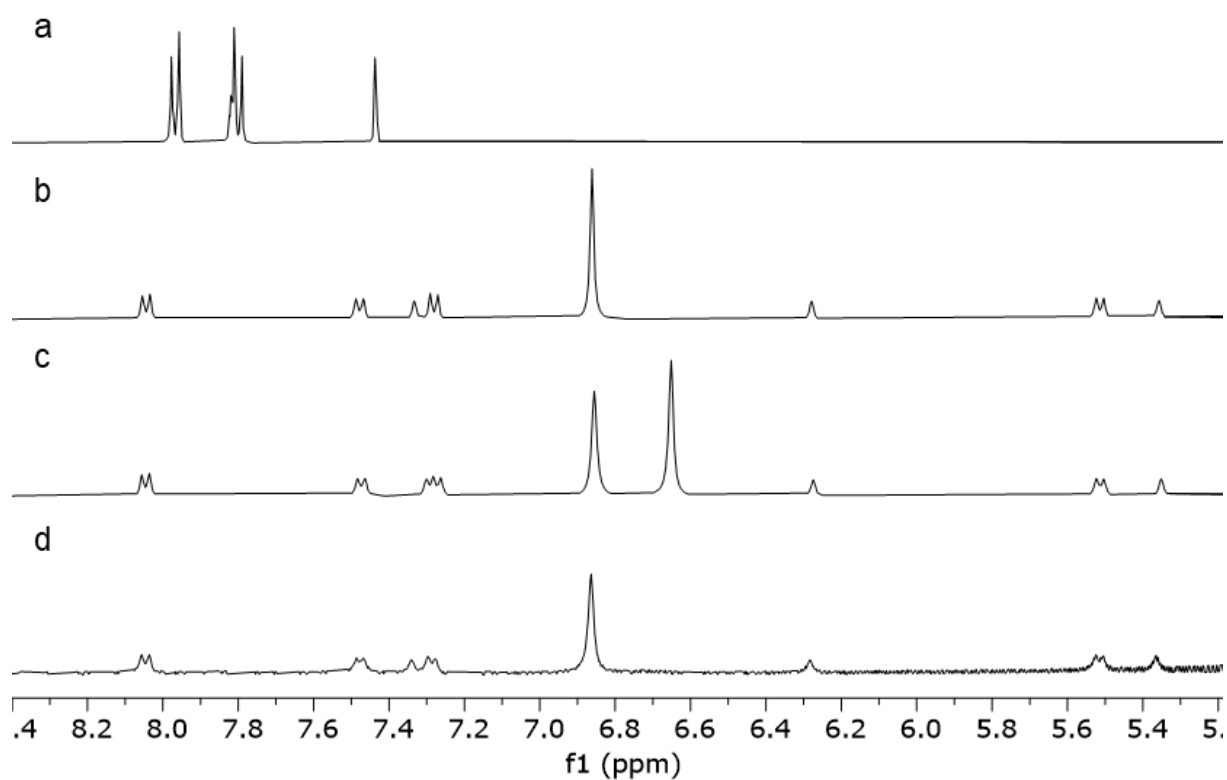


Figure S6: ¹H-NMR spectra (400 MHz) in D₂O of a) stopper **9** at 0.5 mM concentration, b) equimolar mixture of **2** and **9** at 0.5 mM concentration, c) a 2:1 mixture of **2** and **9** at 1 mM and 0.5 mM concentration, respectively, and d) equimolar mixture of **2** and **9** at 0.1 mM concentration.

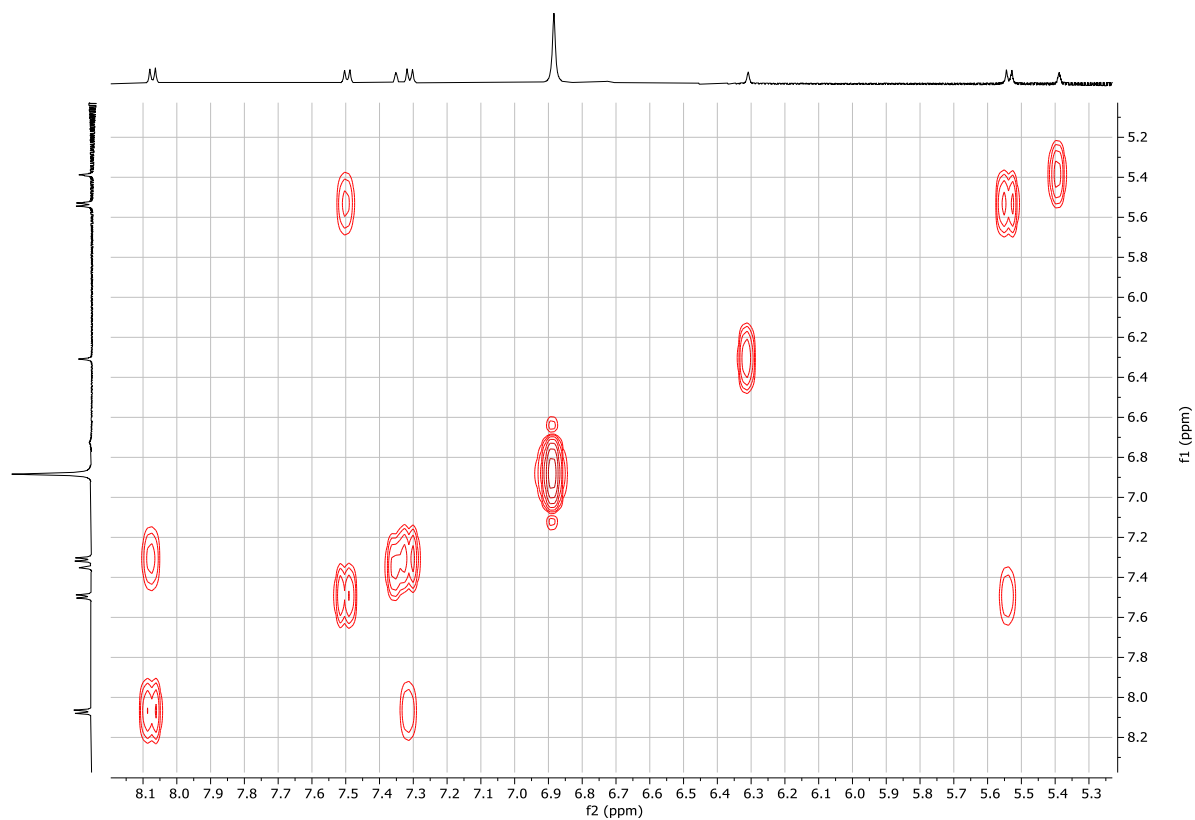


Figure S7: ¹H-COSY NMR spectrum (500 MHz) of the pseudorotaxane **9**⊂**2** at 1 mM concentration in D₂O.

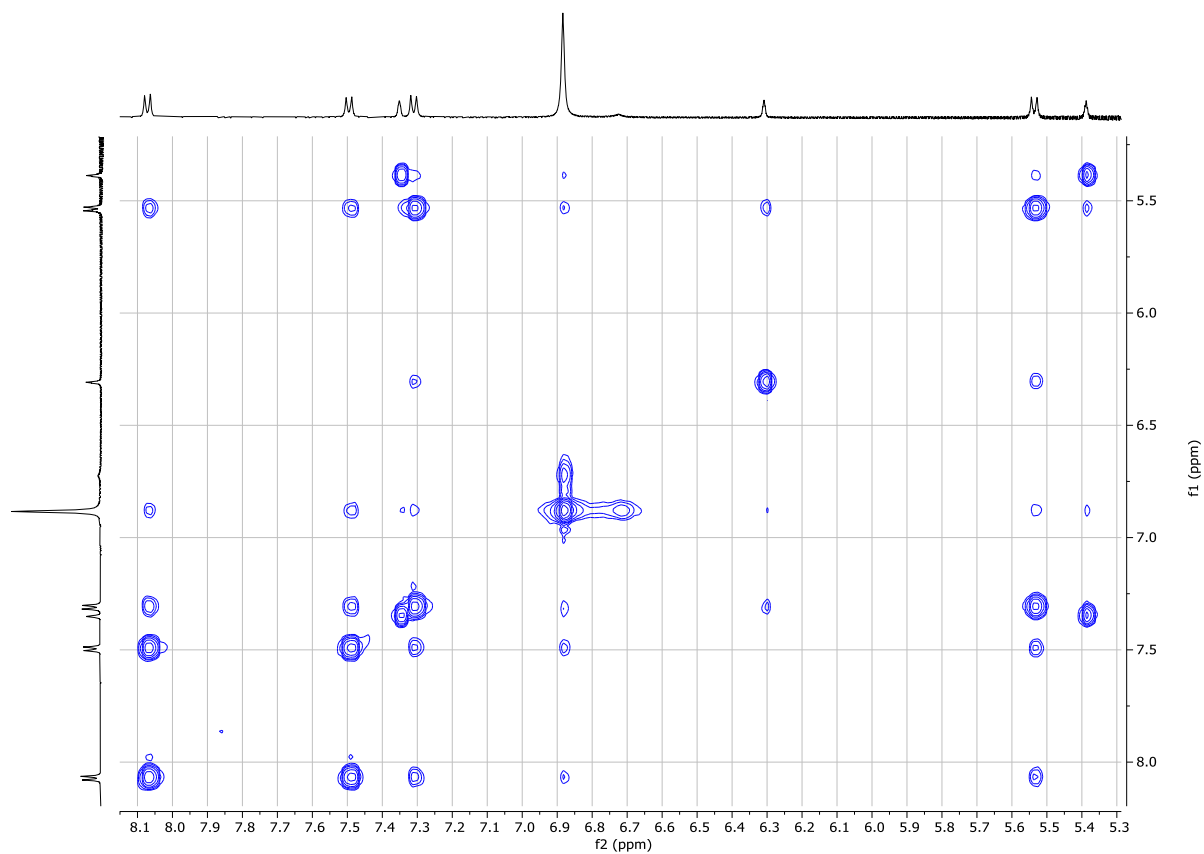


Figure S8: ^1H -NOESY NMR spectrum (500 MHz) of the pseudorotaxane **9c2** at 1 mM concentration in D_2O . Due to the symmetry of the guest molecule and the interchange between the two (identical) positions of the macrocyclic host, exchange signals can be observed along with the intended NOE signals. Due to the molecular weight of the pseudorotaxane, both the EXSY and NOESY signals are in the same phase.

¹H-NMR competition experiment of **1f**, **9**, and **2**

For the ¹H-NMR competition experiment shown in Figure S9e, the chromophore **1f**, stopper **9**, and macrocyclic host **2** were mixed in D₂O in a 1:1:1 ratio to have each component present at 0.5 mM concentration. As a comparison, the ¹H-NMR spectra of free **1f** and **9** are shown in Figure S9a/S9b, and the spectra of **1f****c2** and **9c2** are shown in Figure S9c/S9d. Figure S9e shows the presence of both free stopper **9** (e.g., 7.78 ppm and 7.98 ppm) and its threaded pseudorotaxane state (e.g., 5.35 ppm, 5.50 ppm, 6.28 ppm). Free **1f** cannot be observed clearly, although some broadened peaks are barely protruding from the baseline. The pseudorotaxane **1f****c2** also gives broadened signals, the signals at 5.55, 5.98, and 6.55 ppm indicate its formation. The broadening of the signals complicates the determination of the ratio of formed supramolecular species. Nonetheless, the presence of both pseudorotaxanes simultaneously implies a similar association constant for the two equilibria.

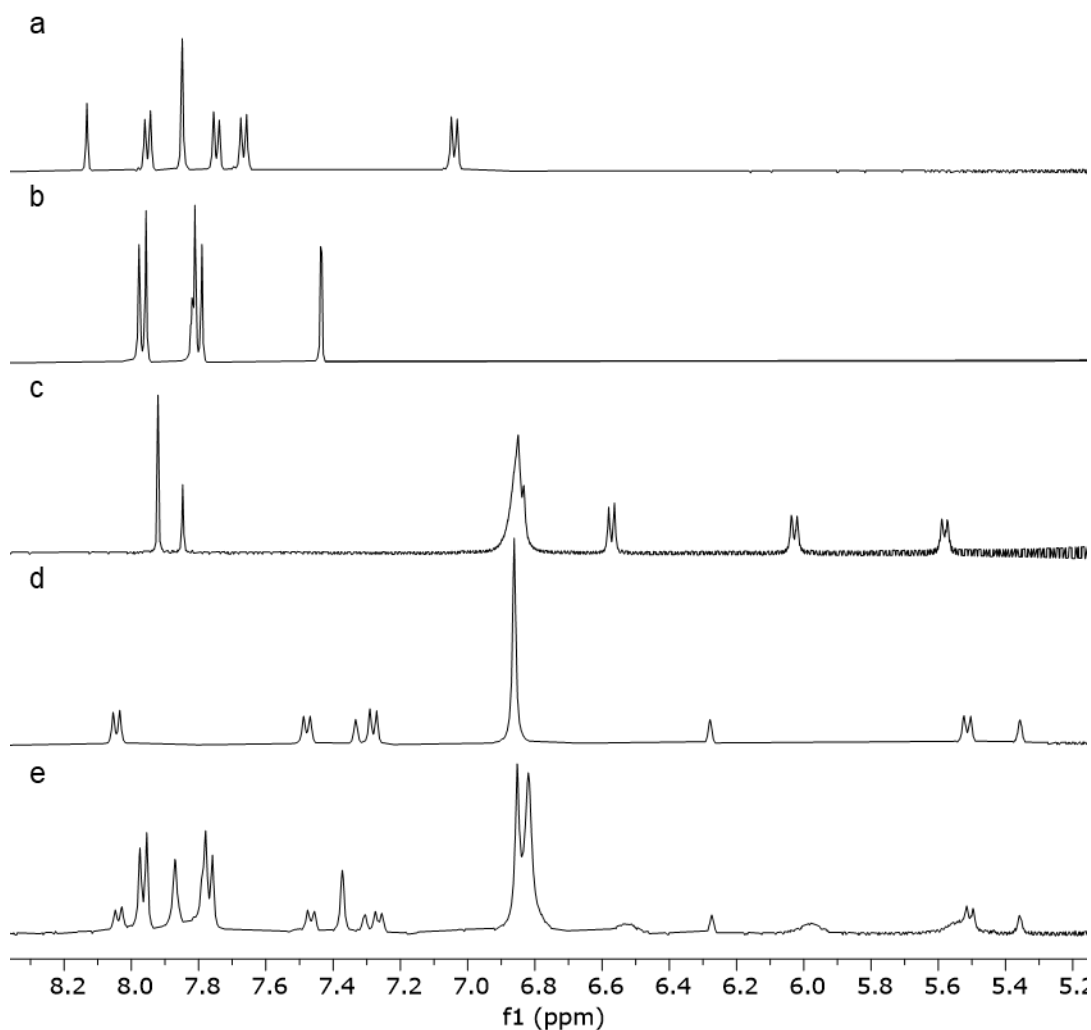


Figure S9: ¹H-NMR spectra (a and c were recorded at 500 MHz frequency; b, d, and e at 400 MHz) of D₂O solutions at 0.5 mM concentration of a) **1f**, b) **9**, c) **1f****c2**, d) **9c2**, e) **1f**, **9**, **2** (1:1:1). The competition experiment in e) shows significantly broadened signals of the pseudorotaxane **1f****c2** (visible in spectrum c), and sharp signals of both the free **9** (b) and pseudorotaxane **9c2** visible in d.

Determination of the association constant of $1f \subset 2$

As NMR spectroscopy was not suited for the determination of the K_a of the equilibrium shown in Scheme S2 in water, we used optical means to monitor the change. At the chosen chromophore concentration of 2.05×10^{-6} M, which was kept constant throughout the titration, addition of a solution of **2** showed relatively small changes in the absorption spectrum (Figure S10) and a significant increase in emission intensity when excited at 400 nm wavelength (Figure S11). In both wavelength regions **2** is spectroscopically “silent” and gives no signal. Fluorescence spectra proved to give more reliable data in this concentration range and was chosen to determine the K_a of the equilibrium. The obtained data was fitted at four wavelengths (640 nm, 650 nm, 660 nm, 670 nm) using the publicly available Matlab script written by P. Thordarson¹ for 1:1 binding (Figure S12). K_a was determined to be 1.5×10^7 M⁻¹ with a 2.9% confidence interval determined by asymptotic error and standard error of the y estimate of 0.116. The difference $k_{\Delta HG}$ of the two proportionality constants k_{HG} and k_H was calculated to be 1.6×10^7 at 640 nm wavelength, while at the other three wavelengths the $k_{\Delta HG}$ is 1.7×10^7 , with 0.2% confidence interval determined by asymptotic error.

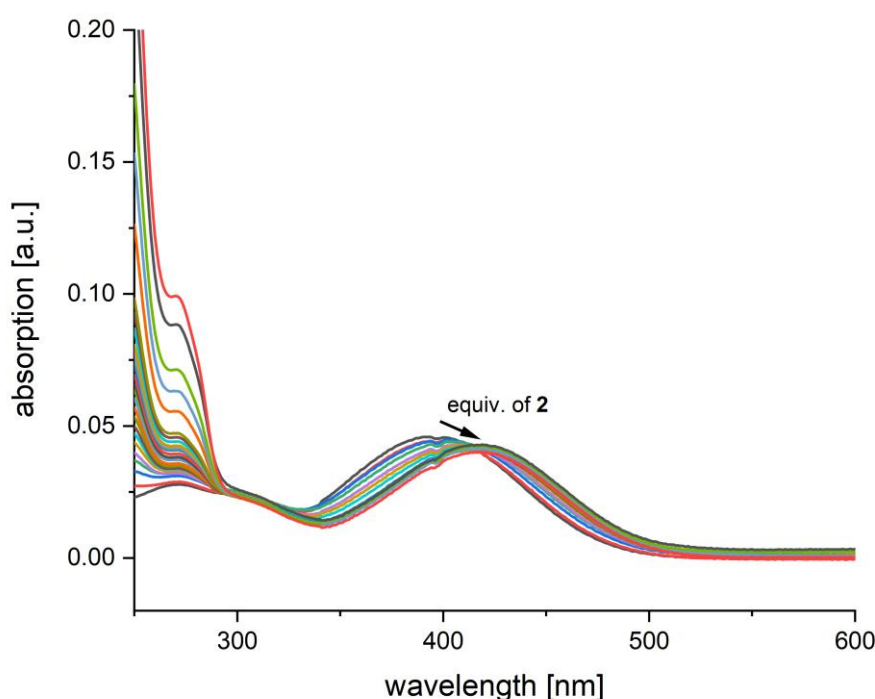


Figure S10: Changes in absorption induced by complexation of **1f** with **2** in aqueous solution, with the arrow indicating the direction of the shift upon addition of **2**.

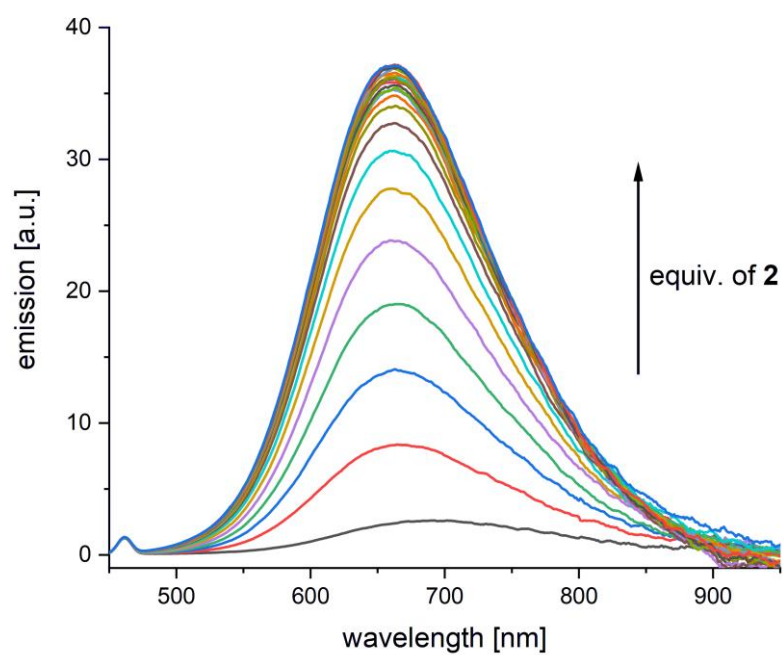


Figure S11: Changes in emission induced by complexation of **1f** with **2** in aqueous solution, with the arrow indicating the increase in emission upon addition of **2**.

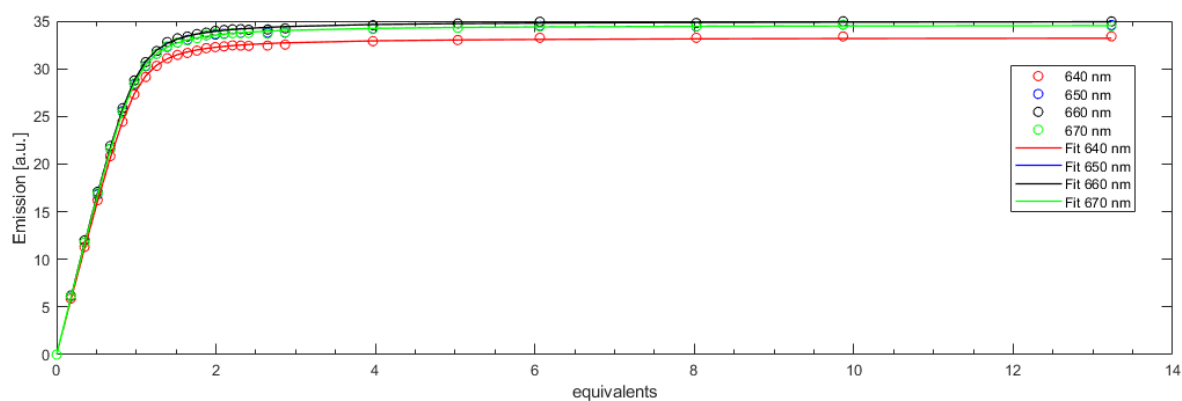


Figure S12: Data points and the calculated fit for all four wavelengths used to calculate K_a .

NOE showing *E*-selective formation of **1f**

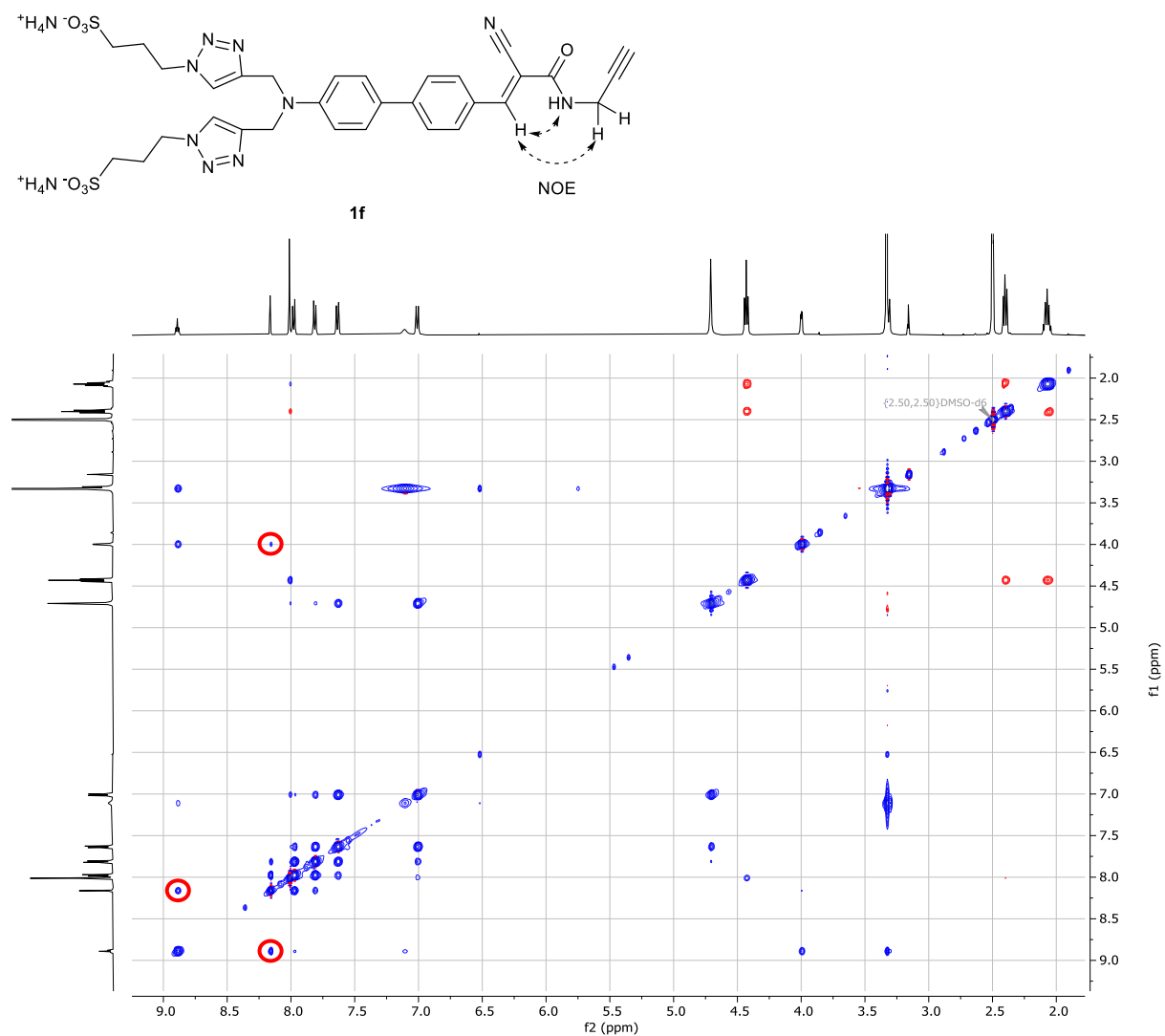


Figure S13: ¹H-NOESY NMR spectrum (500 MHz) of **1f** in DMSO-d₆. Red circles highlight NOEs indicated with dashed arrows in the structure, proving the formation of the *E* isomer.

Optical Spectra of **1a**, **1f**, **1e**, and **1e**2

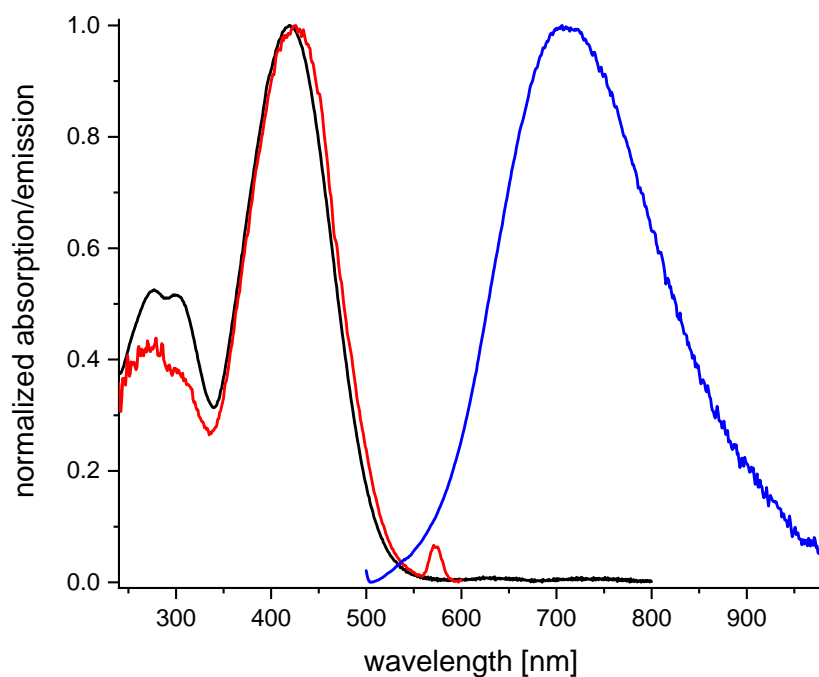


Figure S14: Absorption (black), excitation (red), and emission (blue) spectra of **1a** in H₂O. The emission spectrum was measured with 420 nm excitation light. The excitation spectrum was measured for emission at 710 nm wavelength. The Stokes' shift between the two maxima (420 nm and 710 nm, respectively) is ~ 9725 cm⁻¹. The small peak in the excitation spectrum at 570 nm is a scattering artifact.

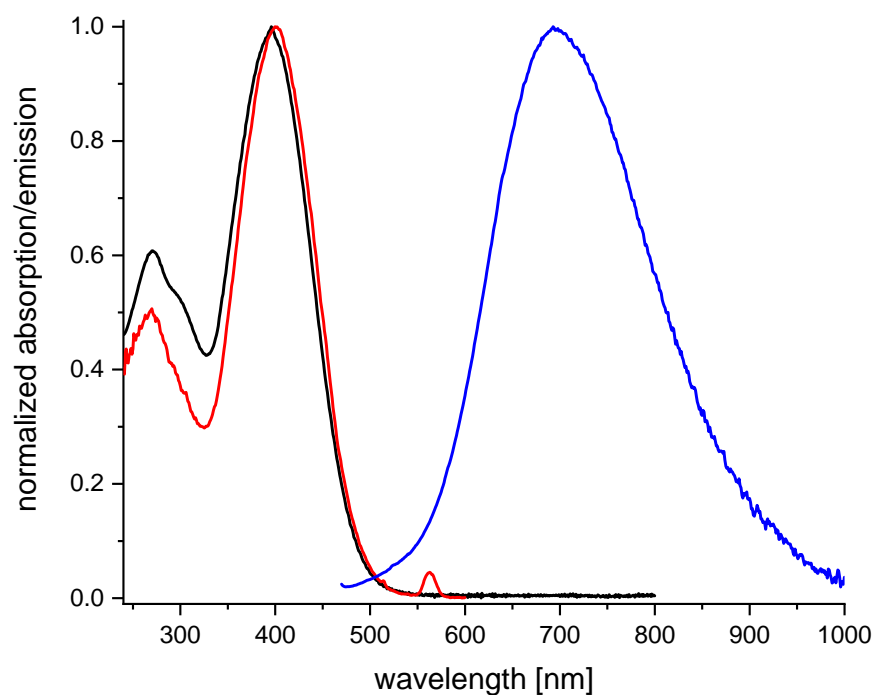


Figure S15: Absorption (black), excitation (red), and emission (blue) spectra of **1f** in H₂O. The emission spectrum was measured with 396 nm excitation light. The excitation spectrum was measured for emission at 695 nm wavelength. The Stokes' shift between the two maxima (396 nm and 693 nm, respectively) is ~ 10820 cm⁻¹. The small peak in the excitation spectrum at 560 nm is a scattering artifact.

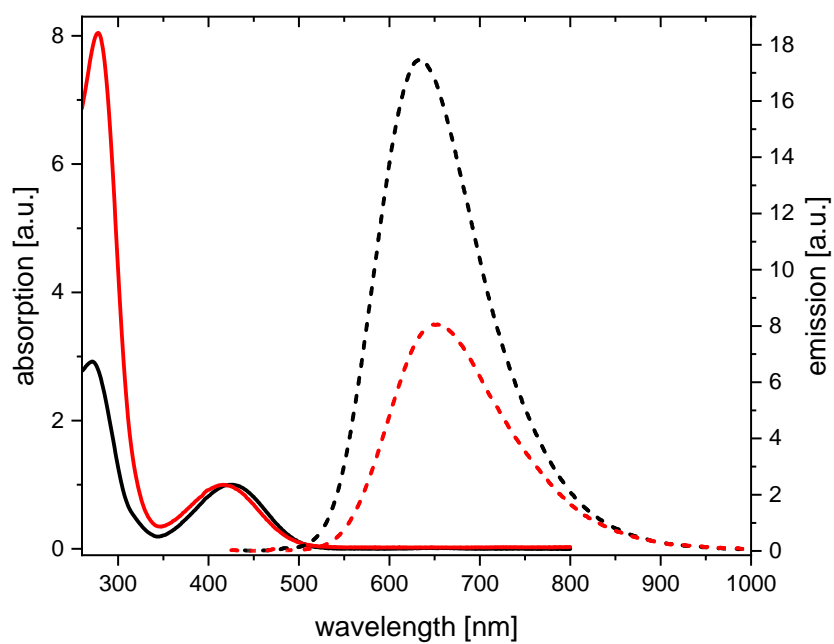


Figure S16: Absorption (solid lines) and emission (dashed lines) spectra of **1ec2** (black) and **1e** (green) in DMSO. Absorption spectra are normalized. Emission spectra were corrected for differences in absorption at the excitation wavelength. **1ec2** was excited at 425 nm wavelength, **1e** at 416 nm.

Quantum Yield Determination for **1e** and **1ec2**

To quantify the difference in emission intensity, we determined the quantum yields of **1e** and **1ec2** in (aerated) phosphate buffered aqueous solution with pH 6.4 on the JASCO Spectrofluorometer FP-8600 equipped with a ILFC-847S integrating sphere, which was continuously purged with N₂ gas during measurements. The integrating sphere was calibrated using a calibrated halogen lamp (ESC-842) and multiple standards² gave accurate results: Rhodamine 6G 96% (Lit.: 94-95%), Ru(bpy)₃Cl₂ 3% (Lit.: 2.8-4.0%), Os(bpy)₃Cl₂ 0.4% (Lit.: 0.5%). An excitation wavelength of 410 nm was chosen, as both molecules absorb at this wavelength. Emission was measured in the range of 380 – 1010 nm. Excitation and emission bandwidths were set to 5 nm. The photomultiplier tube (PMT) voltage was set to 735 V, no beam attenuators or apertures were used. Three types of measurements were used for the calculation of the quantum yield:

1. Blank: The 0.5 cm cuvette with stopper was filled with phosphate buffered aqueous solution and the light reaching the detector was measured during direct irradiation of the solution.
2. Direct excitation: The 0.5 cm cuvette was filled with a solution of either **1e** or **1ec2** and directly irradiated by the excitation light, and the emission was recorded.
3. Indirect excitation: The solution used in the direct measurement was switched to the “out” position and the emission and absorbance from indirect excitation was measured, to correct for this contribution to the measured quantum yield.

Each measurement was performed at a scan rate of 100 nm/min and the average of three cycles was taken to decrease the noise level. The quantum yield was determined using the “Quantum Yield Calculation” software supplied with the instrument.

Due to the small amount of **1ec2** available, we were not able to perform the measurement at precise concentrations. However, different arbitrary concentrations were measured and no concentration dependency was observed for either chromophore. It is important to note that for this instrument, an optical density of at least 0.1 is necessary.

As visible in Figure S17 and S18, the signal-to-noise ratio decreases above 800 nm, which poses a significant problem for low emission intensities. Despite the slow measurements and averaging of three measurement cycles, we were not able to improve the spectra further. Due to this limitation, we integrated the emission only from 500 – 800 nm for **1e** and 500 – 850 nm for **1ec2**, consistently obtaining quantum yields below 1% for **1e** and 10.5 – 11.5% for **1ec2** in the aqueous buffered solution. No precise value for **1e** could be obtained given the poor signal-to-noise in the measurements.

The same measurements were performed in DMSO (Figure S19 and S20). The better signal-to-noise ratio allowed us to integrate in the area of 500 – 900 nm wavelength. The determined quantum yields for **1e** and **1ec2** were 19.0% ±0.9% and 58.5% ±1.5%, respectively.

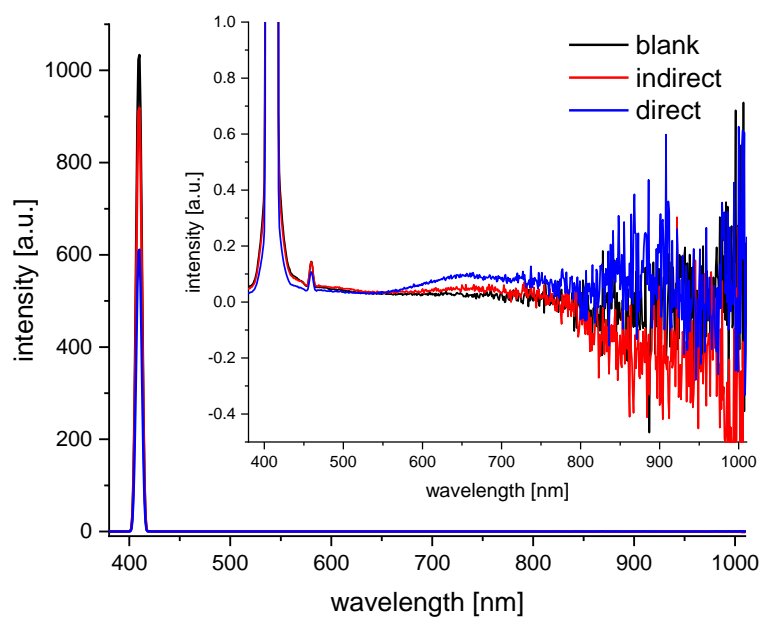


Figure S17: Exemplary spectral dataset used for the determination of the absolute quantum yield of **1e** in phosphate buffered aqueous solution at pH 6.4. Inset shows the spectrum with the y-axis scaled to the emission signal.

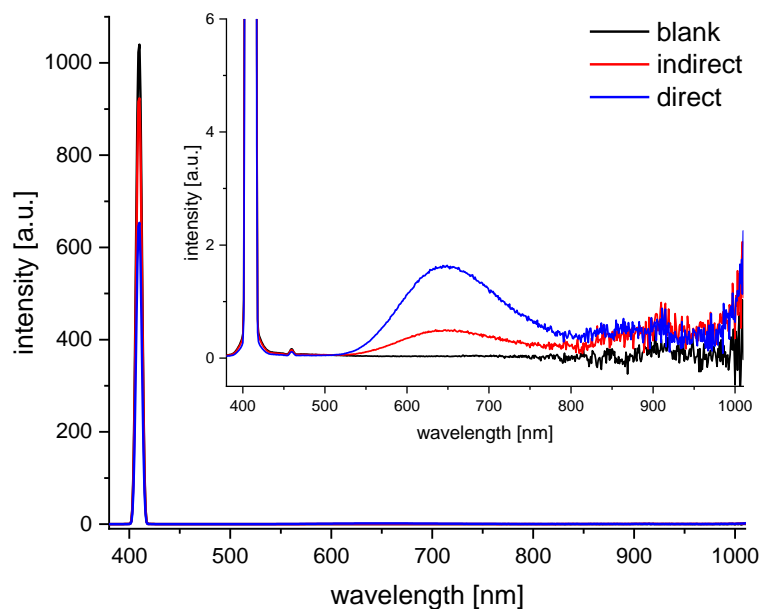


Figure S18: Exemplary spectral dataset used for the determination of the absolute quantum yield of **1ec2** in phosphate buffered aqueous solution at pH 6.4. Inset shows the spectrum with the y-axis scaled to the emission signal.

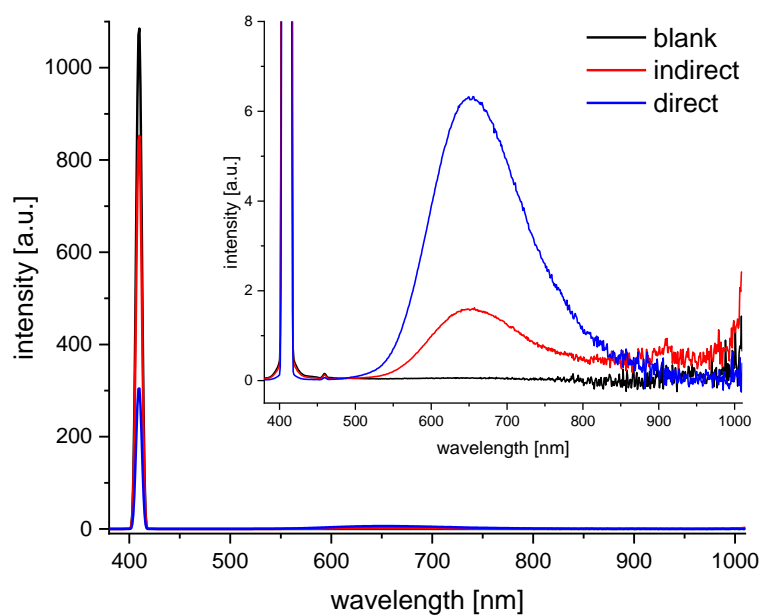


Figure S19: Exemplary spectral dataset used for the determination of the absolute quantum yield of **1e** in DMSO. Inset shows the spectrum with the y-axis scaled to the emission signal.

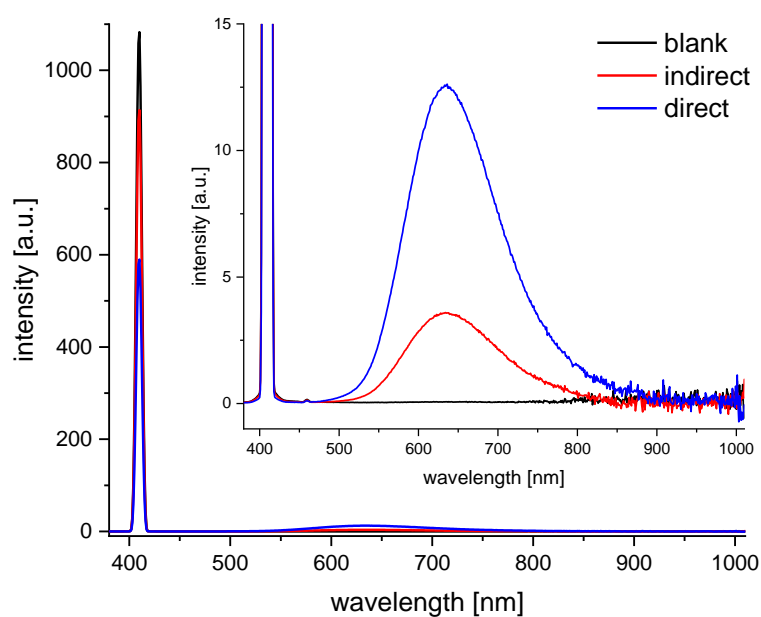


Figure S20: Exemplary spectral dataset used for the determination of the absolute quantum yield of **1ec2** in DMSO. Inset shows the spectrum with the y-axis scaled to the emission signal.

Unedited Photographs of Solid-State Emission and Emission Spectra

For the emission measurements of compounds **3**, **1a**, **1f**, and **1e** in solid state, the solids were finely ground using a mortar and pestle, and the resulting fine powder was transferred onto a glass slide. A second glass slide was pressed on top and PTFE isolating band (chosen due to its white color and lack of luminescence) was wrapped around the top and bottom of the glass slides to hold the solids in place. Due to the lack of sufficient material, **1e****c****2** dissolved in methanol was dropcasted onto a glass slide and the resulting film was dried in vacuum overnight. The samples were fastened in the integrating sphere at a height ensuring direct irradiation of the solids with the excitation laser. All samples were excited at 400 nm wavelength.

Apart from the emission of **3**, all emission spectra show similar shape and maxima for the different chromophores in solid state. The influence of the macrocycle on the emission wavelength of **1e****c****2** appears to be negligible in solid state. The emission is hypsochromically shifted compared to the spectra measured in aqueous solution, which is to be expected due to the lack of solvatochromic effects.

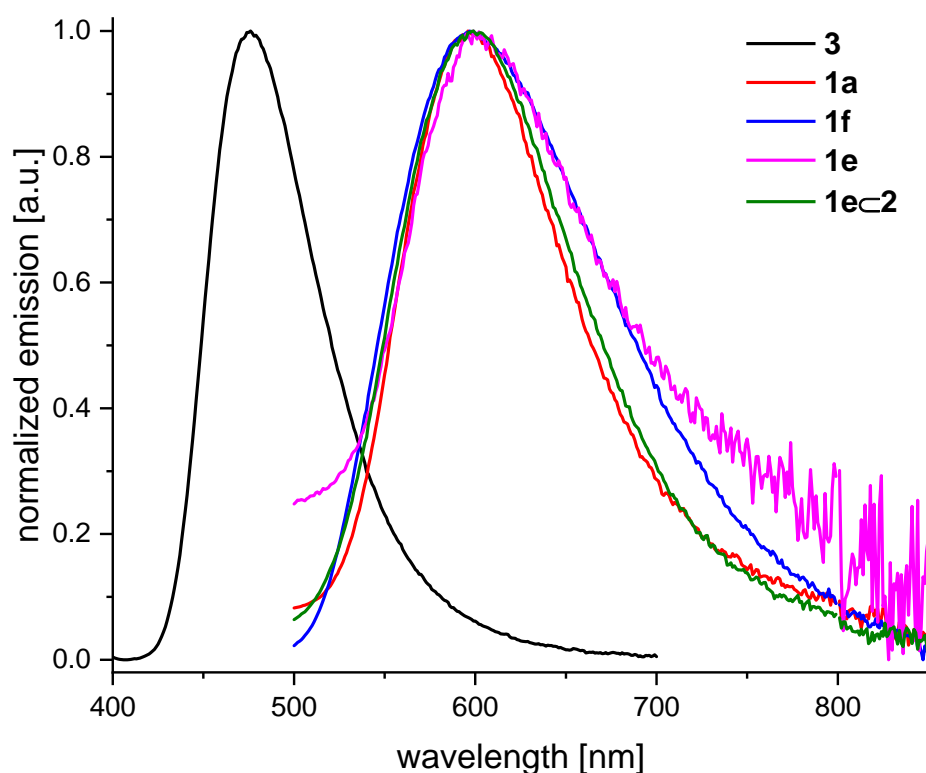


Figure S21: Normalized emission spectra of the powdered solids of **3**, **1a**, **1f**, and **1e**, and a film of **1e****c****2** irradiated at 400 nm wavelength. An artifact at 800 nm wavelength caused by the second harmonic oscillation was removed by deleting this measurement point in all spectra for better visibility.

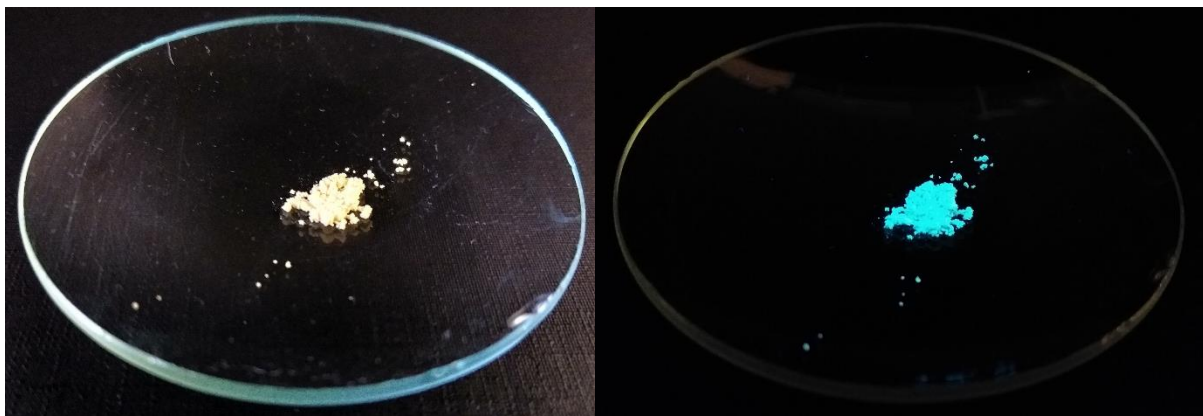


Figure S1: Solids of **3** under ambient light (left) and irradiated by a UV lamp with 366 nm light (right).

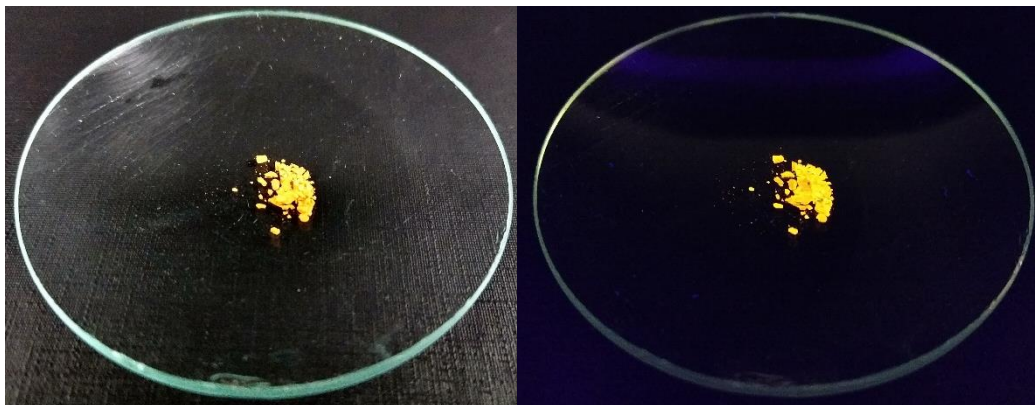


Figure S23: Solids of **1a** under ambient light (left) and irradiated by a UV lamp with 366 nm light (right).



Figure S24: Solids of **1f** under ambient light (left) and irradiated by a UV lamp with 366 nm light (right).

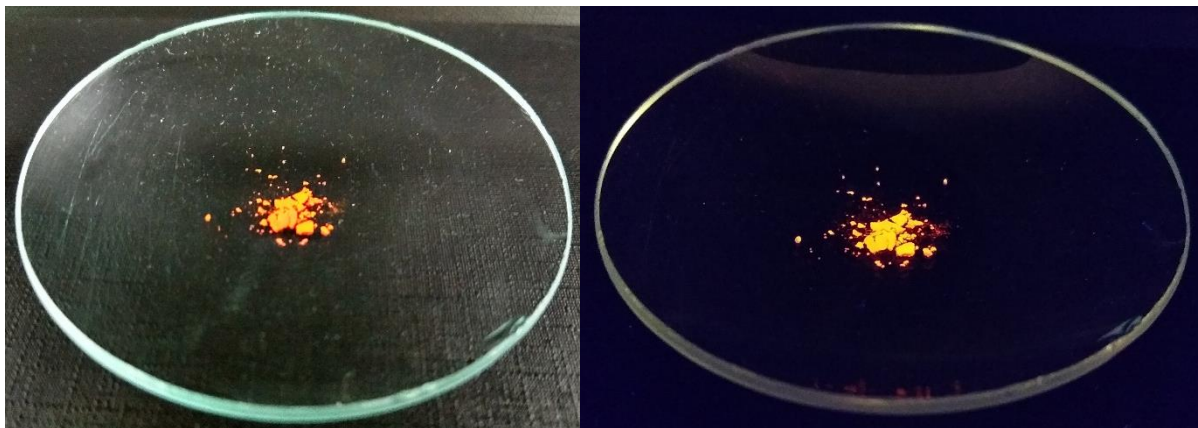


Figure S25: Solids of **1e** under ambient light (left) and irradiated by a UV lamp with 366 nm light (right).



Figure S2: Film of **1ec2** under ambient light (left) and irradiated by a UV lamp with 366 nm light (right).

Deslipping Experiments of **1ec2**

To determine whether the stopper moieties are sufficiently bulky and yielded a stable rotaxane, we performed experiments at elevated temperatures to see if “deslipping” occurs. The association of guests with **2** is mainly driven by the hydrophobic effect and severely diminished in the presence of dipolar aprotic solvents, therefore we chose acetonitrile and DMSO as solvents to guarantee deslipping – if it can occur. For the experiments a solution of **1ec2** in ACN or DMSO was heated to 75 °C or 120 °C in a closed vial, respectively. After certain time intervals the solution was injected into an HPLC-ESI-MS and checked for the presence of either **2** or **1e**, the deslipping products. However, comparison to the chromatograms of either molecule showed no signs of their formation after 16 h of heating (Figure S27).

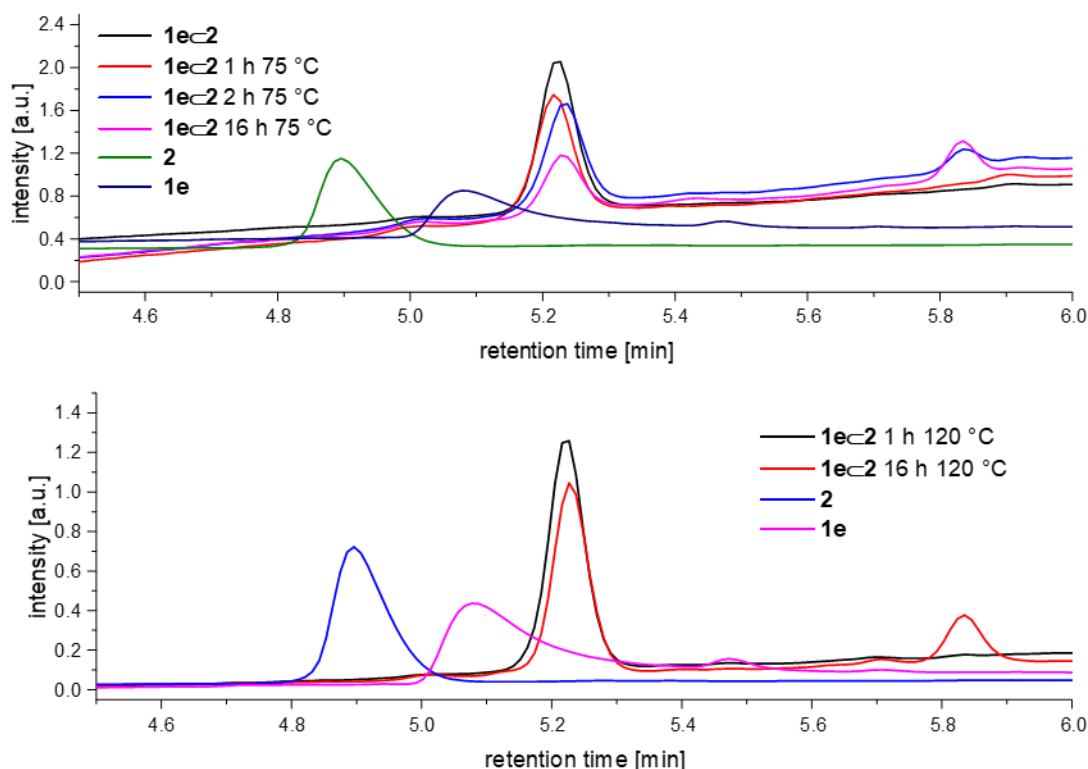
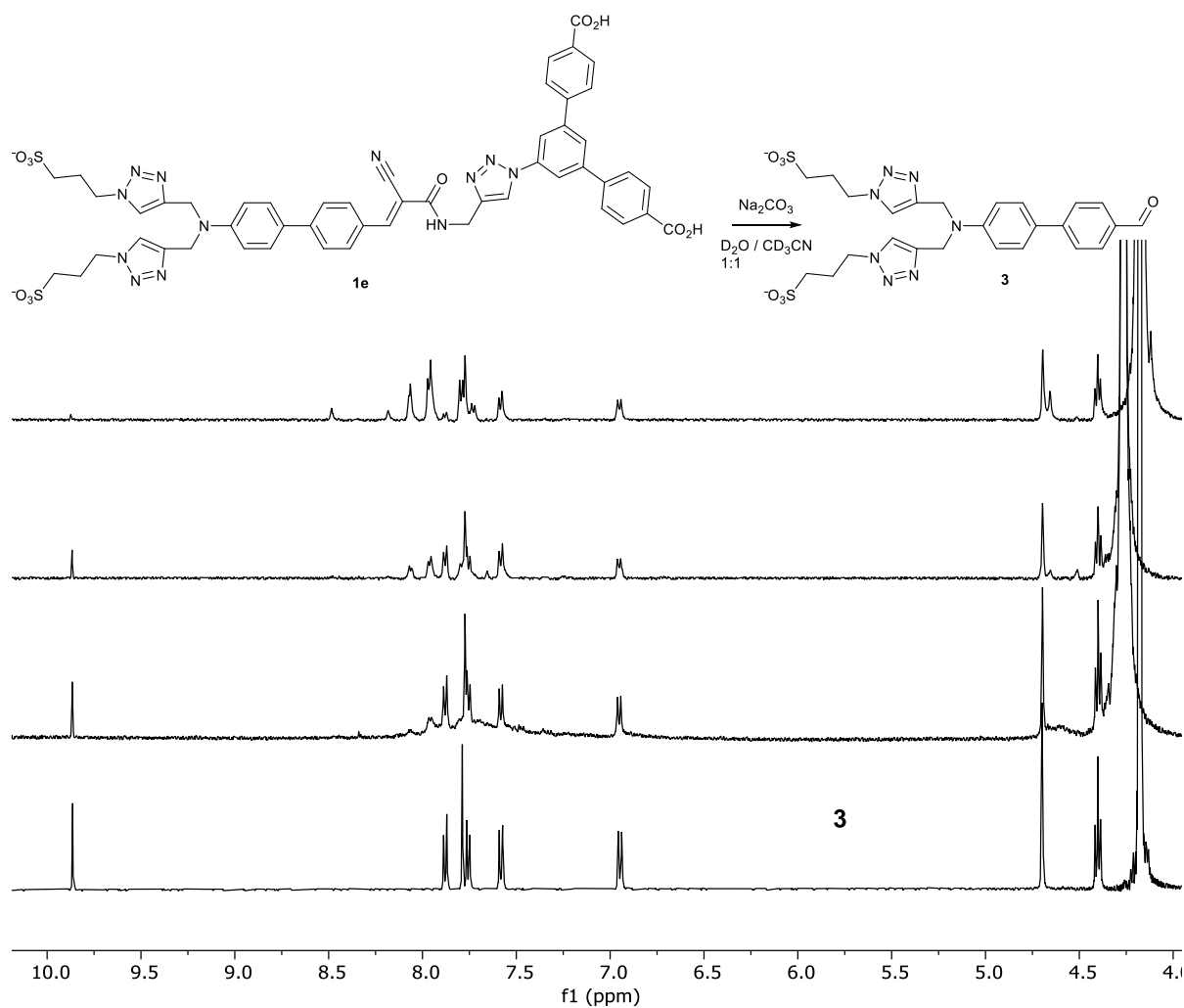


Figure S27: Qualitative HPLC-MS chromatograms (254 nm) of **1ec2** before and after heating to 75 °C in acetonitrile (top) and 120 °C in DMSO (bottom). Chromatograms of **1e** and **2** are shown as comparison. The plotted intensities were adjusted to compensate for different baseline drifts and are not quantitative. As confirmed by the absence of **1e** and **2** after prolonged heating, the isolated rotaxane **1ec2** does not show deslipping under these conditions.

Reversibility of the Knoevenagel Condensation



Scheme S3: Hydrolysis of **1e** to form **3** and various decomposition products of **e** in $\text{D}_2\text{O} / \text{ACN-d}_3$ (1:1) in presence of base (Na_2CO_3) over time. ^1H -NMR spectra (500 MHz) show the reaction over time with the third measurement after 20 h and a comparison to the pure compound **3** (bottom).

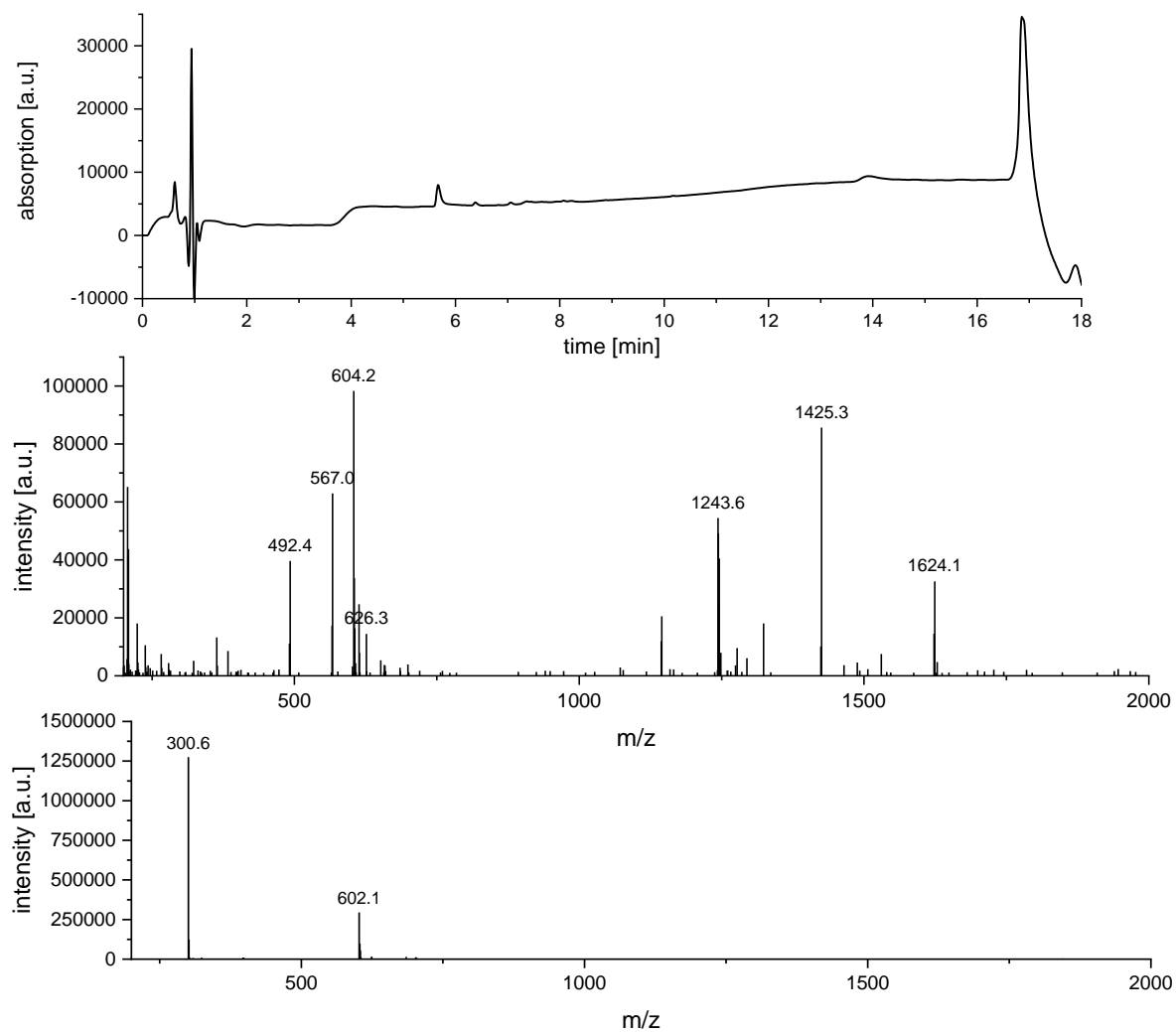
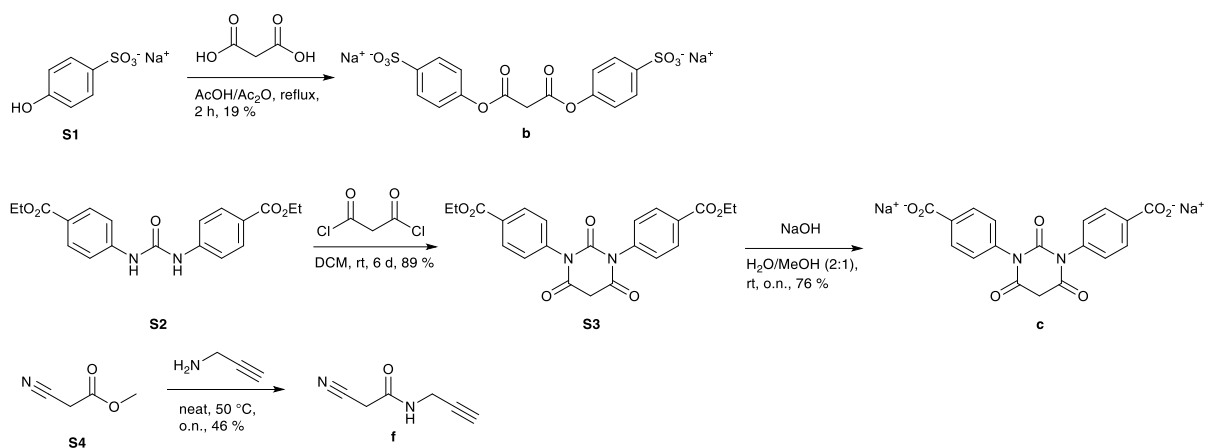
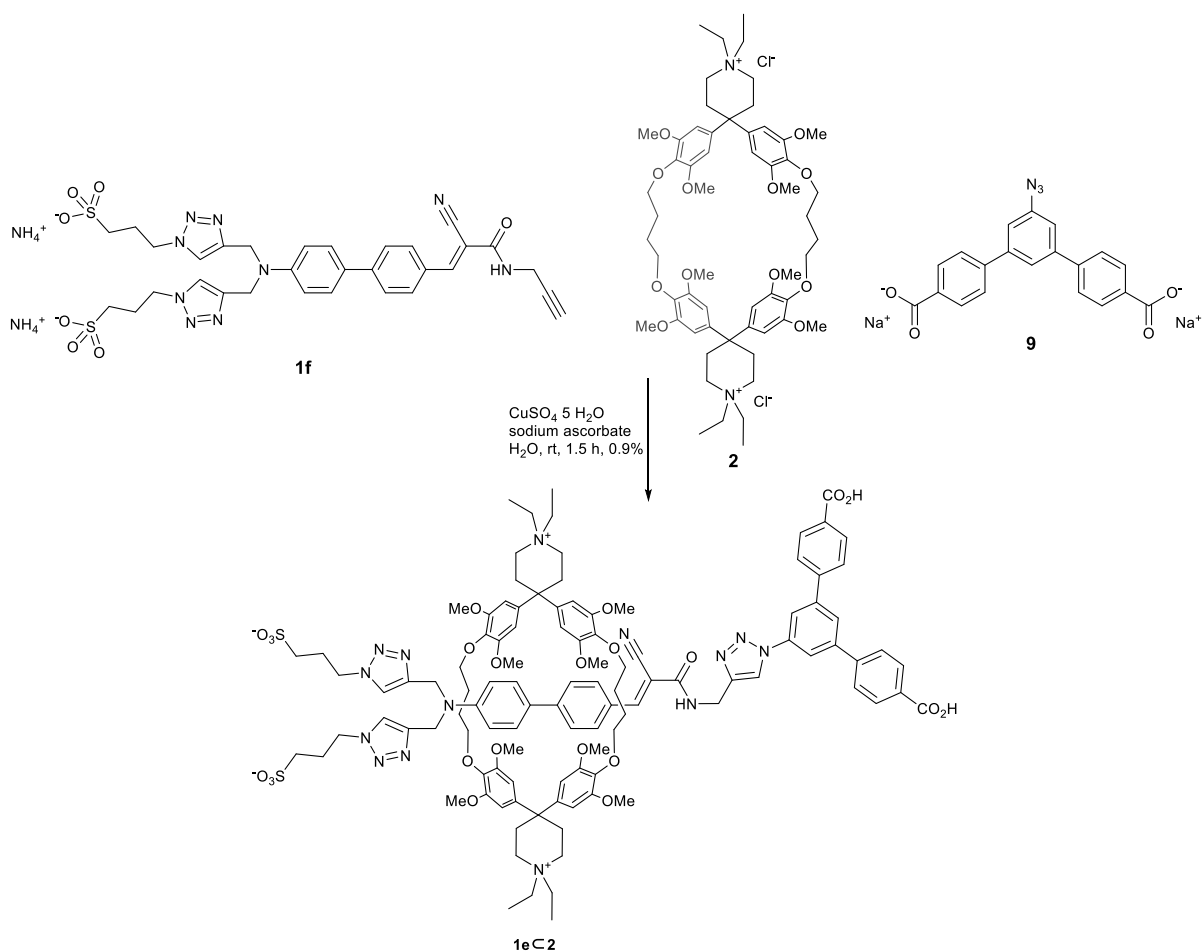
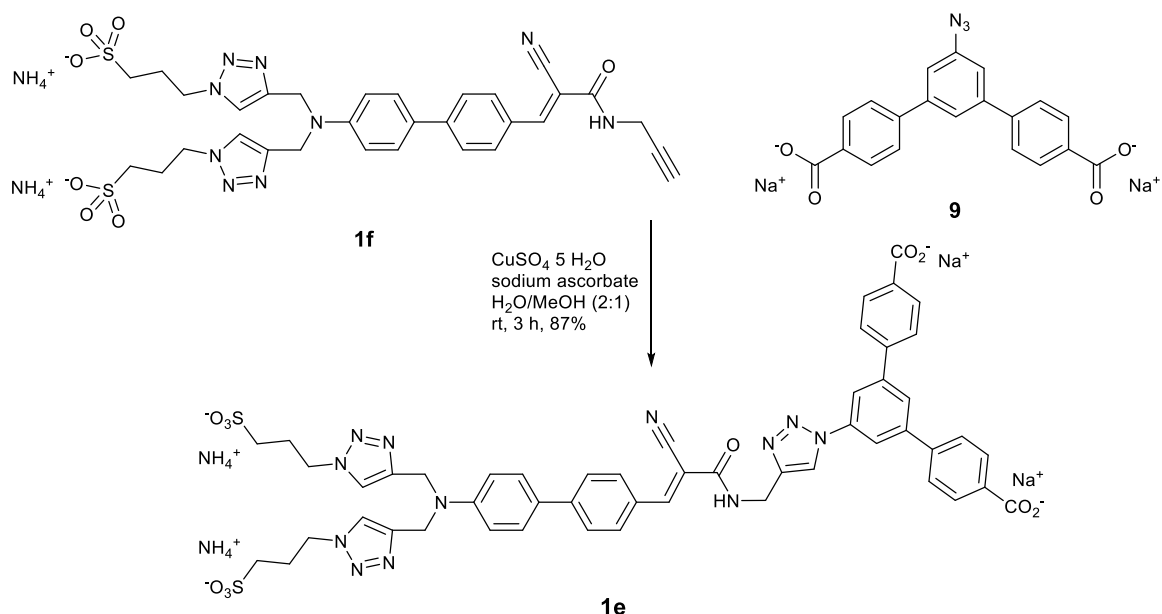


Figure S28: LC-ESI-MS UV-VIS chromatogram (200-800 nm, top) with peak of **3** visible at approx. 5.6 min retention time. Mass spectra of the peak in the positive (middle) and negative (bottom) mode, showing the m/z corresponding to **3** (604 m/z in the positive mode, 602 and 300 m/z in the negative mode).

Supplementary Reaction Schemes

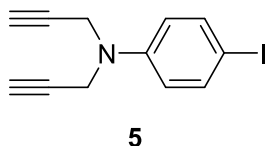
Scheme S4: Synthesis of **b**, **c**, and **f**.

Scheme S5: Assembly of the [2]rotaxane **1ec2** in water via CuAAC.



Scheme S6: Synthesis of reference compound **1e** via CuAAC.

Experimental Procedures

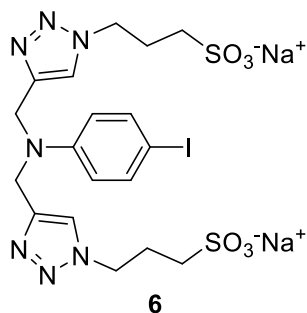


4-Iodoaniline (**4**, 10.2 g, 46.6 mmol, 1.0 equiv.), K_2CO_3 (32.2 g, 233 mmol, 5.0 equiv.) and a solution of propargyl bromide in toluene (80 %, 12 mL, 111 mmol, 2.4 equiv.) were suspended in acetonitrile (160 mL) and the resulting mixture was heated to 60 °C for 3 d. The mixture was allowed to cool to room temperature, insoluble salts were filtered off and the solvent was evaporated. The crude product was purified by flash chromatography (cyclohexane to 40% DCM) and the product was obtained as a yellow liquid (**5**, 9.05 g, 66 %).

^1H -NMR (400 MHz, CDCl_3) δ = 7.57 – 7.52 (m, 2H), 6.74 – 6.69 (m, 2H), 4.09 (d, J = 2.4, 4H), 2.25 (t, J = 2.3, 2H).

^{13}C -NMR (126 MHz, CDCl_3) δ = 147.32, 137.94, 117.71, 81.77, 78.83, 73.09, 40.51.

HR-ESI-MS (m/z): meas. 295.9936 [$\text{M}+\text{H}$] $^+$, calc. 295.9931 ($\text{C}_{12}\text{H}_{11}\text{IN}$) $^+$.



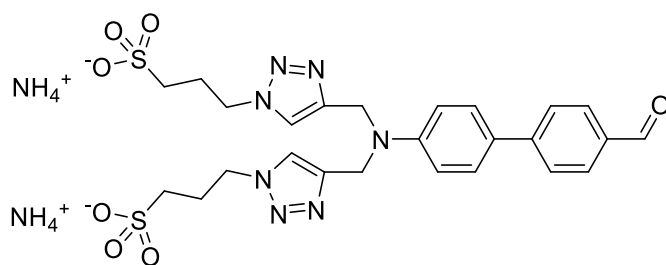
Sodium azide (2.01 g, 30.9 mmol, 4.0 equiv.) was dissolved in H_2O (5 mL), DMF (10 mL) and 1,3-propanesultone (2.7 mL, 30.9 mmol, 4.0 equiv.) was added. After 1 h at rt, TBTA (205 mg, 387 μmol , 0.05 equiv.), $\text{Cu}(\text{CH}_3\text{CN})_4\text{PF}_6$ (144 mg, 387 μmol , 0.05 equiv.) and sodium ascorbate (78 mg, 387 μmol ,

0.05 equiv.) were added, followed by a solution of **5** (2.28 g, 7.73 mmol, 1.0 equiv.) in DMF (5 mL). Additional H₂O (5 mL) and DMF (5 mL) were added and the mixture was stirred at room temperature for 22 h. To destroy remaining azide the reaction mixture was quenched with a few drops of an aqueous Na₂S₂O₃ solution (5%) and a 2:1 I₂/NaI mixture in EtOH (15w%) which was added until the solution assumed a brown color. Subsequently, the Na₂S₂O₃ solution was added to quench excess I₂, observed by decolorization of the reaction mixture. The reaction mixture was washed with DCM 3x and the aqueous layer was concentrated. The crude product was purified by reverse phase column chromatography (C-18, H₂O/ACN 8:2), after which the product was present in a mixture with 3-hydroxypropane-1-sulfonate. The solids were dissolved in a minimal amount of water and the product precipitated by addition of EtOH. After centrifugation and drying under vacuum, the product was obtained as a colorless solid (**6**, 2.33 g, 45 %).

¹H-NMR (400 MHz, D₂O) δ = 7.74 (s, 2H), 7.33 (d, J = 8.3, 2H), 6.61 (d, J = 8.5, 2H), 4.60 (s, 4H), 4.43 (t, J = 7.0, 4H), 2.87 – 2.78 (m, 4H), 2.31 – 2.21 (m, 4H).

¹³C-NMR (101 MHz, D₂O) δ = 147.17, 144.78, 137.84, 124.02, 116.49, 79.18, 48.77, 47.69, 45.91, 25.22.

HR-ESI-MS (m/z): meas. 311.5068 [M]²⁻, calc. 311.5064 (C₁₈H₂₂IN₇O₆S₂)²⁻; meas. 646.0031 [M+Na]⁻, calc. 646.0021 (C₁₈H₂₂IN₇NaO₆S₂)⁻.



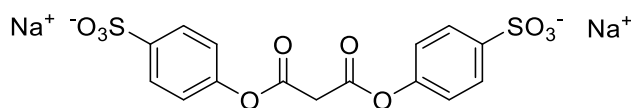
3

6 (4.00 g, 5.98 mmol, 1.0 equiv.), 4-formylphenylboronic acid (1.35 g, 8.97 mmol, 1.5 equiv.), and K₃PO₄ (2.66 g, 12.6 mmol, 2.1 equiv.) in H₂O (200 mL) was degassed for 25 min and Pd(OAc)₂ (67 mg, 299 μ mol, 0.05 equiv.) was added. The mixture was heated to reflux for 1 h, then cooled to room temperature and concentrated. The residue was suspended in EtOH, sonicated and filtered. The solids were redissolved in water and adsorbed on Celite 545, then purified by reverse-phase column chromatography (C-18, H₂O/MeOH 9:1 to 8:2, 20 mM NH₄OAc) to give the product as a bright yellow solid (**3**, 2.96 g, 78 %).

¹H-NMR (400 MHz, D₂O) δ = 9.92 (s, 1H), 7.99 (d, J = 8.2, 2H), 7.87 – 7.83 (m, 4H), 7.71 (d, J = 8.7, 2H), 7.07 (d, J = 8.7, 2H), 4.52 (t, J = 6.9, 4H), 2.84 – 2.79 (m, 4H), 2.34 – 2.25 (m, 4H).

¹³C-NMR (101 MHz, D₂O) δ = 194.85, 147.85, 145.92, 144.69, 133.11, 130.52, 127.94, 126.91, 125.44, 123.80, 113.49, 48.64, 47.62, 45.30, 25.16.

HR-ESI-MS (m/z): meas. 670.1097 [M+3Na]⁺, calc. 670.1101 (C₂₅H₂₇N₇Na₃O₇S₂)⁺.



b

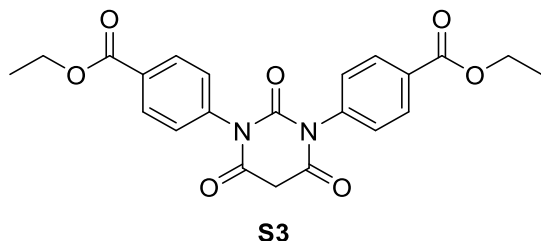
Sodium 4-hydroxybenzenesulfonate dihydrate (2.00 g, 8.62 mmol, 2.0 equiv.) and malonic acid (451 mg, 4.33 mmol, 1.0 equiv.) were suspended in a mixture of AcOH (4.2 mL) and Ac₂O (20.3 mL). The suspension was degassed with argon for 10 min and heated to reflux for 2 h. After allowing it to cool down to room temperature, the formed precipitate was filtered off, washed with Ac₂O and Et₂O. The resulting solids were suspended in methanol (roughly 150 mL) and water was added until the solids

dissolved. Upon cooling, the precipitated product was filtered off and washed with methanol. After drying in vacuum, the product was obtained as a pale yellow powder (384 mg, 19%).

$^1\text{H-NMR}$ (400 MHz, DMSO- d_6) δ = 7.68 – 7.63 (m, 4H), 7.16 – 7.11 (m, 4H), 4.12 (s, 2H).

$^{13}\text{C-NMR}$ (101 MHz, DMSO- d_6) δ = 165.19, 150.03, 146.31, 127.07, 120.87, 41.04.

HR-ESI-MS (m/z): meas. 206.9867 [$\text{M}-2\text{Na}$] $^{2-}$, calc. 206.9863 ($\text{C}_{15}\text{H}_{10}\text{O}_{10}\text{S}_2$) $^{2-}$.

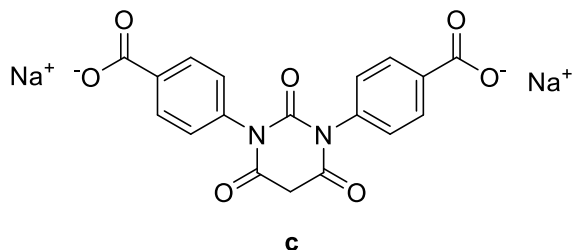


S2 (prepared according to literature³; 356 mg, 1.00 mmol, 1.00 equiv.) and malonyl dichloride (0.1 mL, 1.03 mmol, 1.03 equiv.) were dissolved in dry DCM (40 mL) and stirred at room temperature for 4 d. No further conversion was observed by LC-MS. Additional malonyl dichloride (0.1 mL, 1.03 mmol, 1.03 equiv.) was added and the reaction stirred for 2 d at room temperature. The reaction mixture was treated with aqueous 1 M HCl solution and extracted with EtOAc. The crude product was purified by column chromatography (cyclohexane/ethyl acetate) to give the product (**S3**, 378 mg, 89 %) as a white solid.

$^1\text{H-NMR}$ (500 MHz, DMSO- d_6) δ = 8.09 – 8.04 (m, 4H), 7.49 – 7.44 (m, 4H), 4.33 (q, J = 7.1, 4H), 4.06 (s, 2H), 1.33 (t, J = 7.1, 6H).

$^{13}\text{C-NMR}$ (126 MHz, DMSO- d_6) δ = 165.72, 165.25, 151.28, 139.47, 130.11, 129.90, 129.46, 61.06, 47.74 (splitting caused by partial H/D exchange on the active methylene position), 41.15, 14.20.

HR-ESI-MS (m/z): meas. 447.1161 [$\text{M}+\text{Na}$] $^+$, calc. 447.1163 ($\text{C}_{22}\text{H}_{20}\text{N}_2\text{NaO}_7$) $^+$.

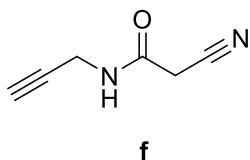


To a degassed solution of NaOH (188 mg, 4.71 mmol, 10.0 equiv.) in $\text{H}_2\text{O}/\text{MeOH}$ (2:1, 12 mL) was added **S3** (200 mg, 471 μmol , 1.0 equiv.) and the mixture was stirred at room temperature over night. The mixture was concentrated and the resulting solids redissolved in a minimal amount of water. A white solid precipitated upon addition of a mixture of EtOH/*i*PrOH and after centrifugation, the solids were suspended in EtOH and sonicated to remove excess NaOH. After centrifugation and drying on high vacuum, the product was obtained as a pure white powder (**c**, 148 mg, 76%).

$^1\text{H-NMR}$ (500 MHz, D_2O) δ = 8.03 – 7.99 (m, 4H), 7.44 – 7.40 (m, 4H), 5.02 (s, 0H). Integral of the CH_2 group is inaccurate due to rapid H/D exchange.

$^{13}\text{C-NMR}$ (126 MHz, D_2O) δ 175.01, 166.64, 154.13, 137.83, 137.00, 130.07, 128.65, 78.80.

HR-ESI-MS (m/z): meas. 413.0353 [$\text{M}+\text{H}$] $^+$, calc. 413.0356 ($\text{C}_{18}\text{H}_{11}\text{N}_2\text{Na}_2\text{O}_7$) $^+$.



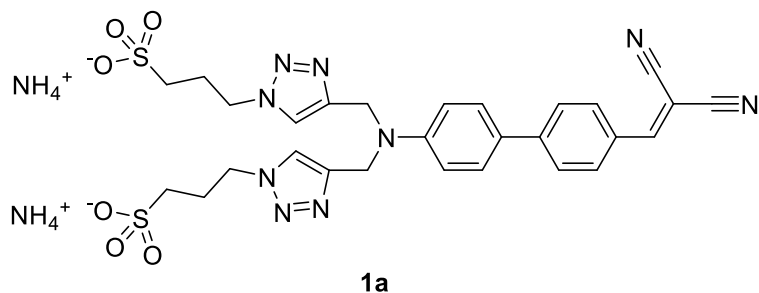
A neat mixture of methyl cyanoacetate (0.58 mL, 650 mg, 6.36 mmol, 1.00 equiv.) and propargylamine (0.42 mL, 363 mg, 6.53 mmol, 1.03 equiv.) was heated to 50 °C over night in a sealed reaction flask. The mixture changed color to deep red within a few minutes. The reaction mixture was allowed to cool to room temperature, the precipitate was collected by filtration and washed thoroughly with DCM. The product⁴ was dried in vacuum and obtained as a pink solid which turned light brown over time (**f**, 370 mg, 46%).

¹H-NMR (500 MHz, DMSO-d₆) δ = 8.69 (br s, 1H), 3.89 (dd, J = 5.4, 2.5, 2H), 3.66 (s, 2H), 3.17 (t, J = 2.5, 1H).

¹H-NMR (500 MHz, CDCl₃) δ = 6.27 (s, 1H), 4.11 (dd, J = 5.3, 2.6, 2H), 3.41 (s, 2H), 2.31 (t, J = 2.6, 1H).

¹³C-NMR (126 MHz, DMSO-d₆) δ = 162.04, 115.93, 80.29, 73.58, 28.45, 25.13.

HR-ESI-MS (m/z): meas. 145.0371 [$M+Na$]⁺, calc. 145.0371 (C₆H₆N₂NaO)⁺.

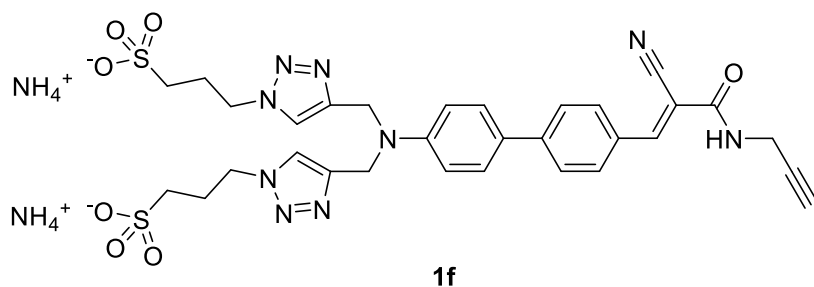


3 (35 mg, 54.9 μ mol, 1.0 equiv.) and malononitrile (7.0 mg, 10.5 μ mol, 1.9 equiv.) were dissolved in H₂O (1 mL) and a color change from yellow to red was observed within the first few minutes. The reaction mixture was stirred at room temperature for 3 h, ACN was added to precipitate the product as an orange solid. After centrifugation, the solids were dried in high vacuum to give the product as a pale orange solid (**1a**, 26 mg, 69%).

¹H-NMR (500 MHz, D₂O) δ = 7.67 (s, 2H), 7.48 (s, 1H), 7.37 (d, J = 8.2 Hz, 2H), 7.23 (d, J = 8.4 Hz, 2H), 7.14 (d, J = 8.2 Hz, 2H), 6.76 (d, J = 8.5 Hz, 2H), 4.58 (s, 4H), 4.29 (t, J = 7.0 Hz, 4H), 2.72 – 2.65 (m, 4H), 2.17 – 2.07 (m, 4H).

¹³C-NMR (126 MHz, D₂O) δ = 161.26, 149.28, 146.21, 145.75, 132.51, 129.24, 128.90, 127.01, 126.19, 124.90, 115.60, 114.62, 114.38, 78.72, 49.73, 48.69, 46.41, 26.22. (A drop of MeOD was added as a reference.)

HR-ESI-MS (m/z): meas. 324.5765 [$M-2(NH_4)$]²⁻, calc. 324.5768 (C₂₈H₂₇N₉O₆S₂)²⁻.



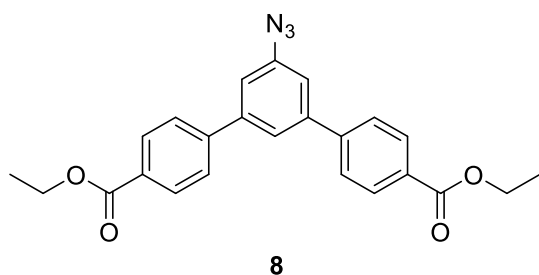
3 (150 mg, 235 μmol , 1.00 equiv.) and **f** (34.4 mg, 282 μmol , 1.20 equiv.) were dissolved in anhydrous DMF (10 mL), degassed for 20 min and heated to 80 °C for 24 h under inert atmosphere, after which time **3** could still be observed in LC-MS. The reaction mixture was cooled to room temperature, additional **f** (11.5 mg, 94 μmol , 0.40 equiv.) was added and heating was resumed for 18 h. The red solution was cooled to room temperature and TBME was added to precipitate the product. After centrifugation, the orange solids were dissolved in 100 mM aqueous NH_4OAc solution to displace dimethylammonium counterions partially present in the product. The solution was concentrated, the solids suspended in EtOH and sonicated to wash out excess salts. After drying on high vacuum, the pure *E* isomer of the product was obtained as an orange solid (**1f**, 63 mg, 36%).

$^1\text{H-NMR}$ (500 MHz, $\text{D}_2\text{O}/\text{CD}_3\text{CN}$ (9:1)) δ = 8.44 (s, 1H), 8.23 (d, J = 8.2 Hz, 2H), 8.14 (s, 2H), 8.02 (d, J = 8.2 Hz, 2H), 7.90 (d, J = 8.5 Hz, 2H), 7.27 (d, J = 8.5 Hz, 2H), 5.05 (s, 4H), 4.77 – 4.73 (m, 5H (overlap with D_2O)), 4.33 (d, J = 2.6 Hz, 2H), 3.09 – 3.04 (m, 4H), 2.93 (t, J = 2.5 Hz, 1H), 2.57 – 2.50 (m, 4H).

$^1\text{H-NMR}$ (500 MHz, DMSO-d_6) δ 8.89 (t, J = 5.5 Hz, 1H), 8.16 (s, 1H), 8.01 (s, 2H), 8.00 – 7.96 (m, 2H), 7.84 – 7.79 (m, 2H), 7.65 – 7.61 (m, 2H), 7.11 (br s, 2H), 7.01 (d, J = 8.9 Hz, 2H), 4.71 (s, 4H), 4.43 (t, J = 7.1 Hz, 4H), 4.00 (dd, J = 5.5, 2.5 Hz, 2H), 3.16 (t, J = 2.5 Hz, 1H), 2.40 (dd, J = 8.3, 6.5 Hz, 4H), 2.11 – 2.04 (m, 4H).

$^{13}\text{C-NMR}$ (126 MHz, $\text{D}_2\text{O}/\text{CD}_3\text{CN}$ (9:1)) δ = 163.59, 153.64, 148.89, 145.95, 145.65, 132.40, 130.19, 128.82, 128.30, 126.97, 124.75, 117.43, 114.75, 103.34, 80.27, 72.82, 49.73, 48.59, 46.84, 30.31, 26.25.

HR-ESI-MS (m/z): meas. 774.1473 [$\text{M}-2(\text{NH}_4)+3\text{Na}$] $^+$, calc. 774.1475 ($\text{C}_{31}\text{H}_{31}\text{N}_9\text{Na}_3\text{O}_7\text{S}_2$) $^+$.

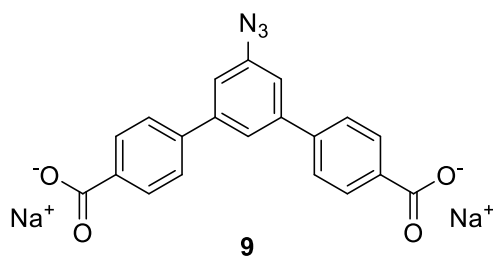


Aniline **7** (prepared according to literature⁵; 600 mg, 1.54 mmol, 1.0 equiv.) was dissolved in DMF (30 mL) and cooled to 0 °C. *tert*-Butyl nitrite (0.92 mL, 7.7 mmol, 5.0 equiv.) and trimethylsilylazide (1.00 mL, 7.7 mmol, 5.0 equiv.) were added, upon which the solution turned orange. The ice bath was removed and the reaction mixture was stirred at room temperature for 6 h, then poured onto water (~400 mL) to precipitate the product. The product was filtered off and washed with water to give a white-beige solid (**8**, 627 mg, 98%). The product contained a minor impurity visible in the $^1\text{H-NMR}$ spectrum at 4.8 ppm and was used as is for the next step. An analytically pure sample was obtained by flash chromatography (cyclohexane/EtOAc 9:1 to 8:2).

$^1\text{H-NMR}$ (500 MHz, CDCl_3) δ = 8.16 – 8.12 (m, 4H), 7.70 – 7.67 (m, 4H), 7.60 (t, J = 1.6, 1H), 7.27 (d, J = 1.6, 2H), 4.42 (q, J = 7.1, 4H), 1.43 (t, J = 7.1, 6H).

^{13}C -NMR (126 MHz, CDCl_3) δ = 166.44, 144.32, 142.78, 141.57, 130.38, 130.24, 127.30, 123.19, 117.53, 61.27, 14.51.

HR-ESI-MS (m/z): meas. 416.1604 $[\text{M}+\text{H}]^+$, calc. 416.1605 ($\text{C}_{24}\text{H}_{22}\text{N}_3\text{O}_4$) $^+$.

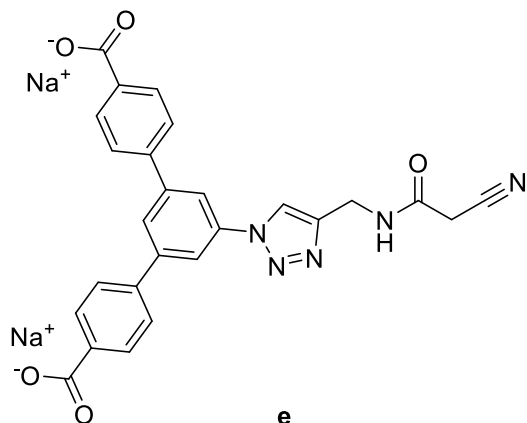


8 (300 mg, 0.72 mmol, 1.0 equiv.) was suspended in a solution of NaOH (289 mg, 7.22 mmol, 10.0 equiv.) in THF/MeOH/ H_2O (4:4:1, 13.5 mL) and heated to 50 °C for 1 h, during which time **8** dissolved. The reaction mixture was allowed to cool to room temperature, the formed precipitate was transferred to a centrifuge tube, and the flask rinsed with THF. After centrifugation, the beige solids were suspended in EtOH and subjected to centrifugation again to remove excess NaOH. The product was obtained as a slightly creamy-white solid after drying in high vacuum (**9**, 280 mg, 96%).

^1H -NMR (500 MHz, D_2O) δ = 7.91 (d, J = 8.0 Hz, 4H), 7.59 (d, J = 8.1 Hz, 4H), 7.49 (s, 1H), 7.13 (s, 2H).

^{13}C -NMR (126 MHz, D_2O) δ = 176.12, 142.73, 142.64, 141.76, 136.58, 130.40, 127.61, 123.12, 117.48. (A drop of MeOD was added as a reference)

HR-ESI-MS (m/z): meas. 358.0853 $[\text{M}-2\text{Na}+1\text{H}]^-$, calc. 358.0833 ($\text{C}_{20}\text{H}_{12}\text{N}_3\text{O}_4$) $^+$.



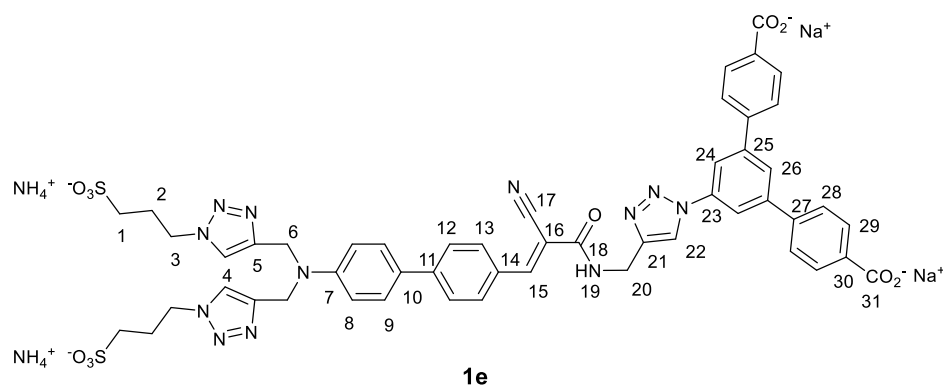
f (15 mg, 123 μmol , 1.24 equiv.) and **9** (40 mg, 99 μmol , 1.00 equiv.) were dissolved in H_2O /MeOH (1.5 mL, 2:1) and $\text{CuSO}_4 \cdot 5 \text{H}_2\text{O}$ (2.5 mg, 9.9 μmol , 0.10 equiv.) and sodium ascorbate (2.6 mg, 12.9 μmol , 0.13 equiv.) were added under argon. The reaction mixture was stirred for 1 h and the product was precipitated as a white solid by addition of ACN. After centrifugation and drying in vacuum, the product was obtained as a white solid (**e**, 34 mg, 65%).

^1H -NMR (500 MHz, D_2O) δ = 7.50 – 7.38 (m, 5H), 6.83 – 6.74 (m, 7H), 4.08 (s, 2H), 3.33 (s, 0H). Contains ACN as an impurity. Active methylene group visible with wrong integral due to H/D exchange in D_2O .

^1H -NMR (500 MHz, D_2O) δ = 7.52 – 7.34 (m, 5H), 6.88 – 6.71 (m, 7H), 4.07 (s, 2H). After complete removal of solvent residues, the peaks are broadened and the active methylene group is not visible due to H/D exchange.

^{13}C -NMR (126 MHz, D_2O) δ = 174.40, 164.54, 143.83, 140.10, 139.50, 135.76, 135.22, 129.08, 125.50, 123.86, 120.66, 115.90, 115.55, 34.51, 25.28 (low intensity likely due to splitting into quintet caused by H/D exchange).

HR-ESI-MS (m/z): meas. 504.1270 $[\text{M}+2\text{H}-\text{Na}]^+$, calc. 504.1278 ($\text{C}_{26}\text{H}_{19}\text{N}_5\text{NaO}_5$) $^+$.



1f (1.00 eq, 20.6 mg, 28 μmol) was dissolved in $\text{H}_2\text{O}/\text{MeOH}$ (2:1, 3 mL), **9** (1.03 eq, 11.6 mg, 29 μmol) was added and to the suspension was added $\text{CuSO}_4 \cdot 5 \text{H}_2\text{O}$ (0.20 eq, 1.4 mg, 6 μmol) and sodium ascorbate (0.22 eq, 1.2 mg, 7 μmol) under argon atmosphere. The mixture was stirred at room temperature for 3 h, during which time the suspension turned into a clear orange solution. ACN (~30 mL) was added, and the precipitate was collected by centrifugation. The solids were dried in high vacuum to obtain the pure product (**1e**, 23.9 mg, 81 %) as an orange-red solid.

^1H -NMR spectrum of a concentrated sample used for 2D-NMR and ^{13}C -NMR measurements, which was used for the assignment of the signals to the structure:

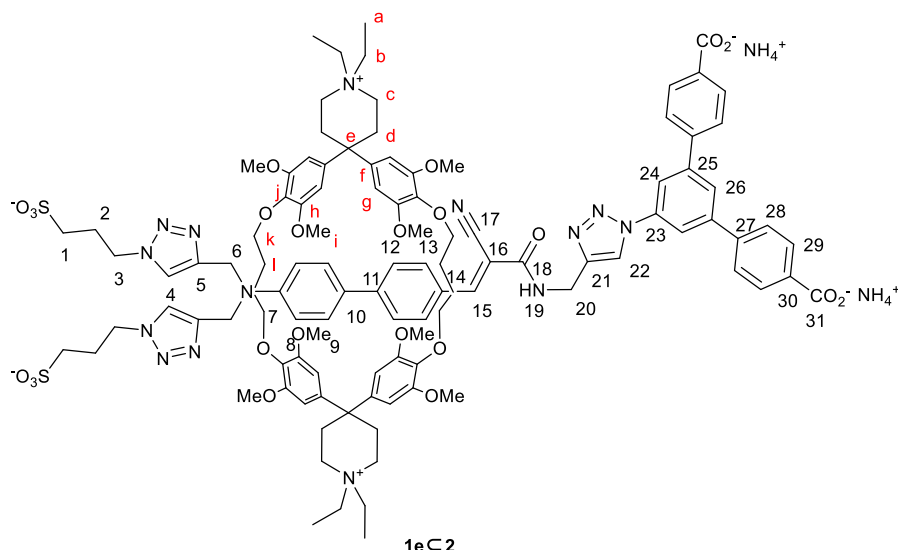
^1H -NMR (500 MHz, $\text{DMSO}-d_6 + \text{AcOH}$) δ = 9.10 (s, 1H, H19), 9.01 (s, 1H, H22), 8.23 (s, H15), 8.22 (s, H24), 8.10 (s, H28, H29, H26), 8.03 (s, H4), 7.99 (d, J = 8.3, H13), 7.82 (d, J = 8.1, 2H, H12), 7.64 (d, J = 8.2, 2H, H9), 7.02 (d, J = 8.3, 2H, H8), 4.71 (s, 4H, H6), 4.62 (s, 2H), 4.44 (t, J = 7.1, 4H, H3), 2.44 – 2.41 (m, H1), 2.12 – 2.08 (m, H2). Integrals for peaks from 8.23 to 7.99 could not be determined separately in this spectrum, due to broadening of the peaks; the total integral is 16. The aliphatic H1 and H2 overlap with AcOH.

^1H -NMR spectrum of a sample with lower concentration, used for comparison to [2]rotaxane **1ec2**:

^1H -NMR (400 MHz, $\text{DMSO}-d_6 + \text{AcOH}$) δ = 9.10 (t, J = 5.7, 1H), 9.02 (s, 1H), 8.28 (s, 2H), 8.21 (s, 1H), 8.14 (s, 1H), 8.11 – 8.04 (m, 8H), 8.03 (s, 2H), 7.98 (d, J = 8.4, 2H), 7.82 (d, J = 8.3, 2H), 7.63 (d, J = 8.6, 2H), 7.00 (d, J = 8.5, 2H), 4.71 (s, 4H), 4.62 (d, J = 5.1, 2H), 4.42 (t, J = 7.1, 4H), 2.40 – 2.37 (m, 4H), 2.07 – 2.04 (m).

^{13}C -NMR (126 MHz, $\text{DMSO}-d_6 + \text{AcOH}$) δ = 161.6 (C18), 150.4 (C15), 148.3 (C7), 145.9 (C21), 144.3 (C5, extracted from HMBC), 144.1 (C11), 142.0 (C23), 141.6 (C27), 138.0 (C25), 131.0 (C13), 129.2 (C14), 128.4 (C29 or C28), 127.6 (C9), 126.1 (C10), 125.8 (C12), 125.3 (C28 or C29), 123.2 (C4), 121.8 (C22), 118.1 (traces of $\text{CH}_3^{13}\text{CN}$), 117.7 (C24), 116.8 (C17), 113.1 (C8), 104.1 (C16), 48.6 (C3), 48.1 (C1), 45.6 (C6), 35.4 (C20), 26.5 (C2), 1.2 (traces of $^{13}\text{CH}_3\text{CN}$). H28 and H29 did not show signals in HMBC, making the assignment of C30 and C31 impossible, as they are also not visible in the ^{13}C -NMR spectrum, likely due to different protonation states of the carboxylic acid.

HR-ESI-MS (m/z): meas. 532.1355 $[\text{M}-2\text{Na}-2\text{NH}_4+2\text{H}]^{2-}$, calc. 532.1352 ($\text{C}_{51}\text{H}_{44}\text{N}_{12}\text{O}_{11}\text{S}_2$) $^{2-}$.



Dye **1f** (20 mg, 27.0 μmol , 1.0 equiv.) and host **2** (34.7 mg, 32.4 μmol , 1.2 equiv.) were dissolved in H_2O (16.5 mL) and degassed for 20 min. To this solution was added stopper **9** (12 mg, 29.7 μmol , 1.1 equiv.), $\text{CuSO}_4 \cdot 5 \text{H}_2\text{O}$ (6.7 mg, 27.0 μmol , 1.0 equiv.), and sodium ascorbate (5.5 mg, 27.0 μmol , 1.0 equiv.) as solids. The solution was stirred at room temperature and LC-MS indicated complete consumption of **1f** after 1.5 h. The reaction mixture was concentrated under reduced pressure and the solids purified by consecutive runs of reverse-phase HPLC on C-18 functionalized Silica stationary phase ($\text{H}_2\text{O}/\text{ACN}$, 67/33, containing 0.5% HCO_2H). The orange residue was dissolved in H_2O (~15 mL) and filled into a MWCO 1000 dialysis tube to dialyze against ~3 L Milli-Q H_2O over night. After concentration under reduced pressure, the product was further purified by Sephadex LH-20 in DMF/ H_2O containing 100 mM NH_4OAc as buffer. For mild removal of DMF, toluene was added and the solvents were evaporated under reduced pressure. Dialysis was repeated as above and the pure product was obtained as an orange film after concentration and drying on high vacuum (**1eC2**, 0.5 mg, 0.9 %).

^1H -NMR (600 MHz, $\text{CD}_3\text{CN}/\text{D}_2\text{O}$ 1:1) δ = 8.53 (s, 1H, H22), 8.33 (s, 0H, integral too low due to H/D exchange, H19), 8.11 (s, 1H, H26), 8.09 (s, 2H, H24), 7.97 (d, J = 8.2, 4H, H29), 7.81 (d, J = 8.2, 4H, H28), 7.77 (s, 2H, H4), 7.65 (s, 1H, H15), 6.70 (s, 8H, H-g), 6.64 (d, J = 8.3, 2H, H13), 6.56 (d, J = 8.6, 2H, H8), 6.00 (d, J = 8.5, 2H, H9), 5.54 (d, J = 8.3, 2H, H12), 4.68 (s, 6H, H6, H20), 4.47 (t, J = 7.1, 4H, H3), 3.66 – 3.41 (m, 26H, expected: 24H, H-i), 3.31 – 3.13 (m, 16H, H-b, H-c), 3.05 – 2.95 (m, 10H, expected: 8H, H-k), 2.76 – 2.73 (m, 5H, expected: 4H, H1), 2.26 – 2.21 (m, 4H, H2), 1.24 – 1.11 (m, 30H, expected: 28H, H-a, H-d, H-l).

^{13}C NMR (151 MHz, $\text{CD}_3\text{CN}/\text{D}_2\text{O}$ 1:1) δ = 174.1 (C31**), 163.0 (C18**), 154.0 (C-h), 152.8 (C15*), 148.9 (C7**), 146.4 (C21**), 146.2 (C5), 144.3 (C11**), 143.8 (C30), 141.9 (C27**), 138.8 (C23**), 138.0 (C25**), 135.7 (C-j), 131.4 (C13*), 130.9 (C29), 128.9 (C14**), 128.0 (C9*), 127.8 (C28), 127.1 (C26*), 126.7 (C10**), 125.4 (C12*), 124.4 (C4), 123.2 (C22*), 119.1 (C24*), 117.8 (C17**), 113.7 (C8*), 104.1 (C-g*), 102.6 (C16**), 73.1 (C-k), 69.2 (C-b**), 56.6 (C-i), 56.3 (C-c*), 49.8 (C3), 48.7 (C1), 46.9 (C6*), 44.1 (C-e), 36.2 (C20*), 29.9 (C-d), 26.6 (C2), 26.0 (C-l), 7.4 (C-a). * Extracted from HMQC. ** Extracted from HMBC.

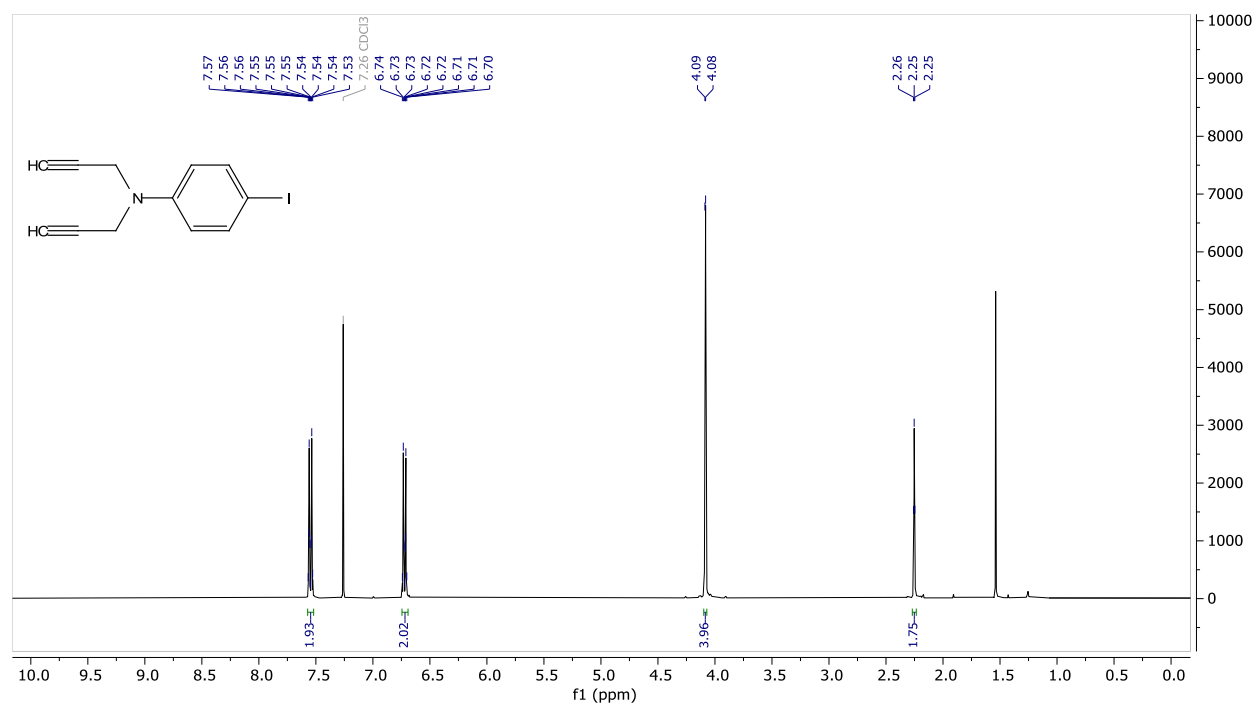
HR-ESI-MS (m/z): meas. 1033.4423 $[\text{M}+2\text{H}]^{2+}$, calc. 1033.4432 ($\text{C}_{109}\text{H}_{130}\text{N}_{14}\text{O}_{23}\text{S}_2$) $^{2+}$; 1044.4337 $[\text{M}+\text{H}+\text{Na}]^{2+}$, calc. 1044.4342 ($\text{C}_{109}\text{H}_{129}\text{N}_{14}\text{NaO}_{23}\text{S}_2$) $^{2+}$; 1055.4252 $[\text{M}+\text{Na}_2]^{2+}$, calc. 1055.4251 ($\text{C}_{109}\text{H}_{128}\text{N}_{14}\text{Na}_2\text{O}_{23}\text{S}_2$) $^{2+}$; 1066.4152 $[\text{M}+\text{H}+\text{Na}_3]^{2+}$, calc. 1066.4161 ($\text{C}_{109}\text{H}_{127}\text{N}_{14}\text{Na}_3\text{O}_{23}\text{S}_2$) $^{2+}$.

References

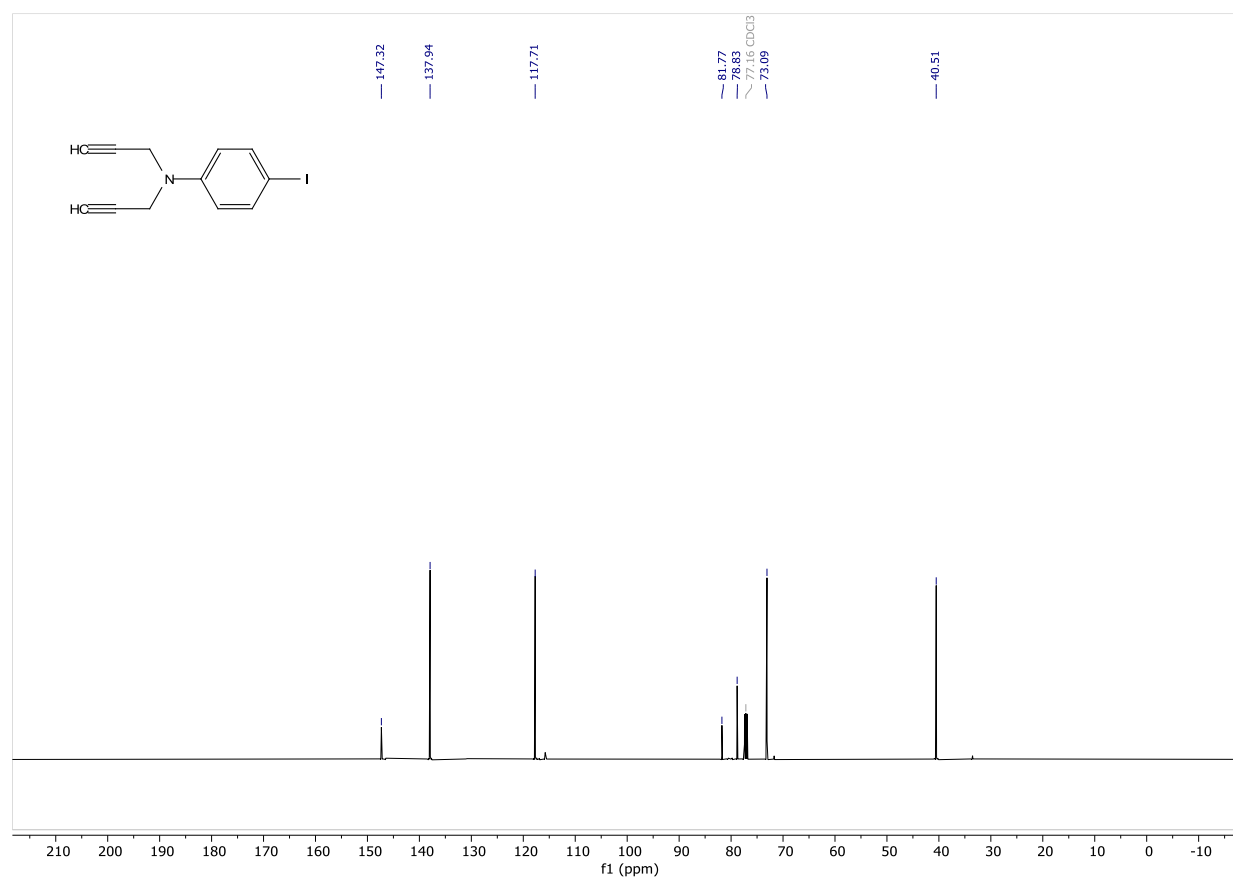
- 1 P. Thordarson, *Chem Soc Rev*, 2011, **40**, 1305–1323.
- 2 A. M. Brouwer, *Pure Appl. Chem.*, 2011, **83**, 2213–2228.
- 3 A. Azhdari Tehrani, L. Esrafil, S. Abedi, A. Morsali, L. Carlucci, D. M. Proserpio, J. Wang, P. C. Junk and T. Liu, *Inorg. Chem.*, 2017, **56**, 1446–1454.
- 4 D. Dziuba, R. Pohl and M. Hocek, *Chem. Commun.*, 2015, **51**, 4880–4882.
- 5 P. Martinez-Bulit, B. H. Wilson and S. J. Loeb, *Org. Biomol. Chem.*, 2020, **18**, 4395–4400.

NMR Spectra

¹H-NMR spectrum of **5**



¹³C-NMR spectrum of **5**



Chemical structure of compound 10 is shown as an inset. The structure consists of a central benzene ring substituted with an iodine atom (I) and two 1,2,4-triazole rings. Each triazole ring is further substituted with a propylsulfonate group (CH₂CH₂CH₂SO₃⁻ Na⁺).

¹H NMR spectrum (D₂O) of compound 10. The x-axis represents the chemical shift in ppm (f1), ranging from -0.5 to 10.0. The y-axis represents intensity, ranging from -1000 to 20000. The spectrum shows several peaks corresponding to the protons in the molecule.

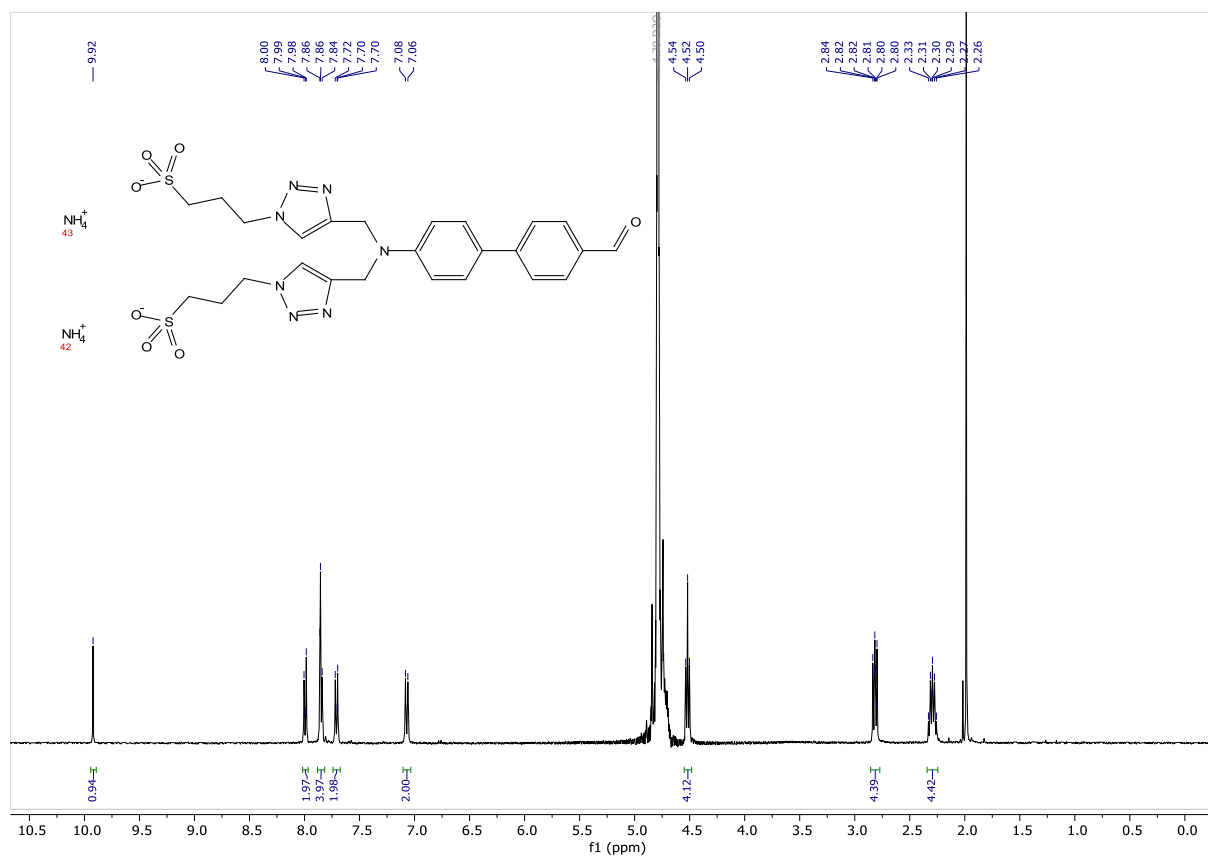
Peak assignments and integrations are provided:

- 7.74 (1.90)
- 7.34 (2.02)
- 7.32 (2.02)
- 6.62 (2.02)
- 6.60 (2.02)
- 4.79 (4.10)
- 4.60 (4.31)
- 4.45 (4.18)
- 4.43 (4.37)
- 4.41 (4.18)
- 2.84 (2.83, 2.82, 2.80, 2.30, 2.28, 2.26, 2.24, 2.23) (4.18)
- 2.30 (4.37)

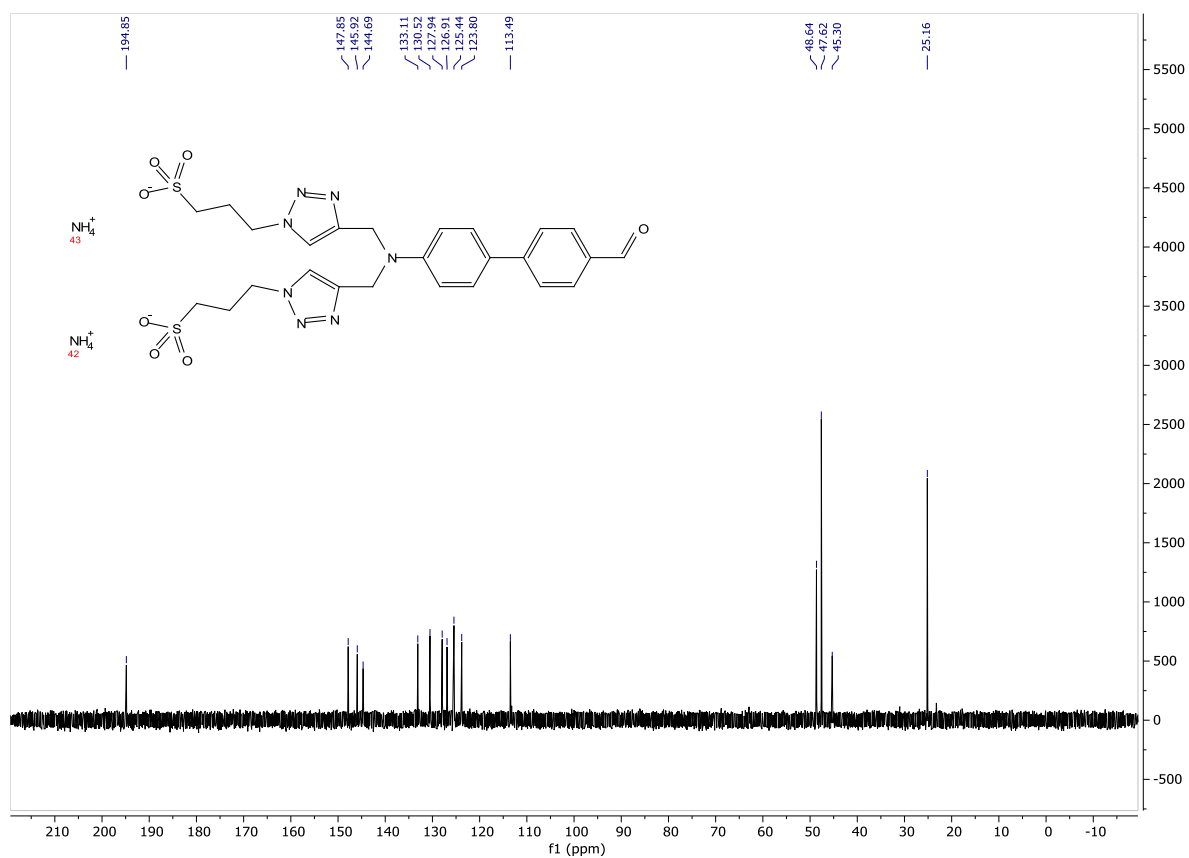
Chemical structure of the sodium salt of compound 10 is shown. The structure consists of a central benzene ring substituted with an iodine atom and two 4-(4-sulfamoylphenyl)-1H-1,2,4-triazol-1-ylmethyl groups. The sodium salt is indicated by Na⁺ ions.

¹³C NMR spectrum (f1 (ppm)) showing peaks at the following chemical shifts (ppm): 147.17, 144.78, 137.84, 124.02, 116.49, 79.18, 48.77, 47.69, 45.91, and 25.22.

¹H-NMR spectrum of **3**



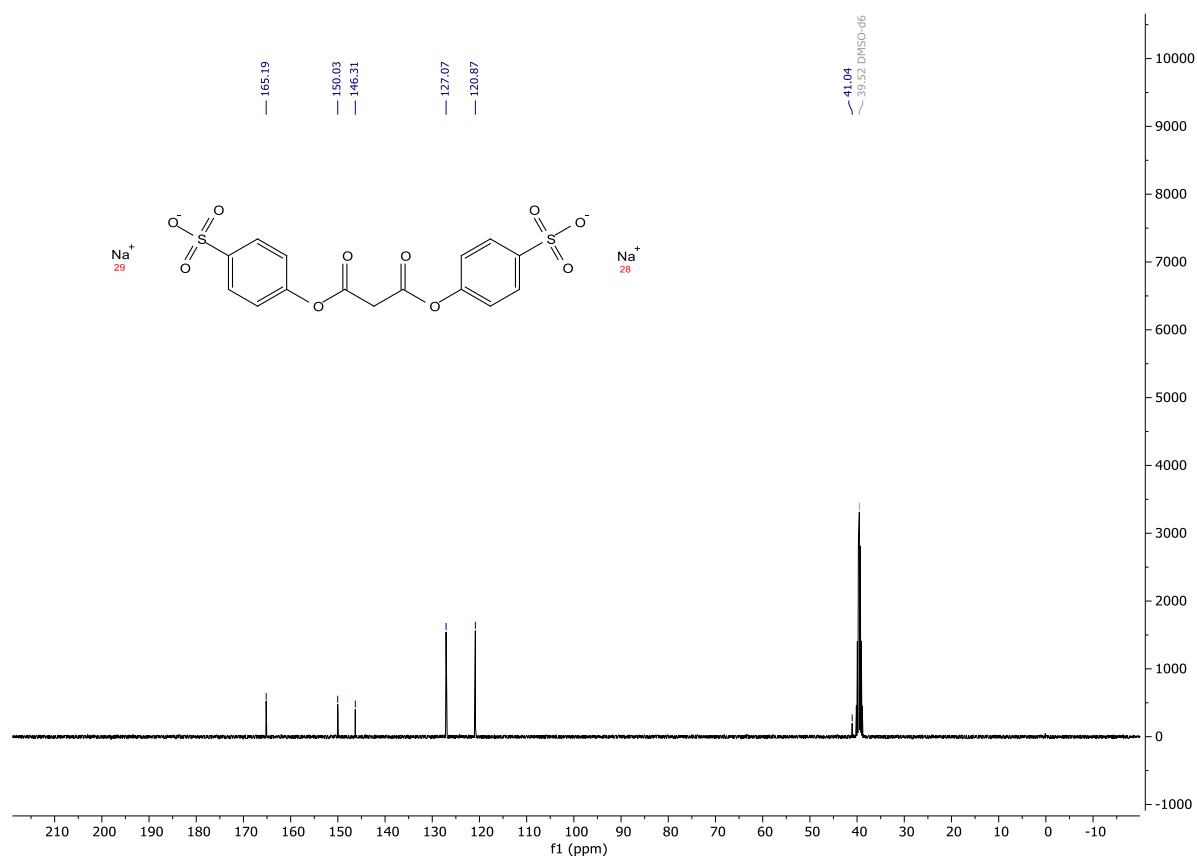
¹³C-NMR spectrum of **3**



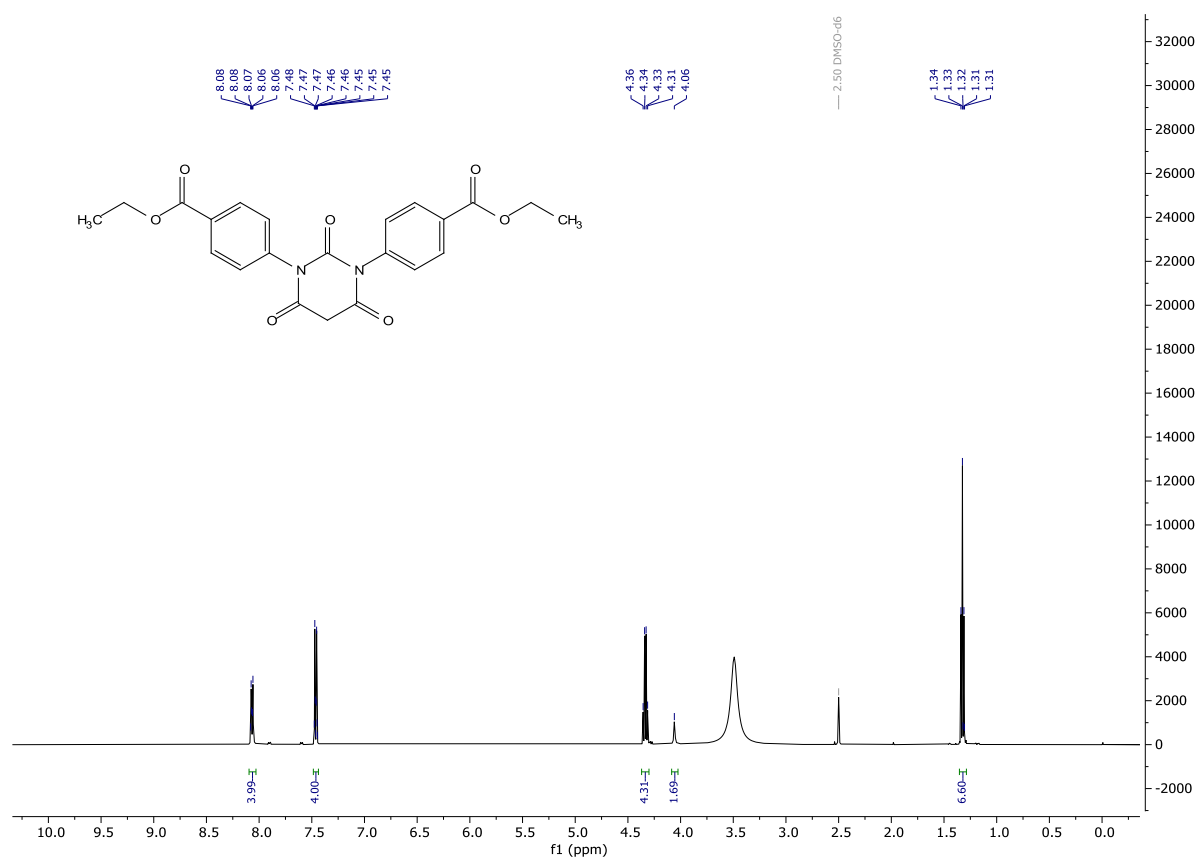
¹H-NMR spectrum of **b**



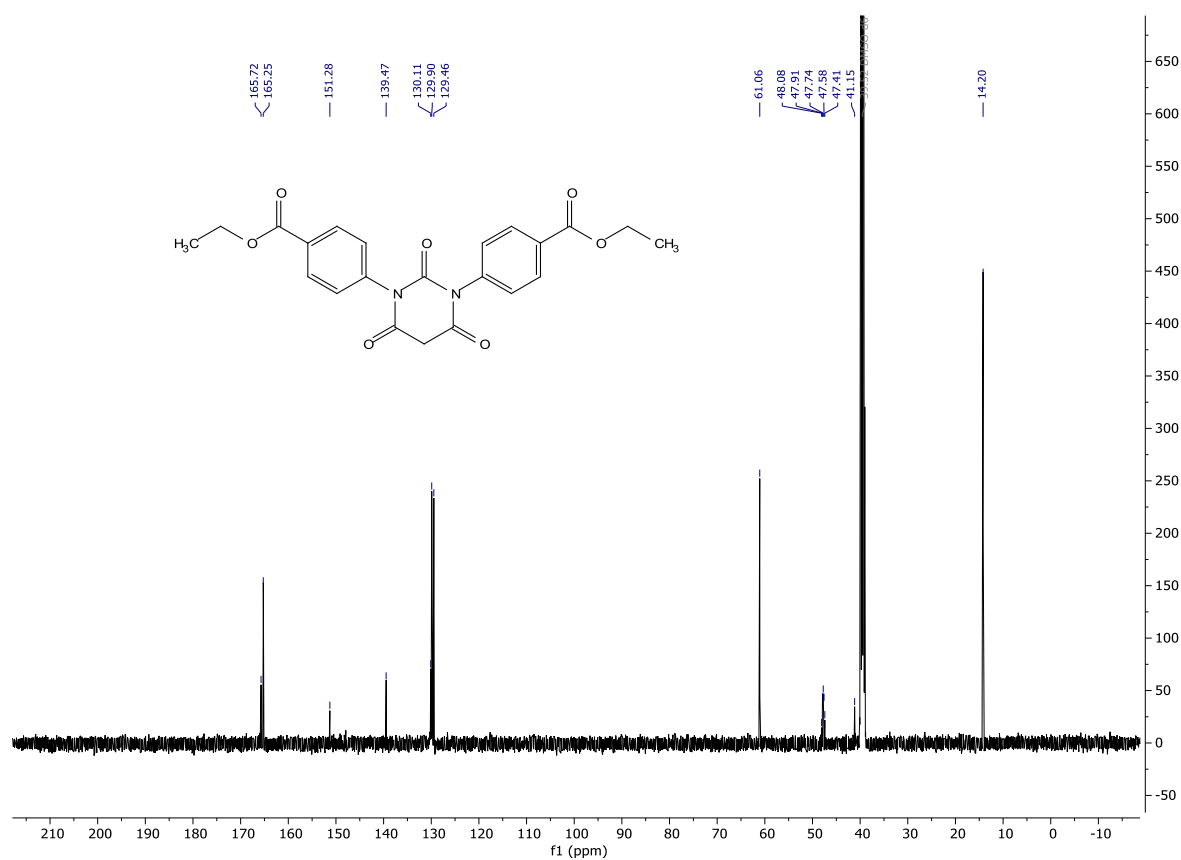
¹³C-NMR spectrum of **b**



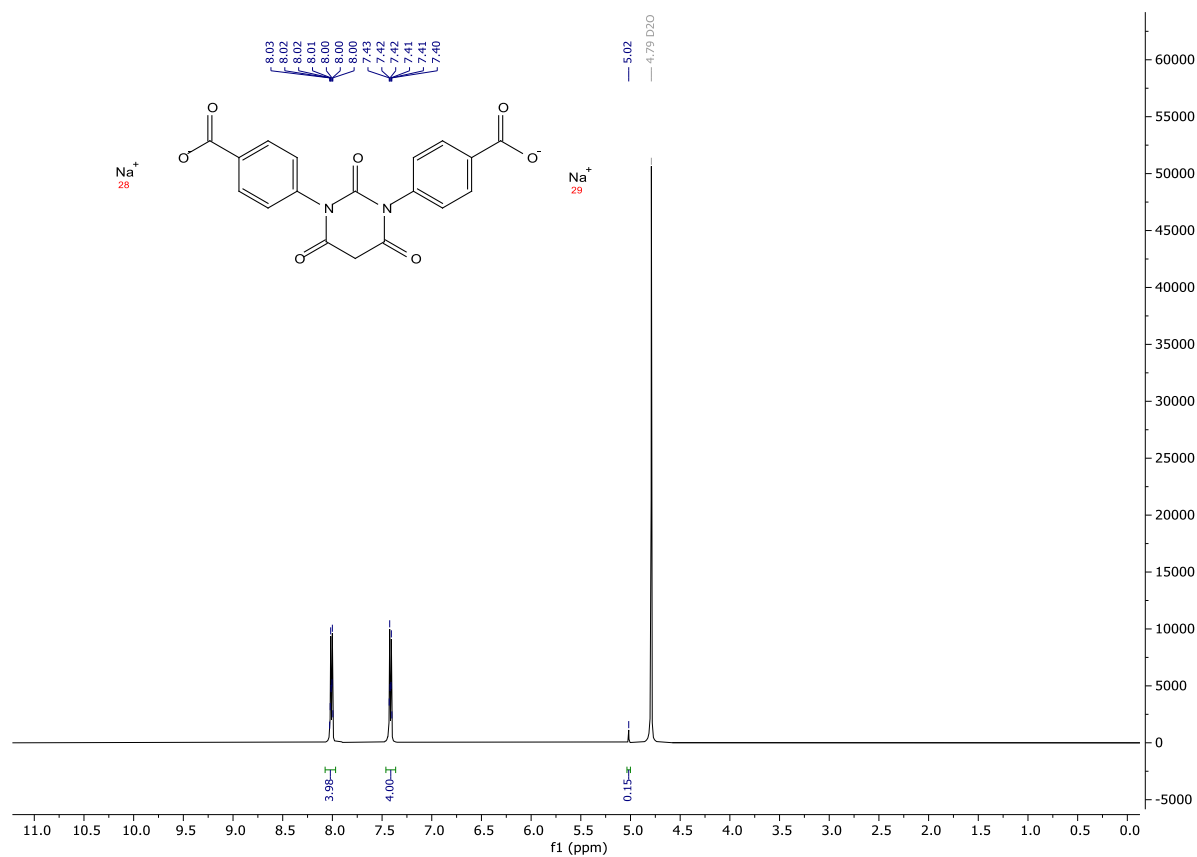
¹H-NMR spectrum of **S3**



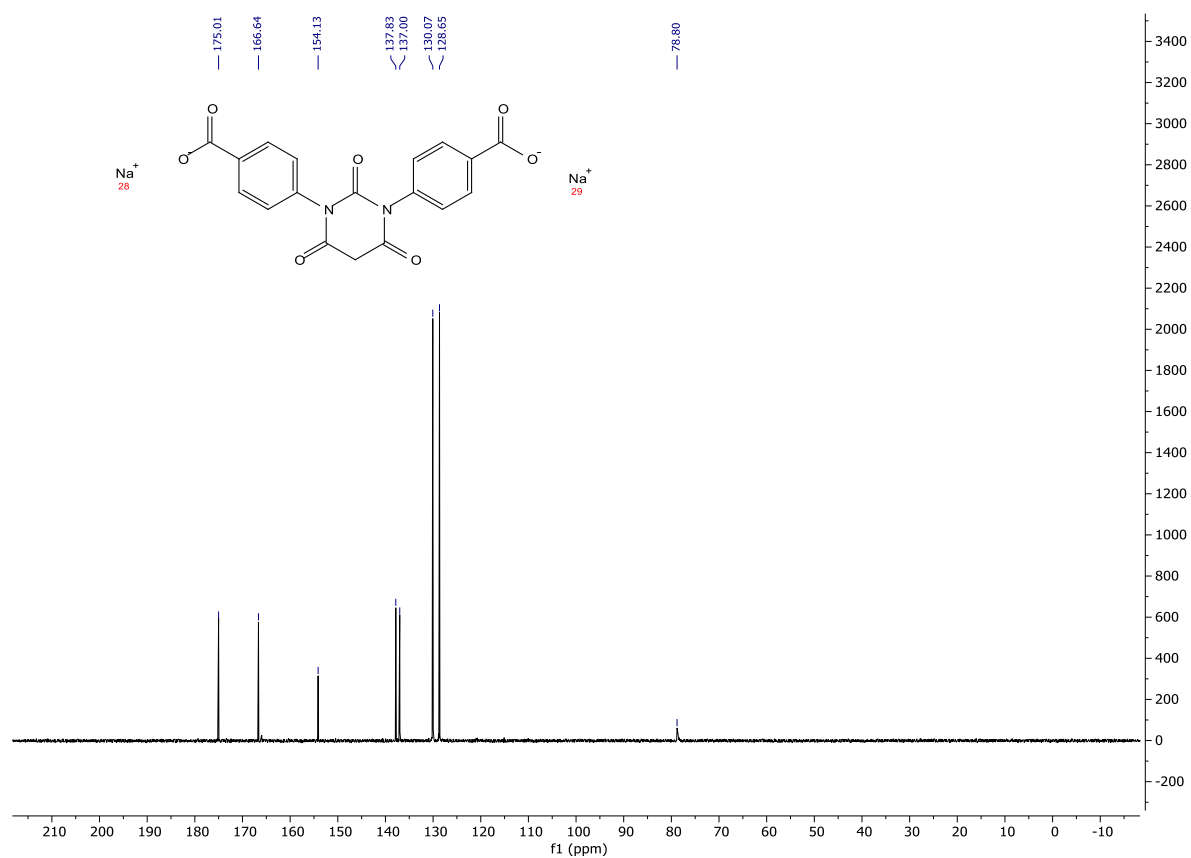
¹³C-NMR spectrum of **S3**



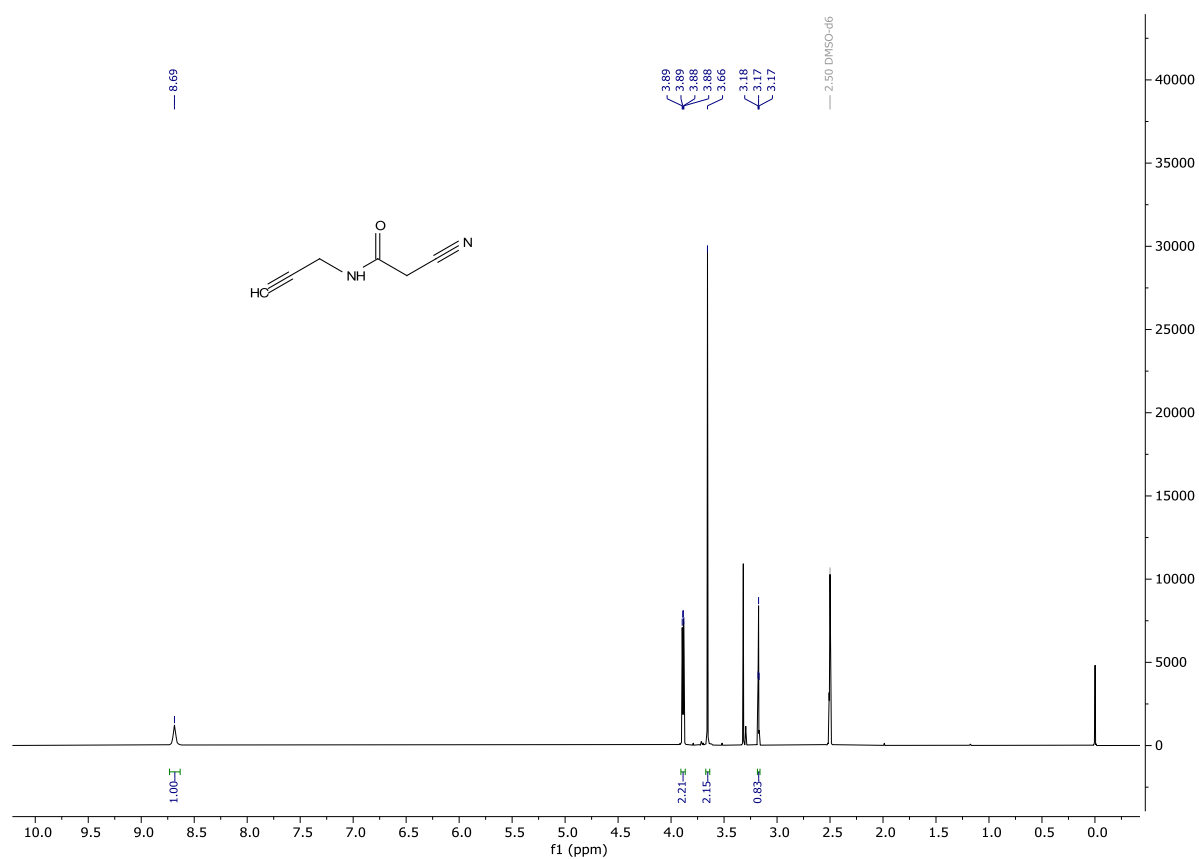
¹H-NMR spectrum of **c**



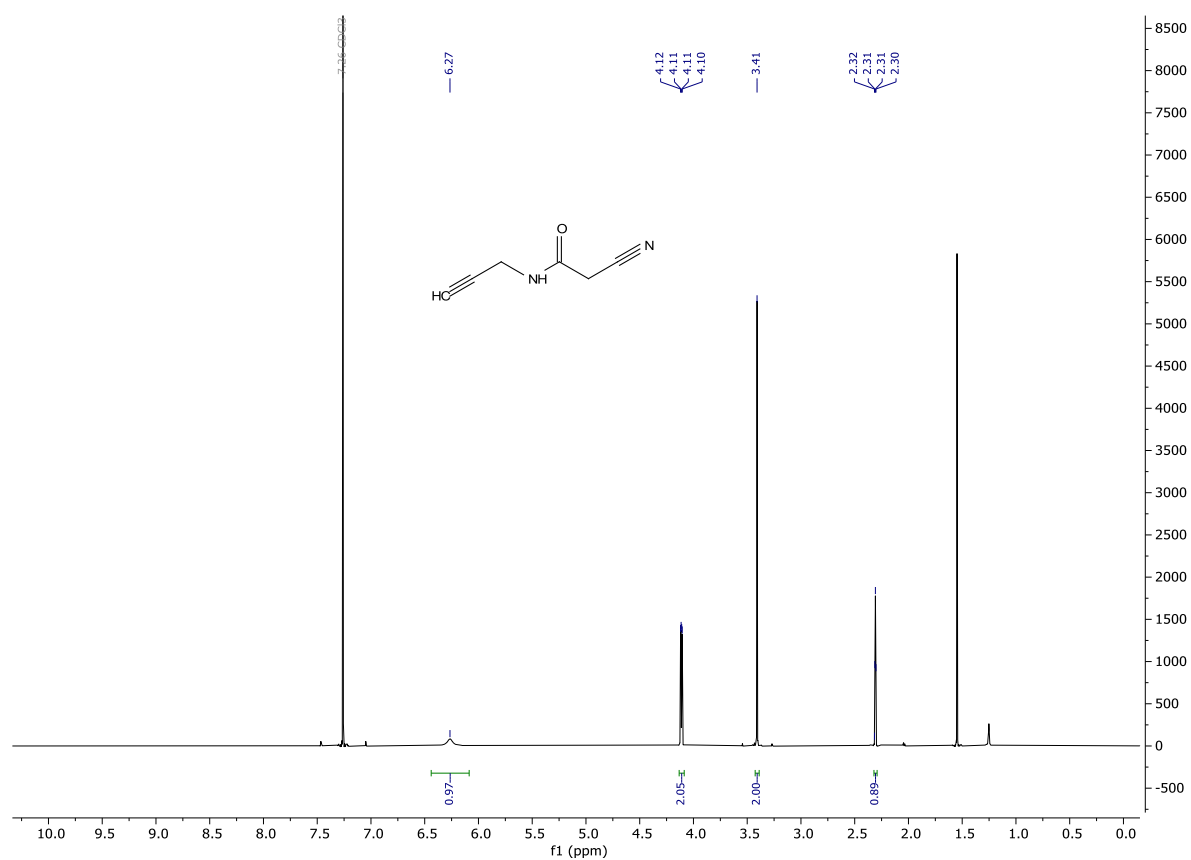
¹³C-NMR spectrum of **c**



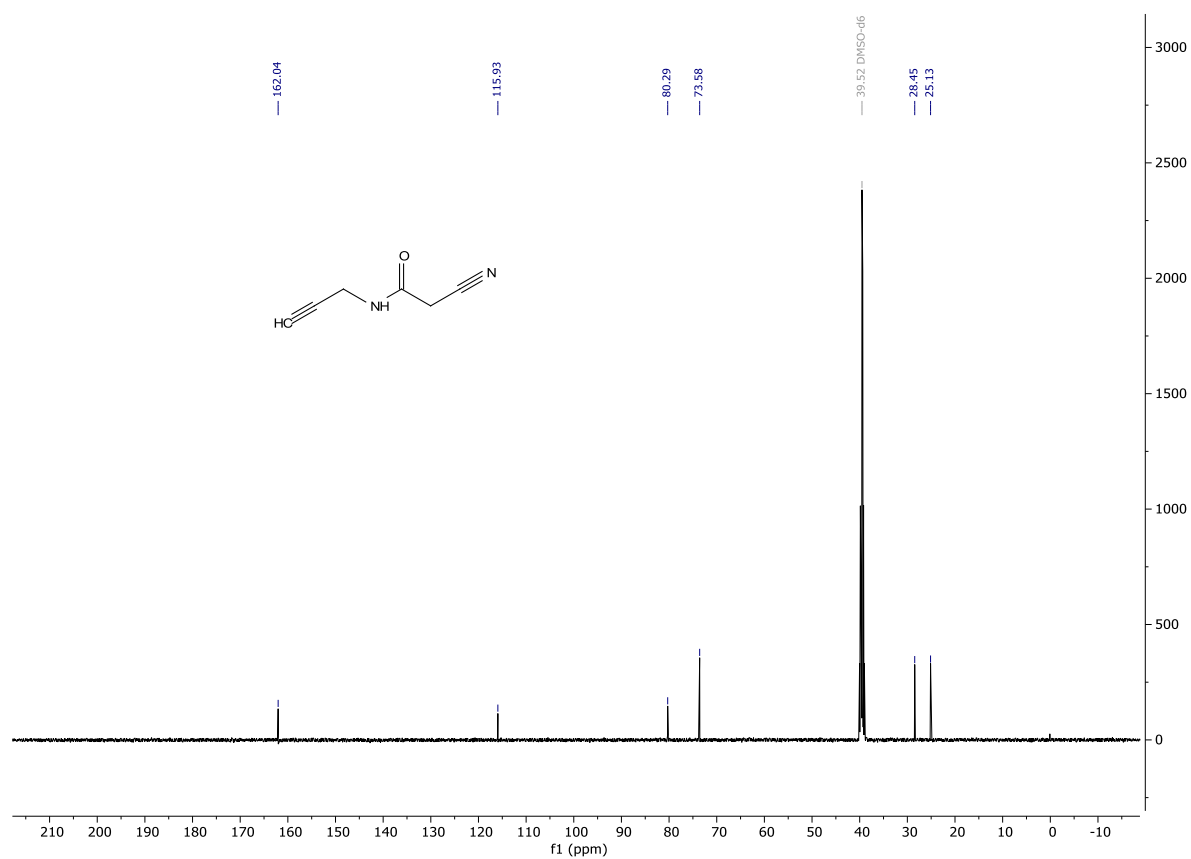
¹H-NMR spectrum of **f** in DMSO-d₆



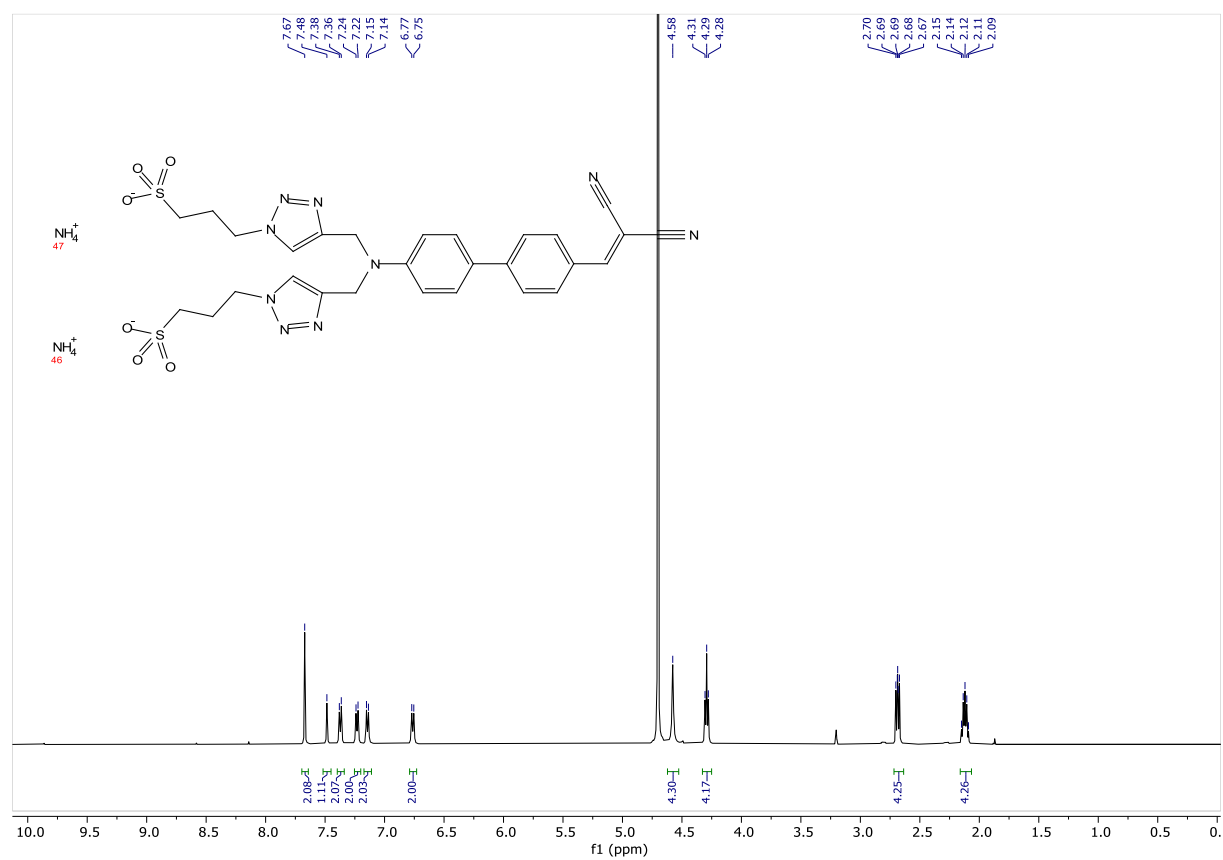
¹H-NMR spectrum of **f** in CDCl₃



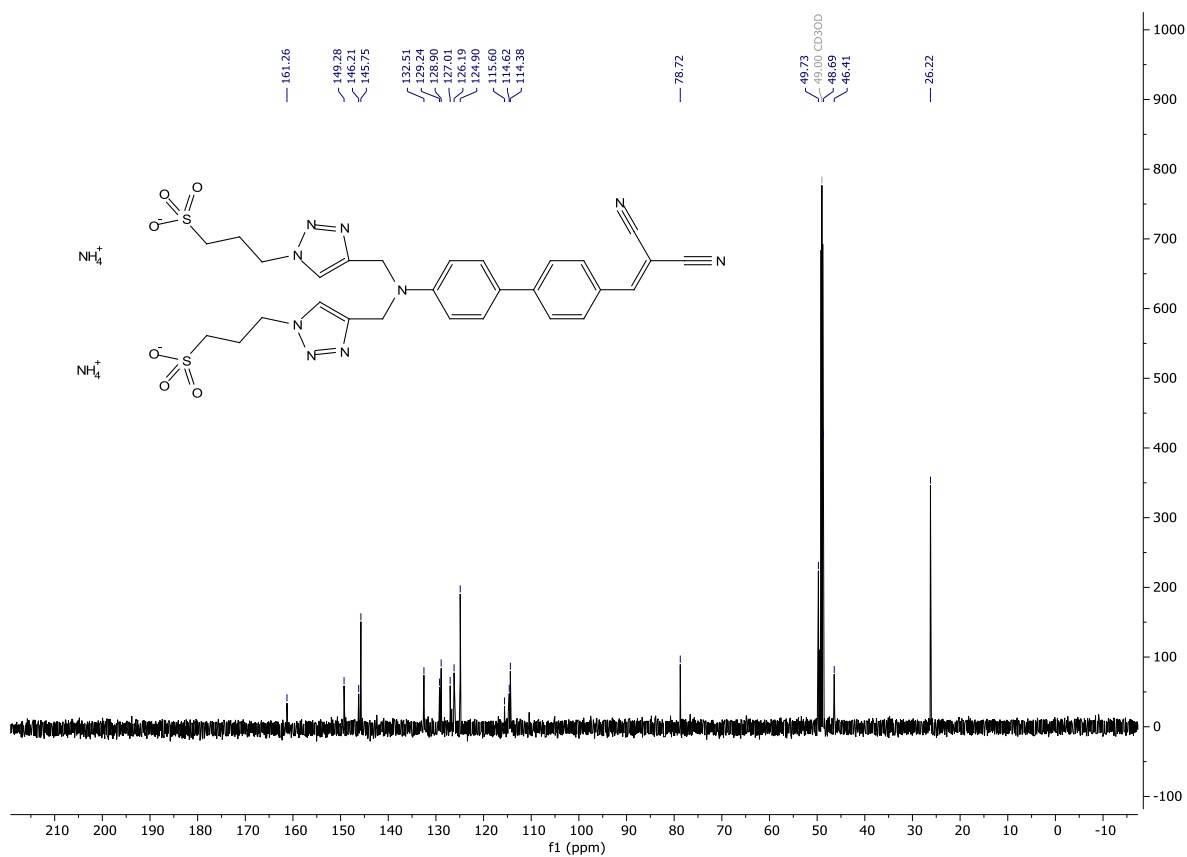
^{13}C -NMR spectrum of **f** in DMSO- d_6



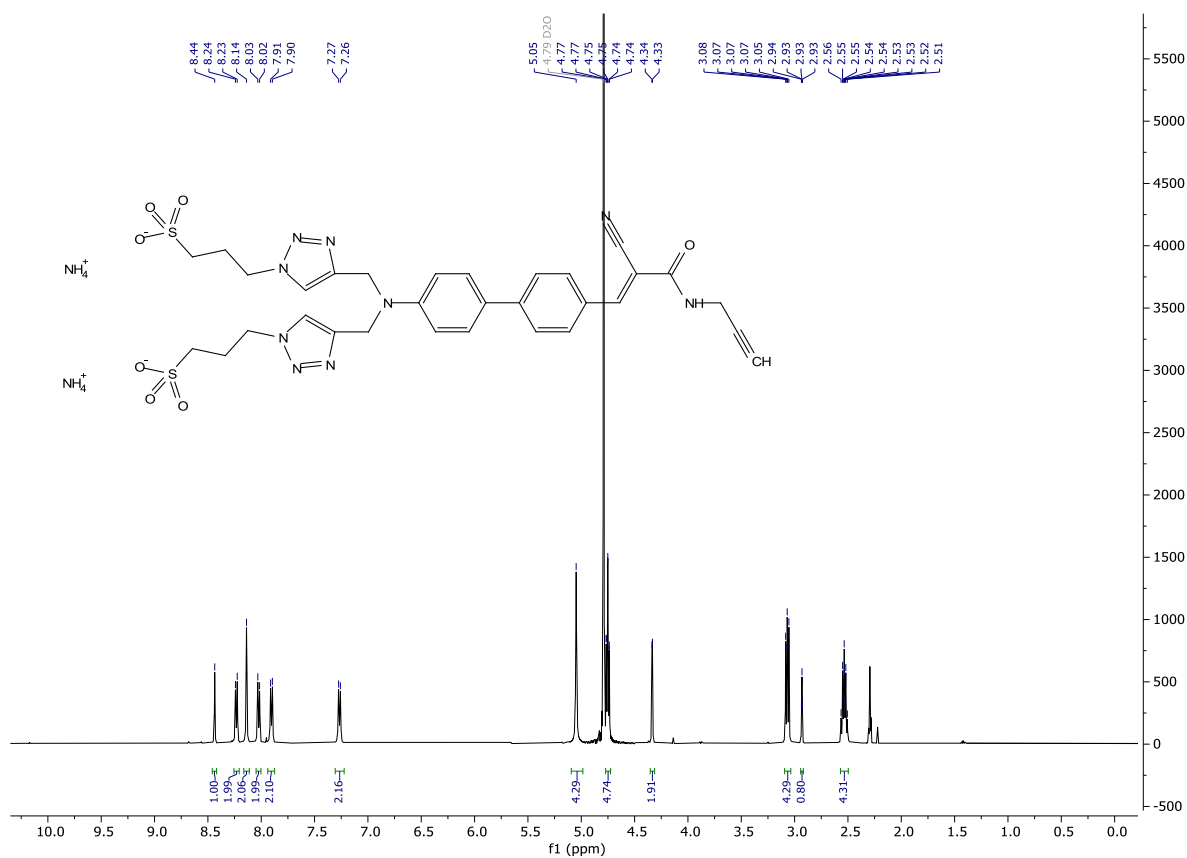
^1H -NMR spectrum of **1a**



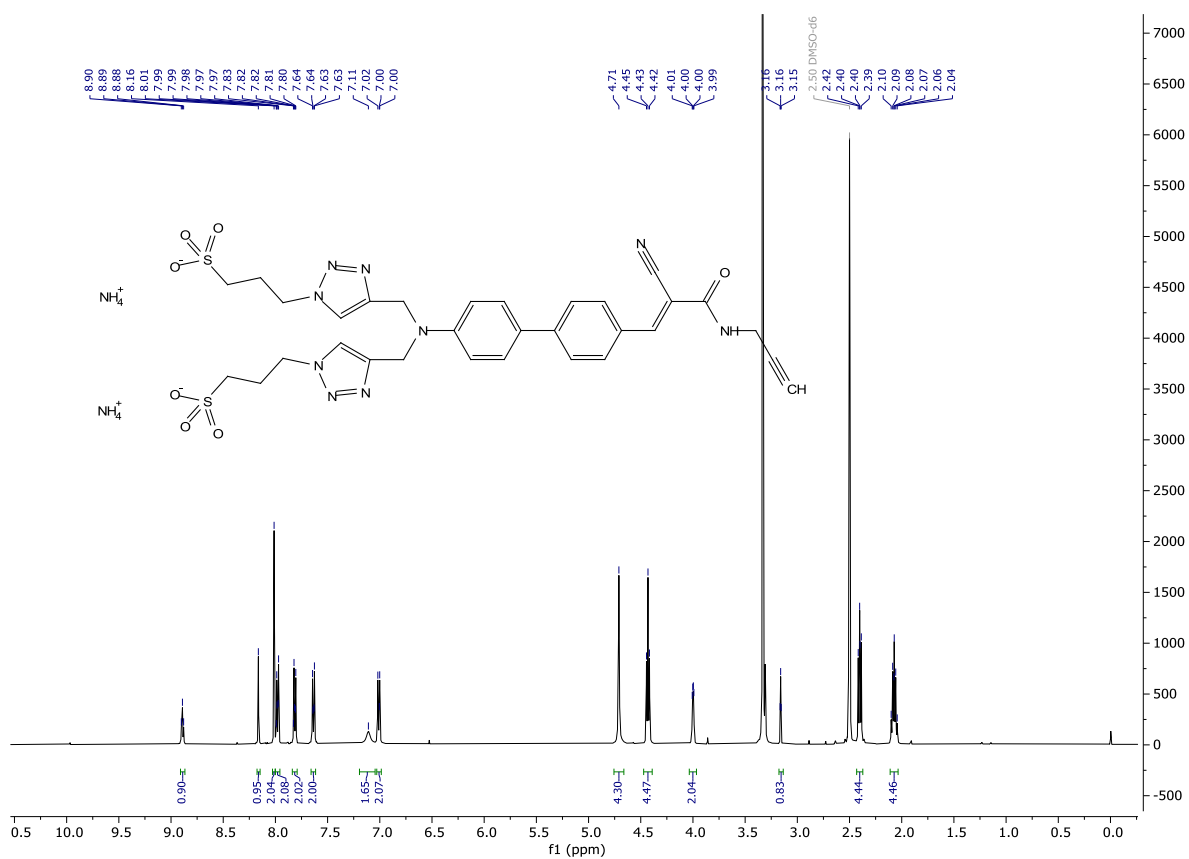
¹³C-NMR spectrum of **1a**



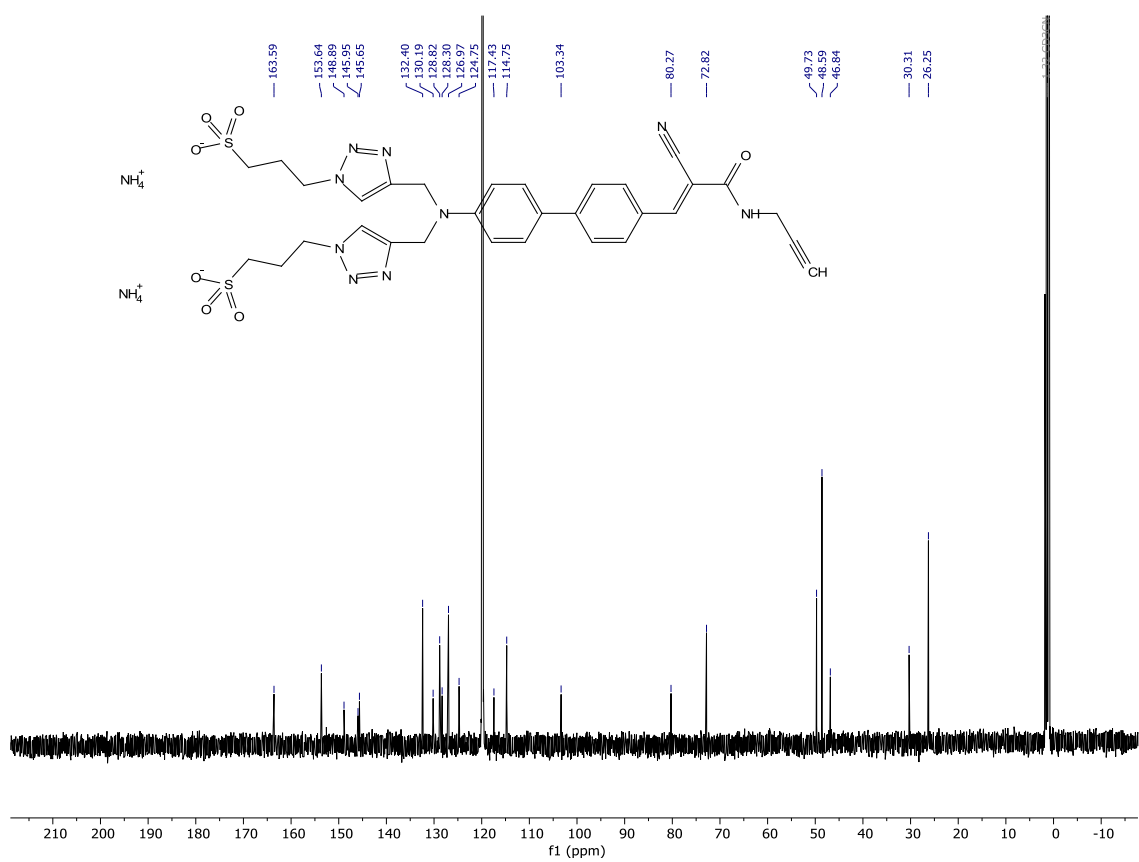
¹H-NMR spectrum of **1f** in D₂O/CD₃CN 9:1



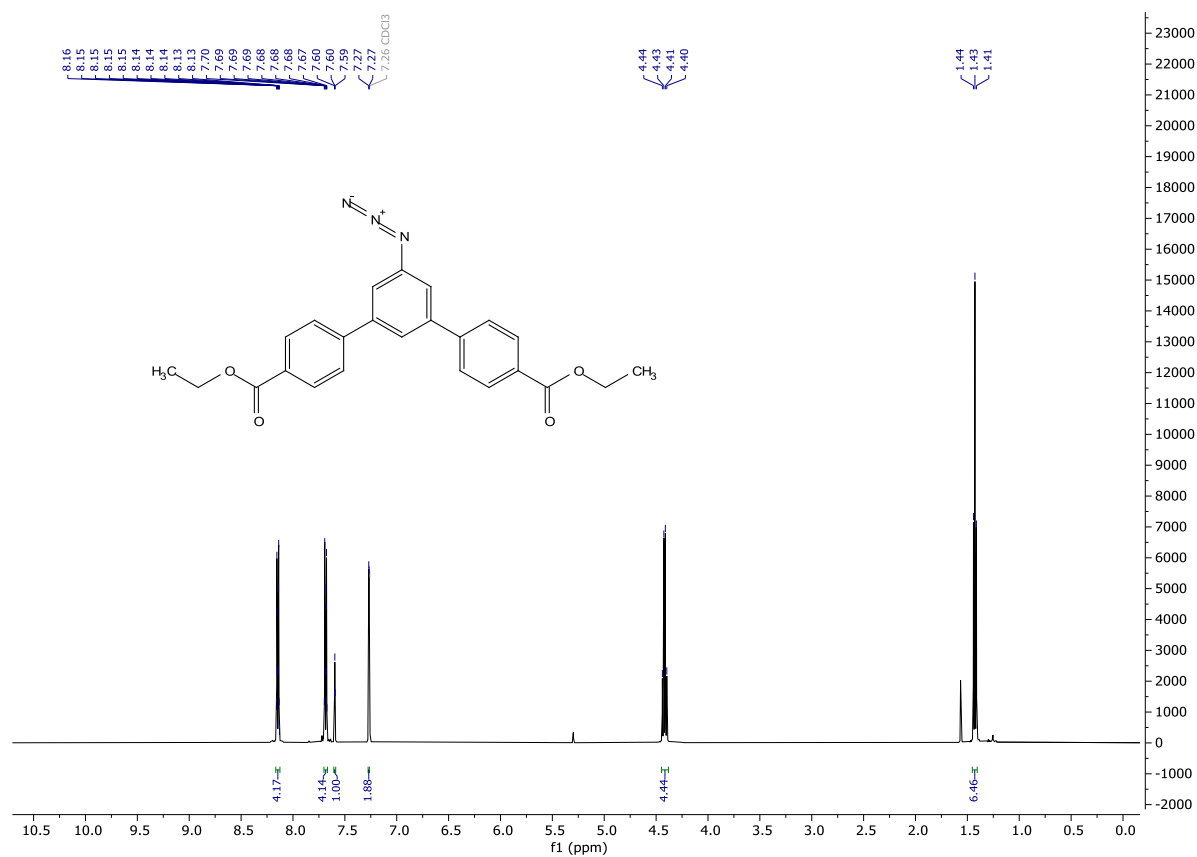
^1H -NMR spectrum of **1f** in DMSO- d_6



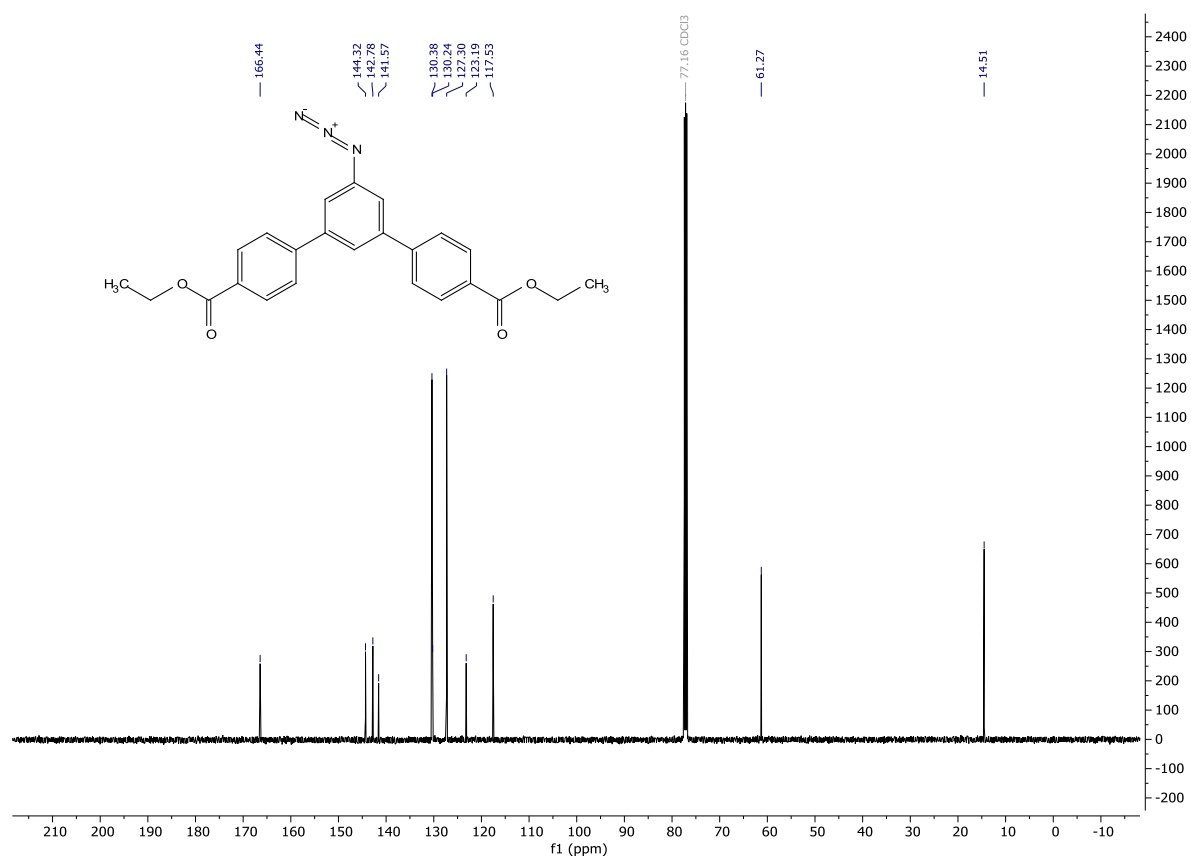
^{13}C -NMR spectrum of **1f** in $\text{D}_2\text{O}/\text{CD}_3\text{CN}$ 9:1



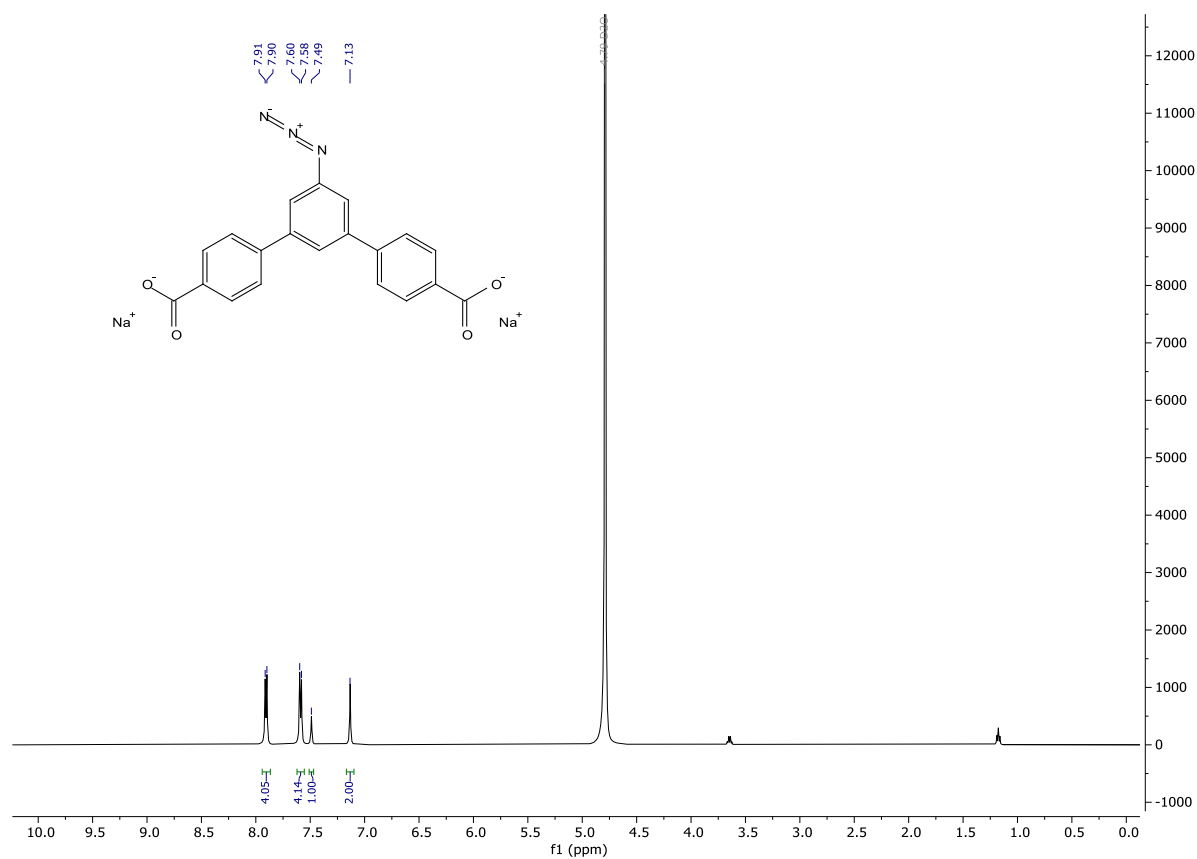
¹H-NMR spectrum of **8**



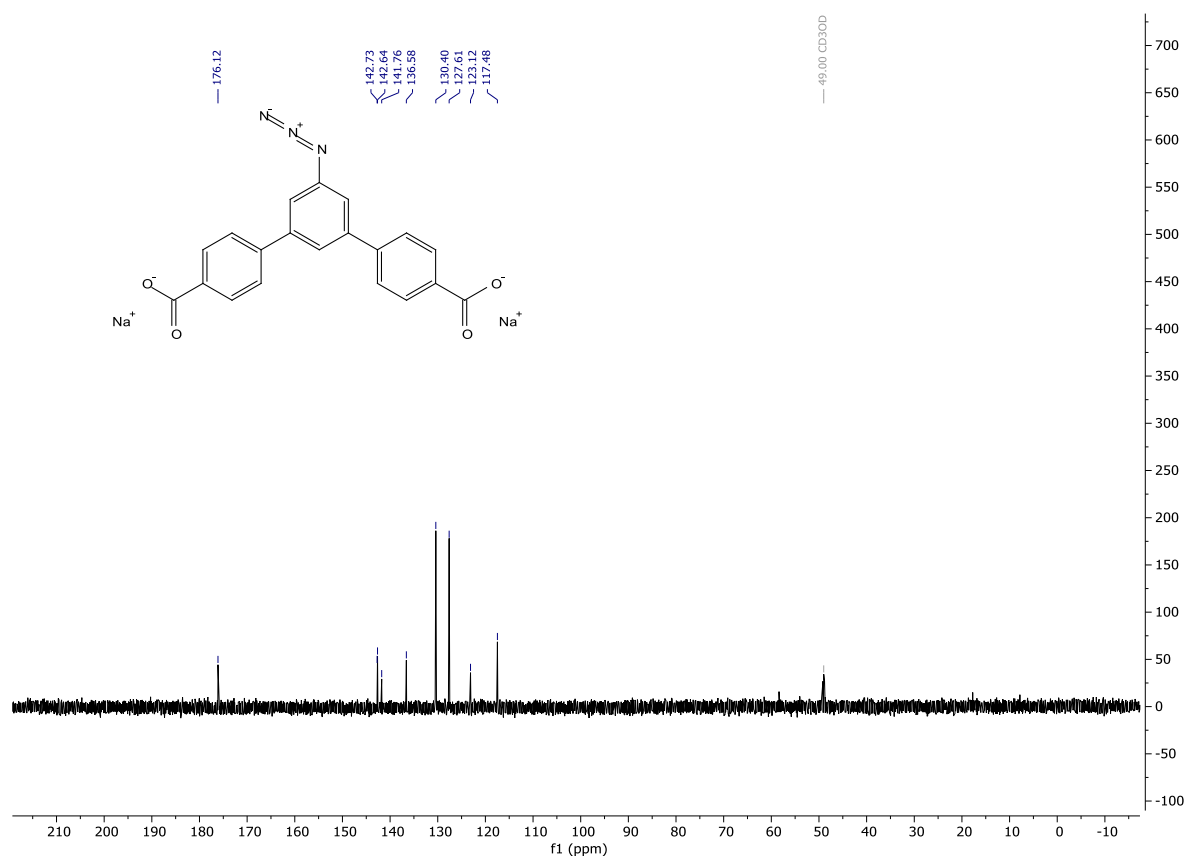
¹³C-NMR spectrum of **8**



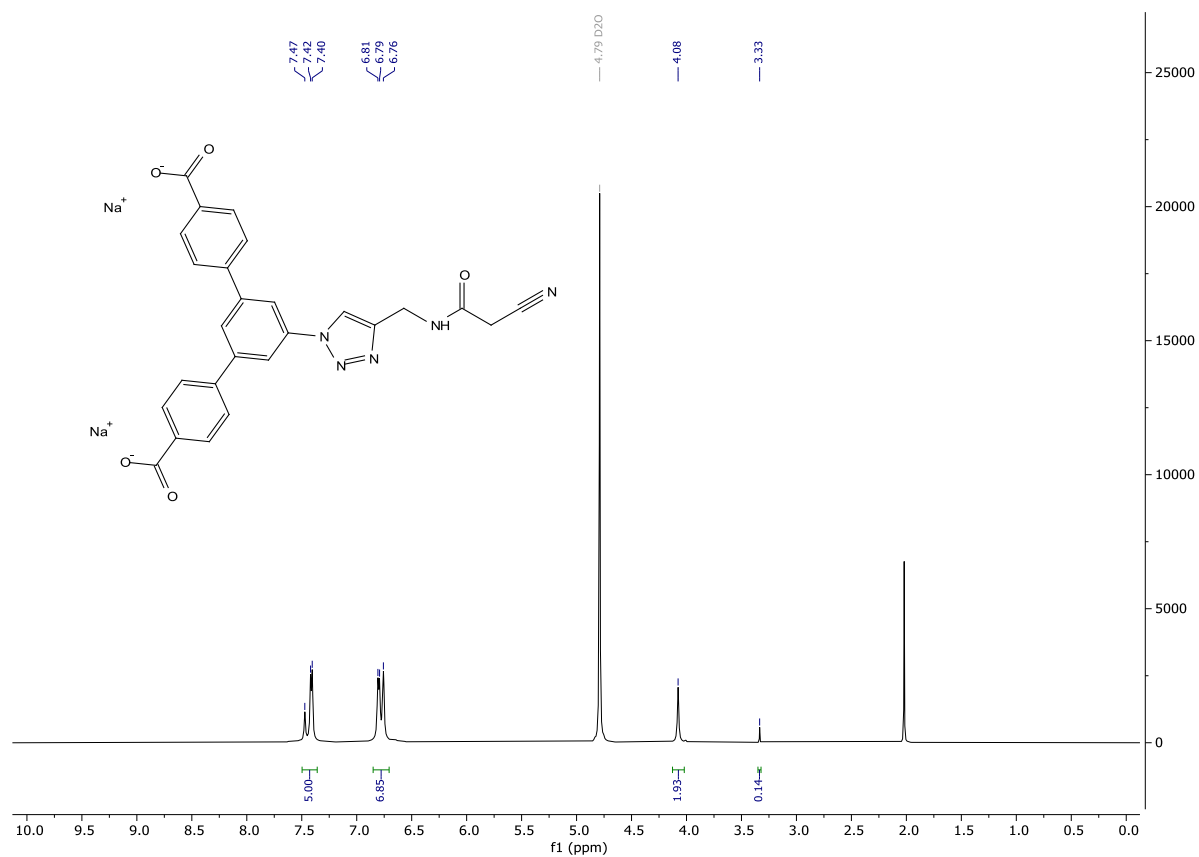
¹H-NMR spectrum of **9**



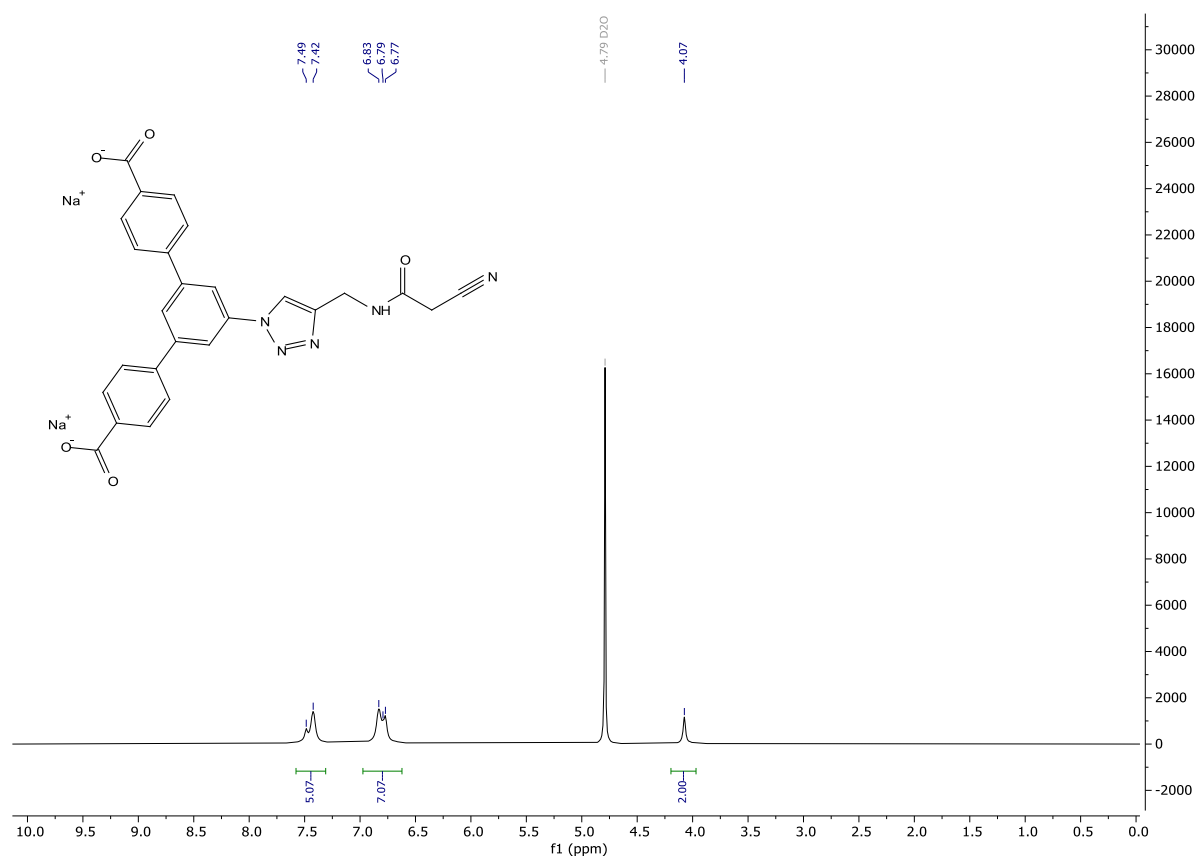
¹³C-NMR spectrum of **9**



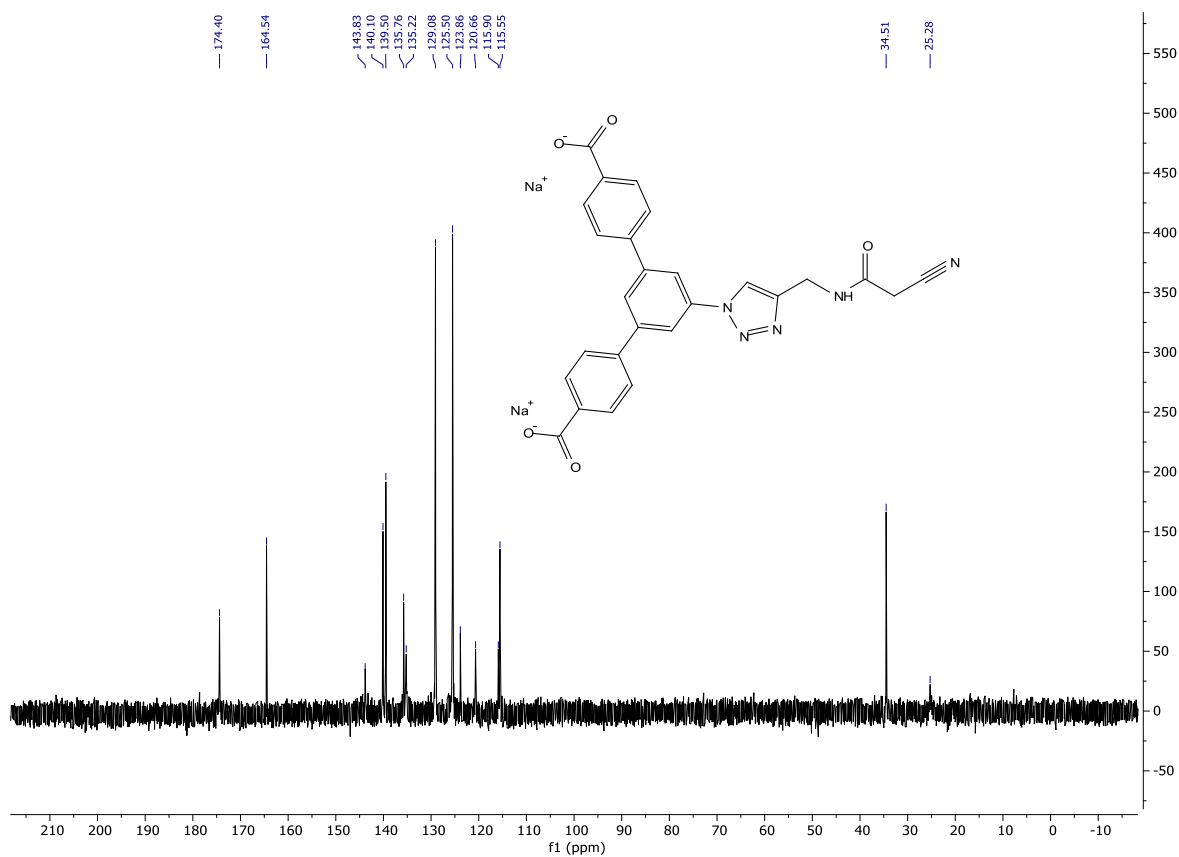
^1H -NMR spectrum of **e** containing ACN as impurity, but with visible acidic CH_2 group



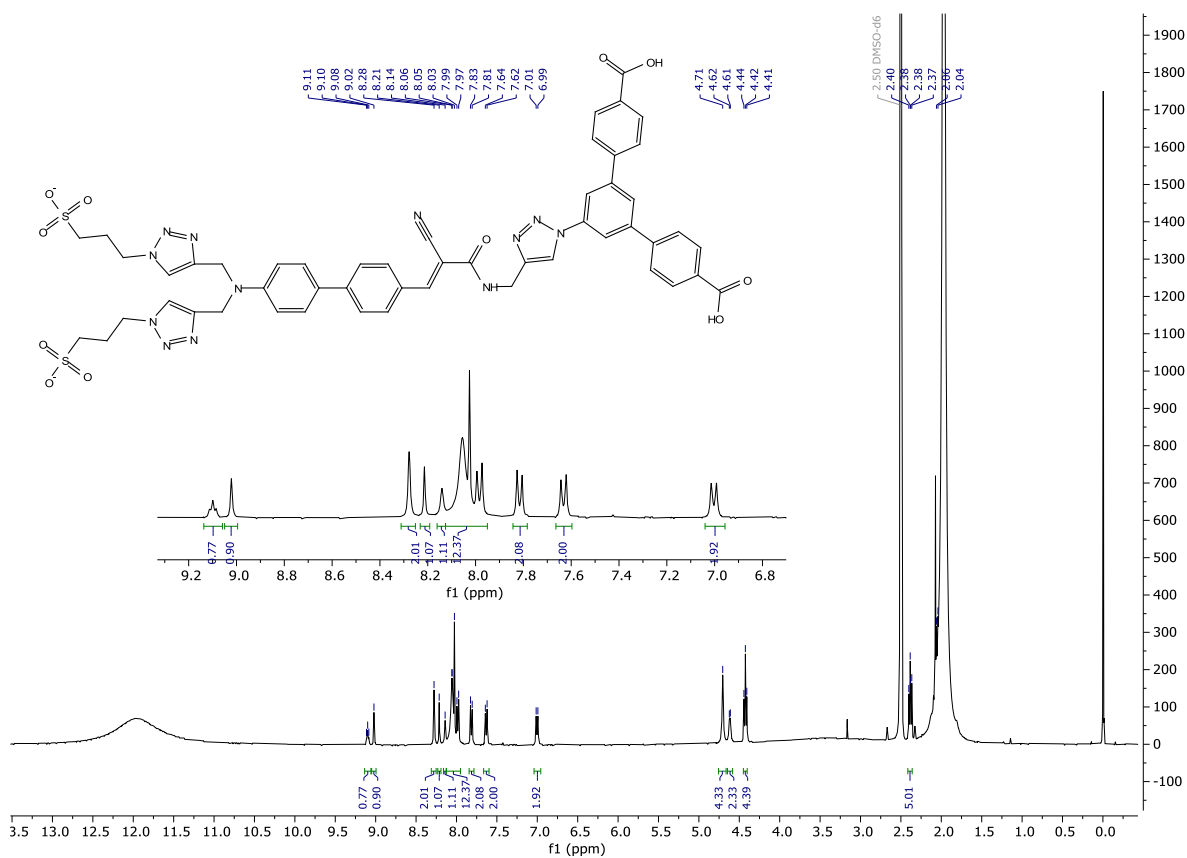
^1H -NMR spectrum of **e**



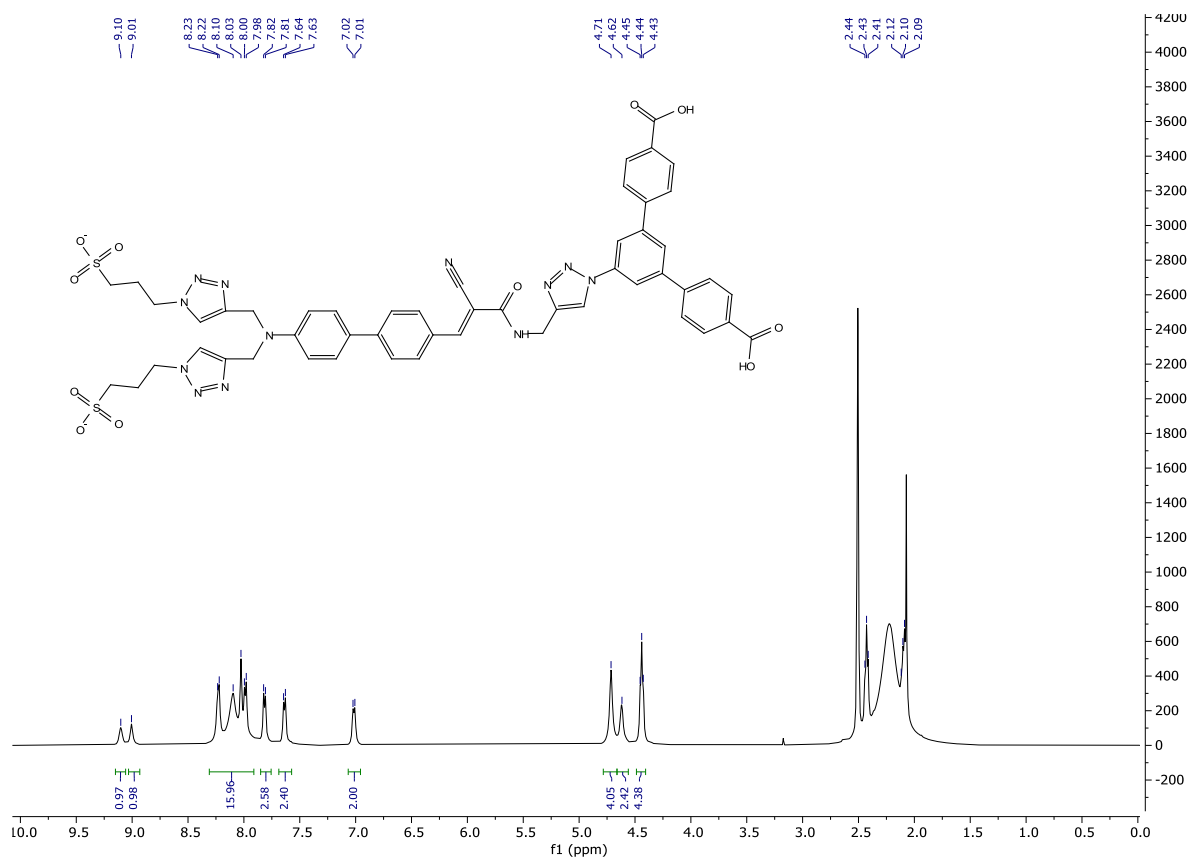
¹³C-NMR spectrum of **e**



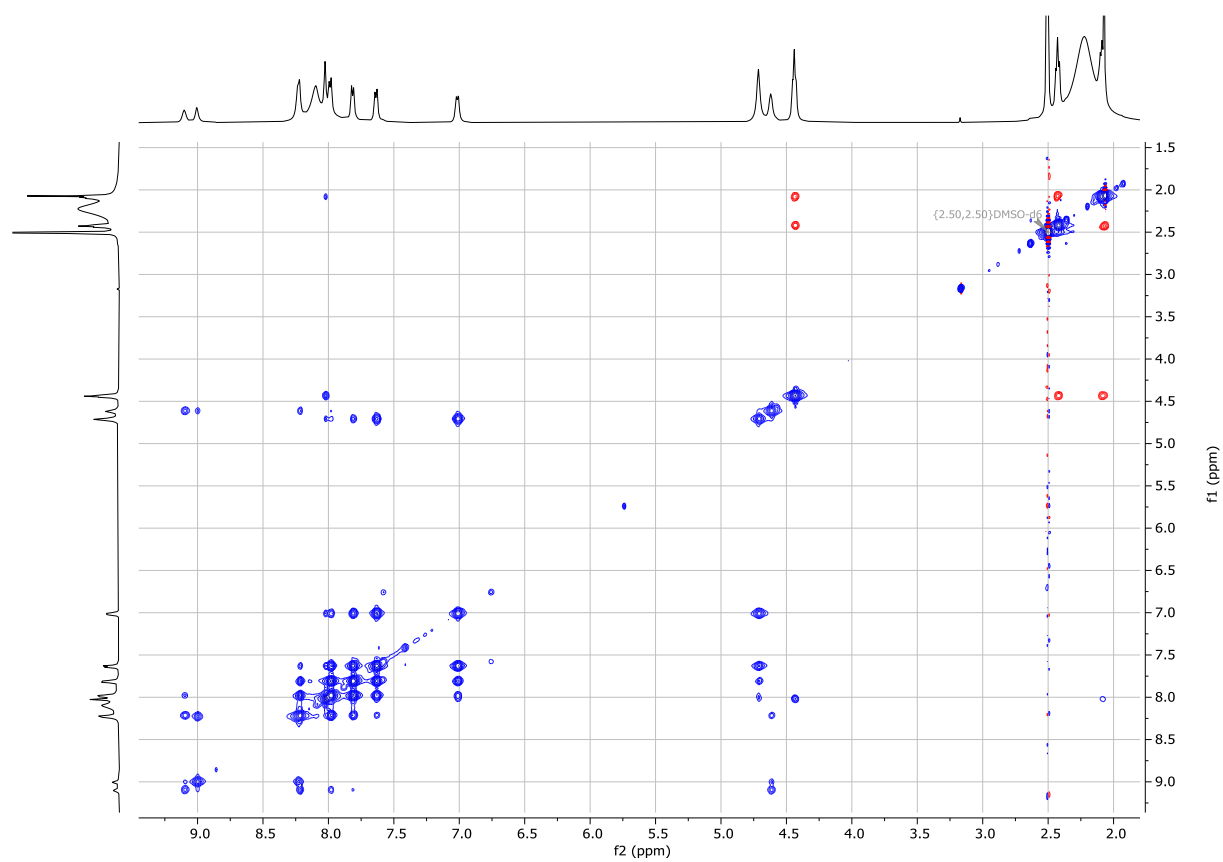
Low concentration ¹H-NMR spectrum of **1e** in DMSO-d₆ with AcOH as additive



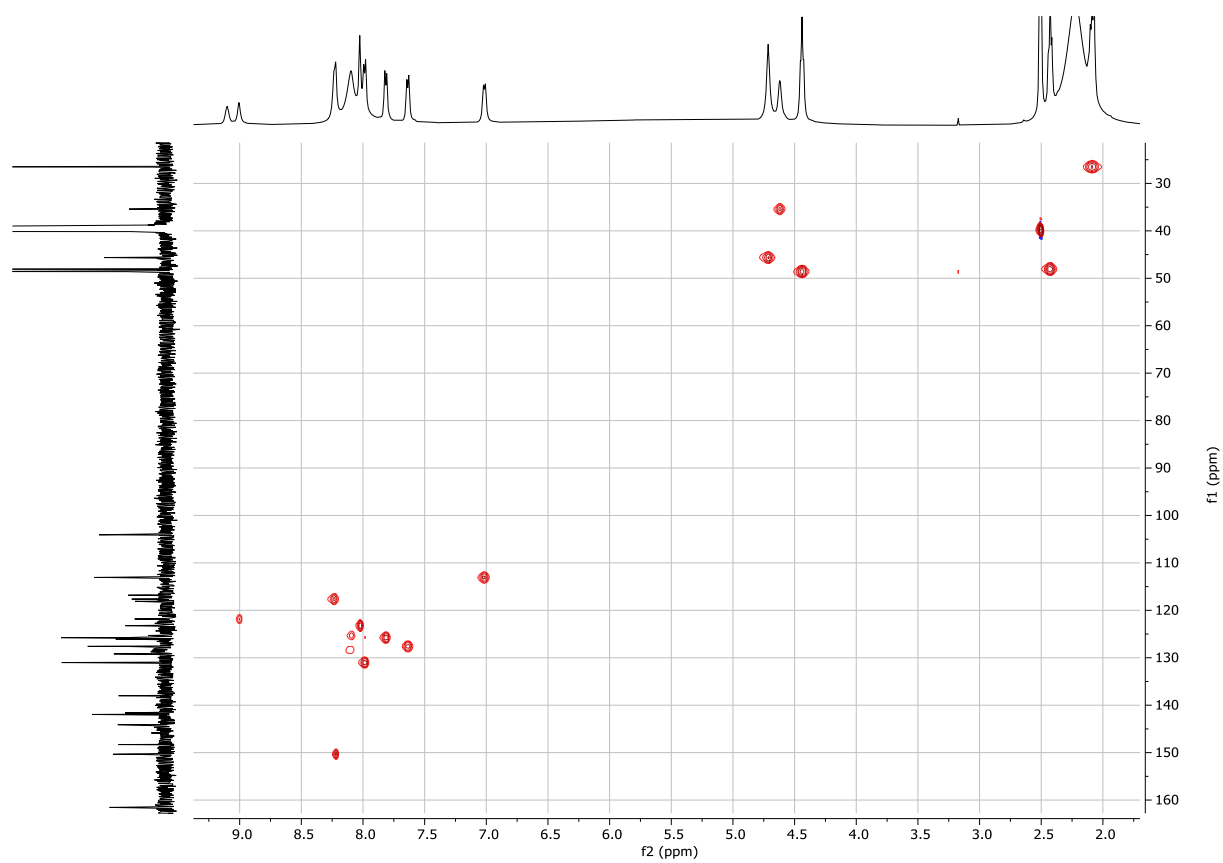
High concentration ^1H -NMR spectrum of **1e** in DMSO- d_6 with AcOH as additive



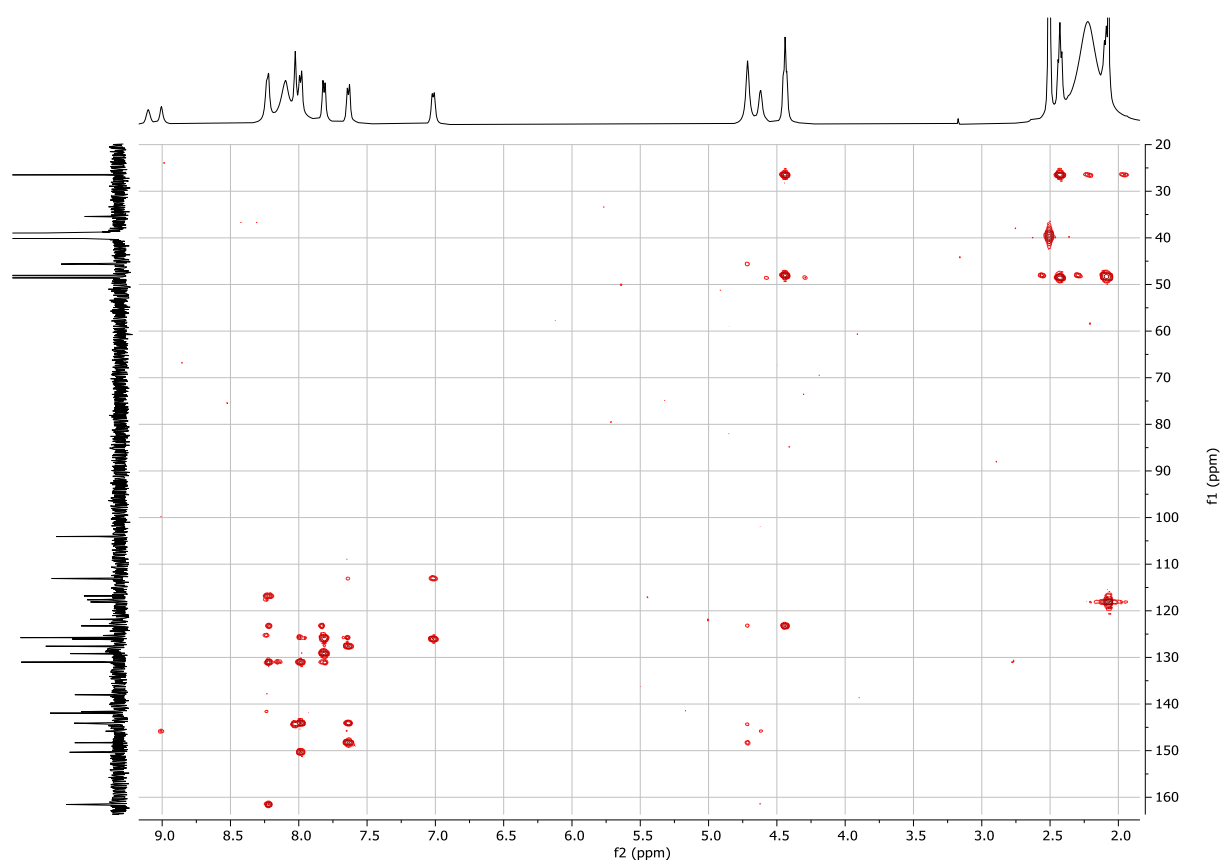
NOESY spectrum of **1e**



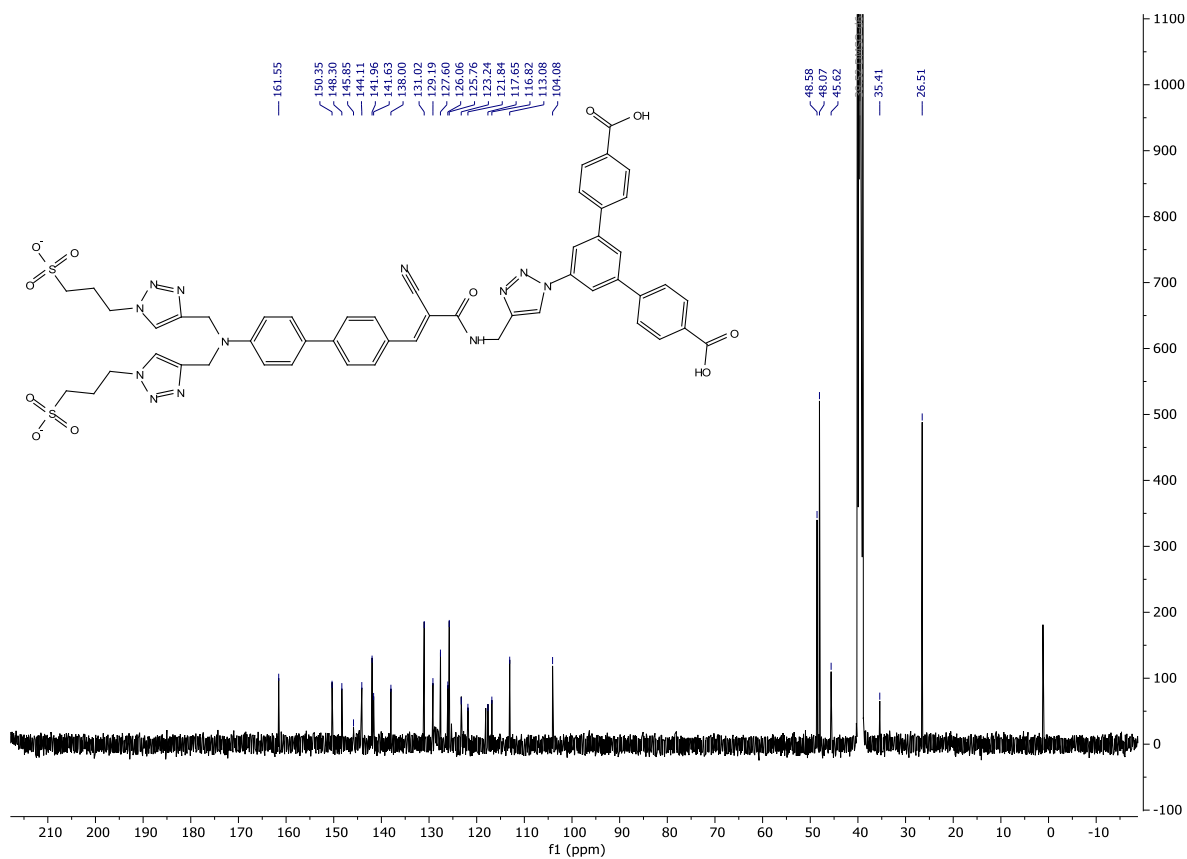
HMQC spectrum of **1e**



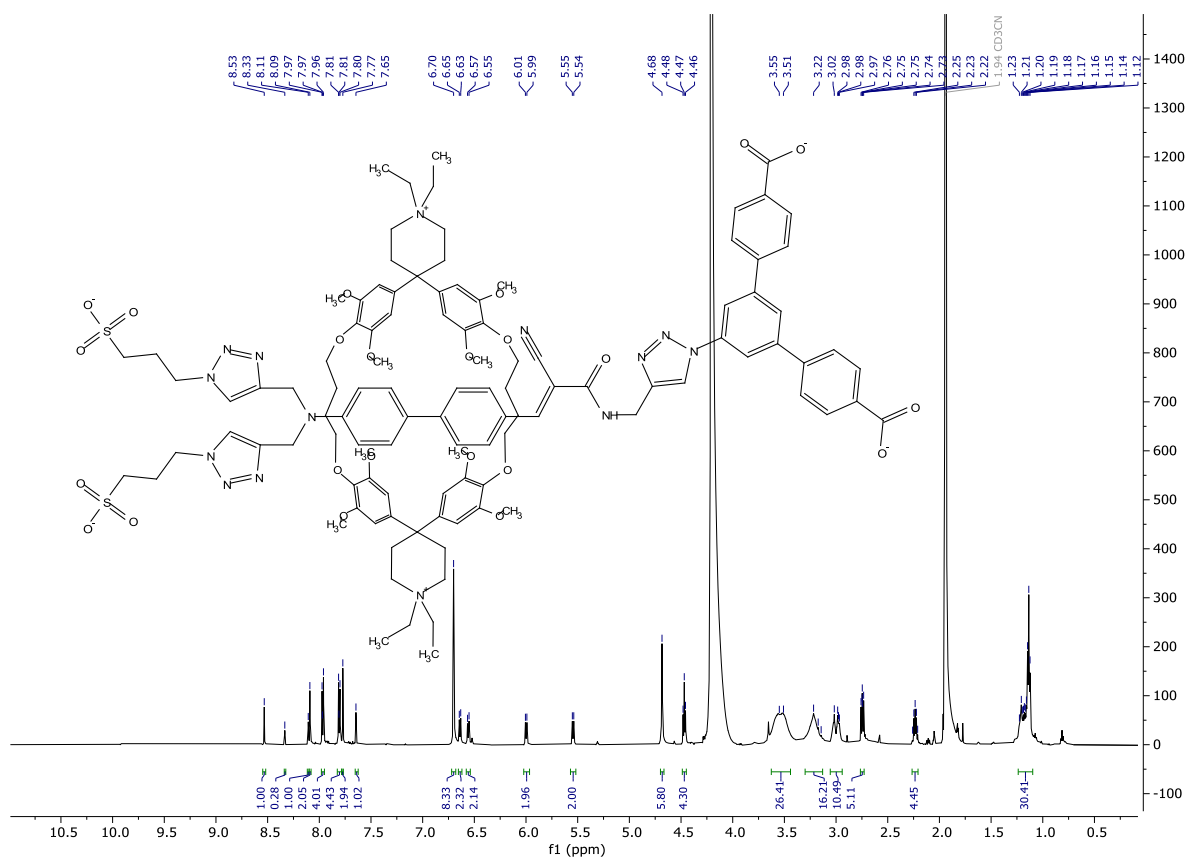
HMBC spectrum of **1e**



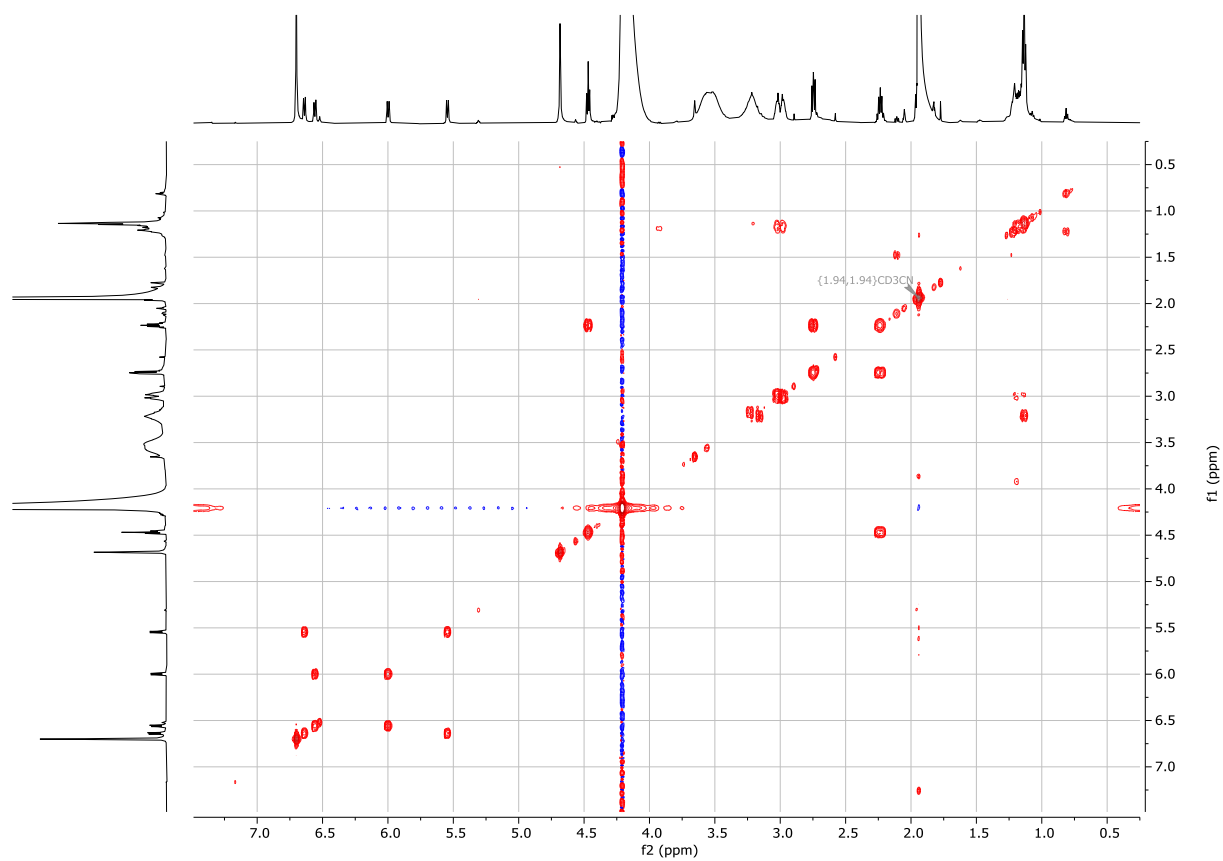
^{13}C -NMR spectrum of **1e**



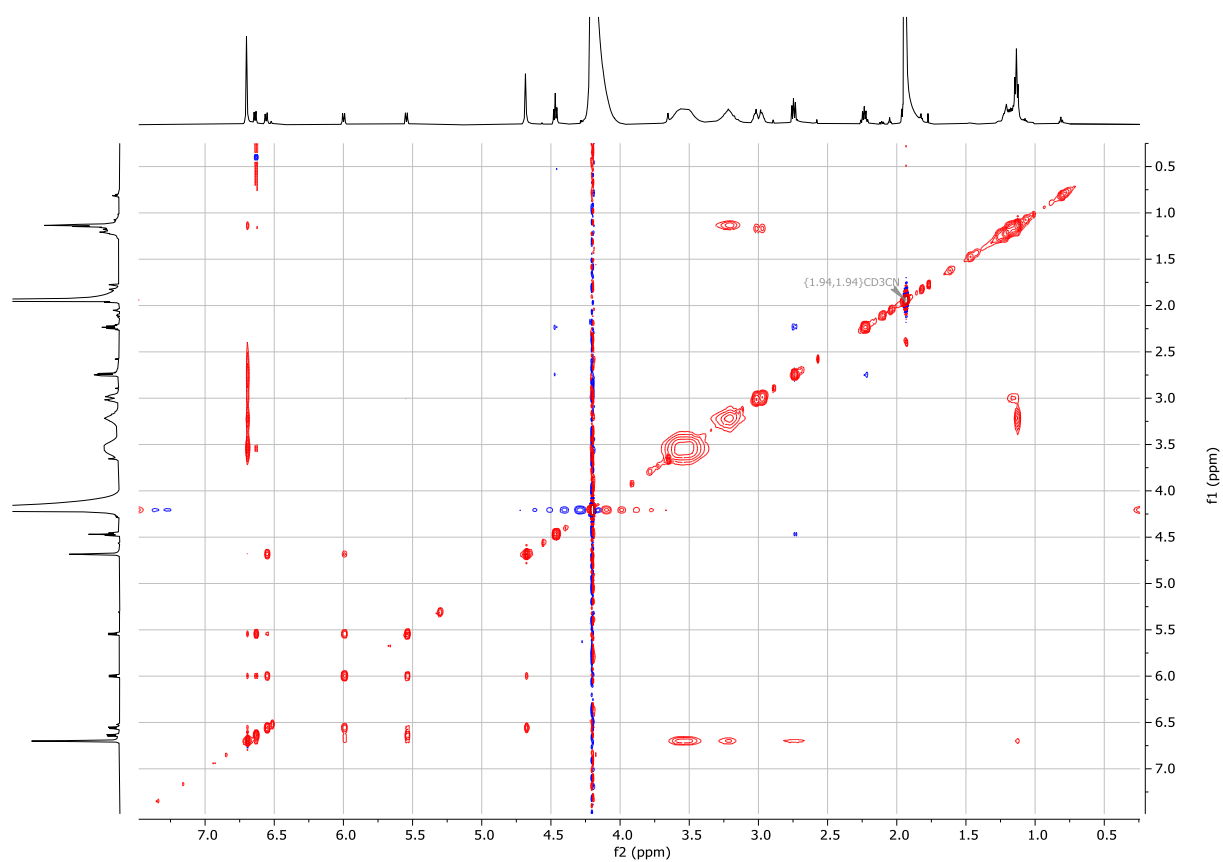
^1H -NMR spectrum of **1e** in $\text{CD}_3\text{CN}/\text{D}_2\text{O}$ 1:1



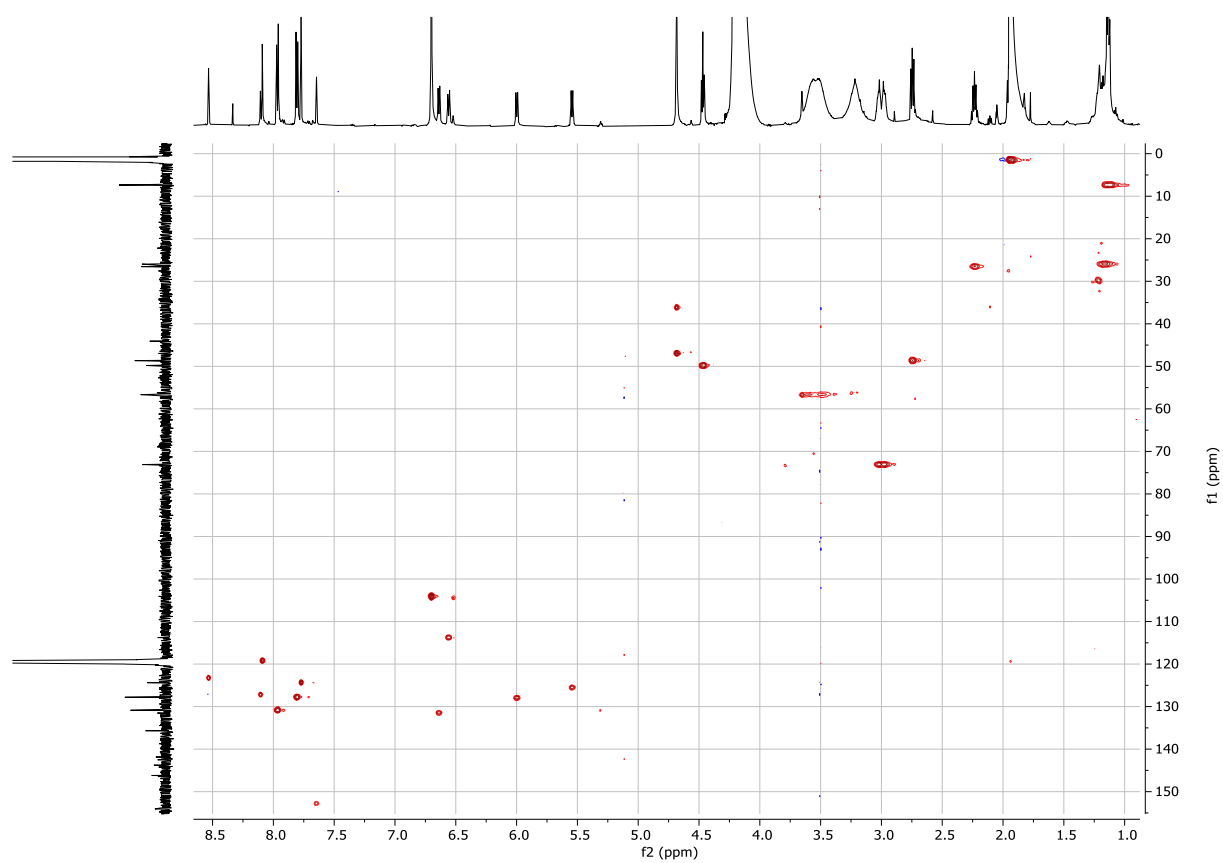
COSY spectrum of **1e**c2



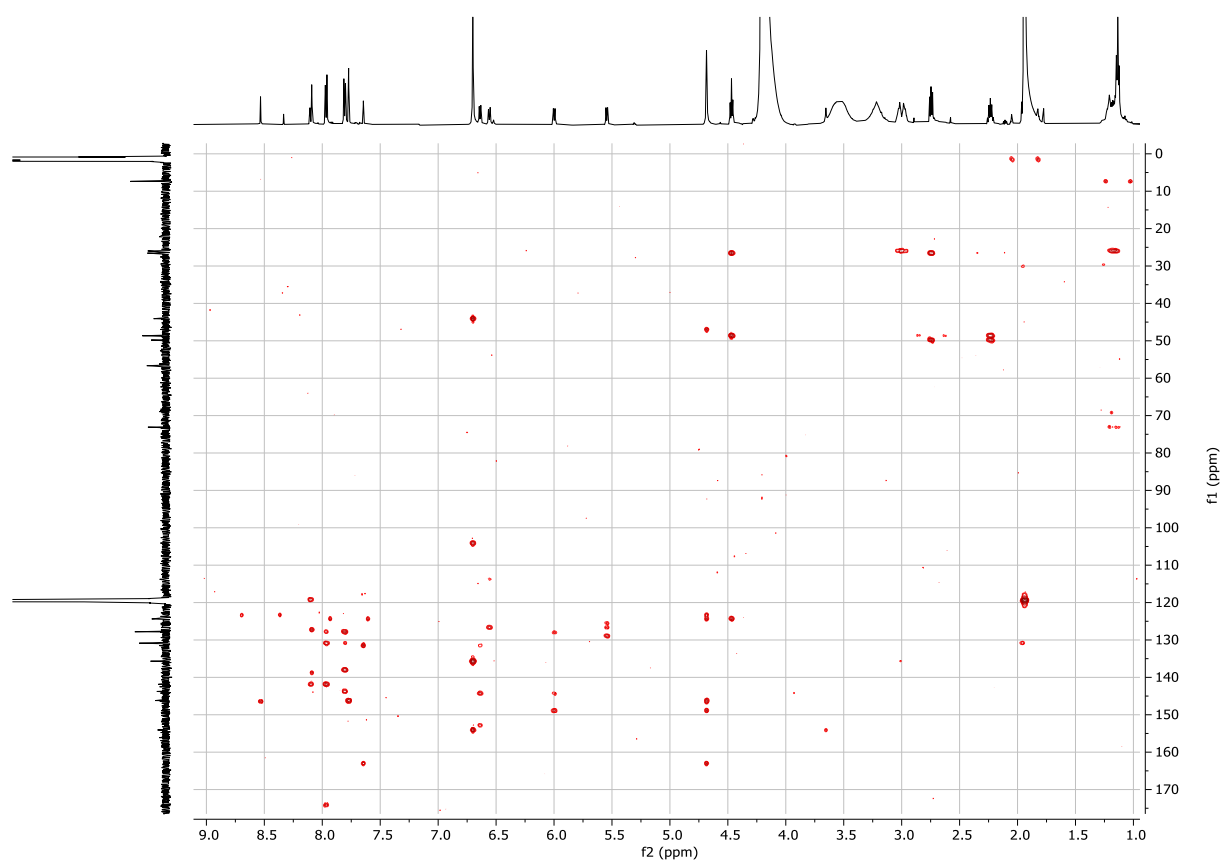
NOESY spectrum of **1e**c2



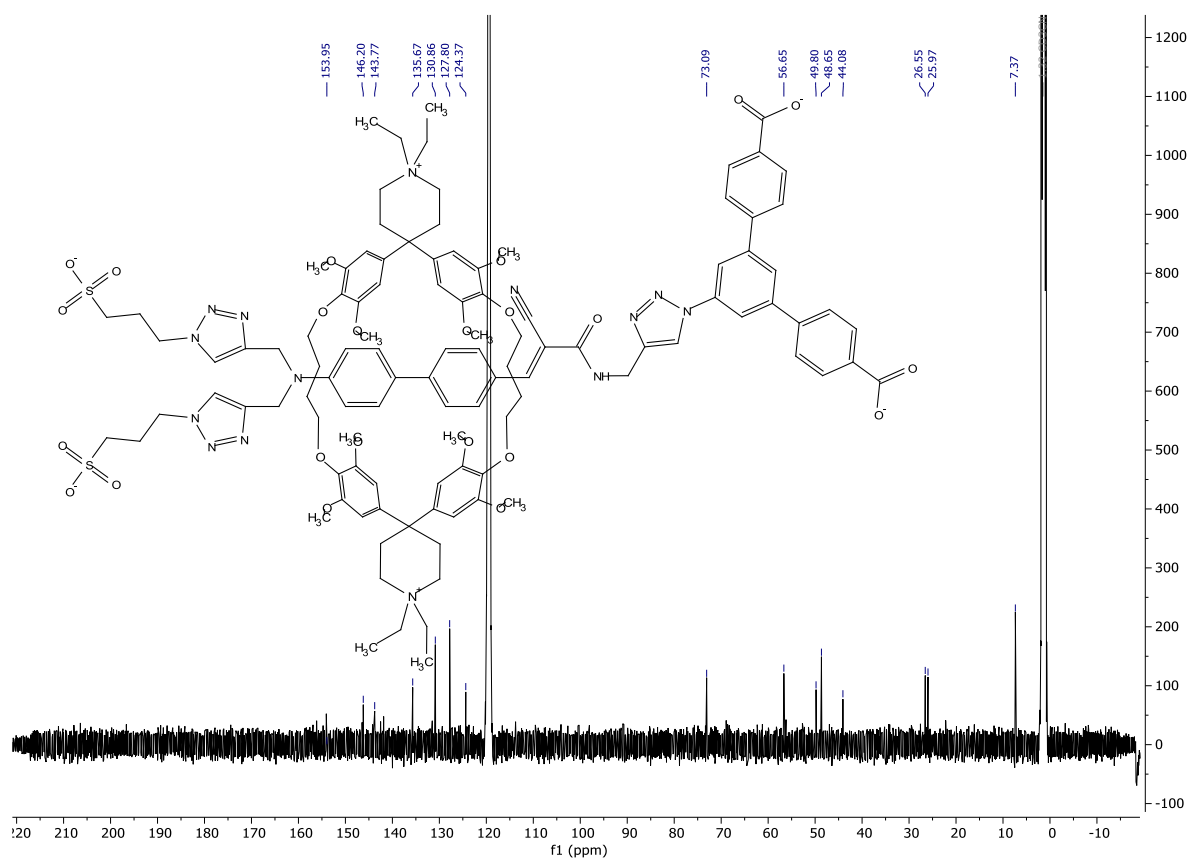
HMQC spectrum of **1e**c2



HMBC spectrum of **1e**c2

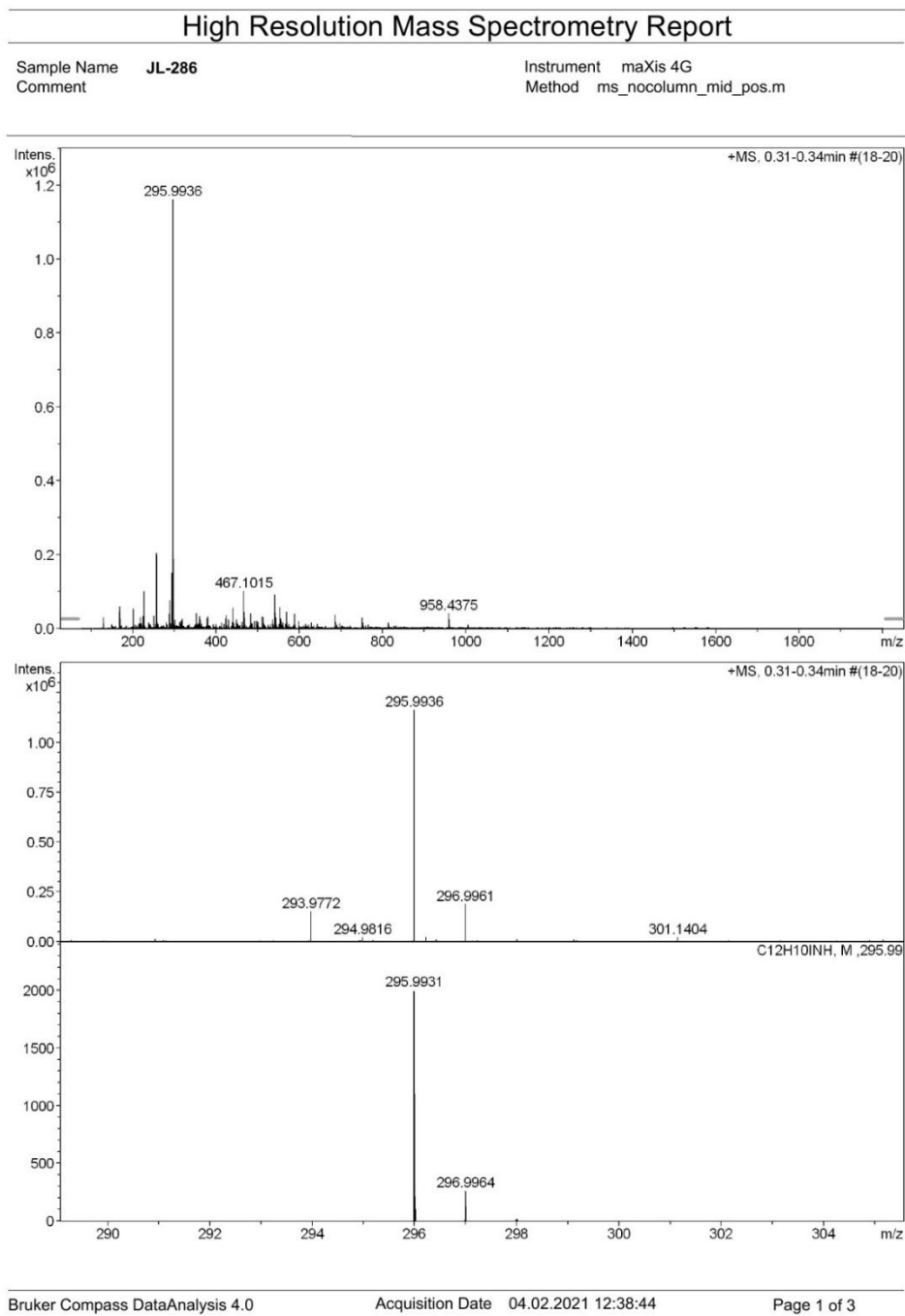


^{13}C -NMR spectrum of **1ec2** (16384 scans)



HR-MS Spectra

HR-MS Spectrum of 5



High Resolution Mass Spectrometry Report

Measured m/z vs. theoretical m/z

Meas. m/z	#	Formula	Score	m/z	err [mDa]	err [ppm]	mSigma	rdb	e ⁻ Conf	z
295.9936	1	C ₁₂ H ₁₁ I _N	100.00	295.9931	-0.6	-1.9	16.1	7.5	even	1+

Mass list

#	m/z	I %	I
1	130.0656	2.6	30019
2	131.0727	1.2	14358
3	168.0807	3.9	45548
4	169.0883	5.1	59307
5	170.0955	2.3	26306
6	201.1094	4.6	52950
7	214.9170	1.2	13936
8	217.1043	1.0	11349
9	218.9535	2.7	30893
10	220.9341	1.2	14412
11	224.9926	2.8	32453
12	226.9512	8.6	99729
13	238.8838	1.3	15609
14	239.1612	1.1	12243
15	250.9919	2.9	33418
16	255.1560	1.0	12183
17	256.9694	17.6	204577
18	257.0626	1.0	11532
19	257.9769	17.0	197091
20	258.9801	1.4	16537
21	281.0476	1.4	15935
22	288.2891	3.3	38568
23	288.9216	6.5	75739
24	290.9248	1.2	13733
25	293.9772	13.0	150572
26	294.9816	1.8	21069
27	295.9936	100.0	1161490
28	296.2190	2.0	23569
29	296.9961	16.1	187403
30	301.1404	1.9	22246
31	312.8879	1.4	16247
32	316.3204	1.5	16980
33	317.2443	1.7	19955
34	319.2600	2.2	25714
35	335.1668	1.0	11577
36	350.8917	1.0	11593
37	353.2656	3.5	41218
38	356.9085	1.2	13780
39	360.3229	2.8	33075
40	362.9257	2.0	23436
41	365.1055	1.1	12381
42	379.1453	2.4	27538
43	379.1933	1.5	17855
44	381.1006	1.2	14363
45	381.2969	2.8	32969
46	413.2654	1.4	15695
47	423.2194	2.3	26302
48	424.8962	3.0	35301
49	430.9132	2.0	23505
50	439.1242	1.5	17398
51	441.2969	4.8	56023
52	442.3002	1.3	15231
53	443.3334	1.0	12049
54	448.8628	2.0	23223
55	450.8597	1.2	13446
56	463.0659	1.5	17075
57	467.1015	8.7	101481
58	467.2445	2.8	32717
59	468.1020	3.8	44061
60	469.0996	2.4	28271
61	483.2082	3.4	39521
62	484.2112	1.2	13951

High Resolution Mass Spectrometry Report

#	m/z	I %	I
63	486.8668	1.2	13517
64	487.3598	1.0	11465
65	492.8839	1.6	18476
66	497.3955	1.7	19418
67	501.0217	1.6	18027
68	511.2718	2.8	32049
69	513.1430	2.6	30270
70	513.3695	1.2	14415
71	514.1441	1.2	14251
72	536.1645	2.0	23260
73	537.1651	1.0	11465
74	541.1201	7.8	90884
75	542.1208	3.8	43713
76	543.1184	2.5	29362
77	550.9466	1.0	11932
78	553.3888	1.8	21451
79	553.4583	5.0	57665
80	554.4614	1.9	22636
81	554.8537	1.0	11350
82	555.2980	2.3	27044
83	557.0939	1.6	19114
84	560.8708	1.3	15652
85	566.8876	1.0	11548
86	569.4323	3.8	44074
87	570.4355	1.5	16864
88	588.9028	3.3	38111
89	599.3240	1.6	18409
90	615.1385	1.0	11694
91	628.8585	1.3	15324
92	685.4340	3.1	36470
93	686.4373	1.5	17192
94	696.8454	1.2	13557
95	750.4062	2.5	28764
96	751.4093	1.2	13727
97	752.4057	1.3	14653
98	813.5561	1.4	15731
99	958.4375	3.6	41248
100	959.4404	2.1	24087

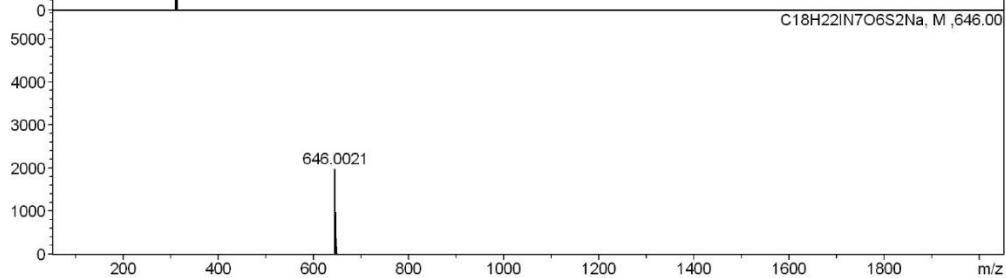
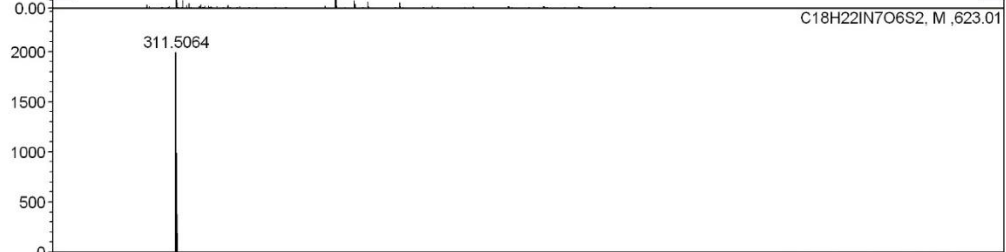
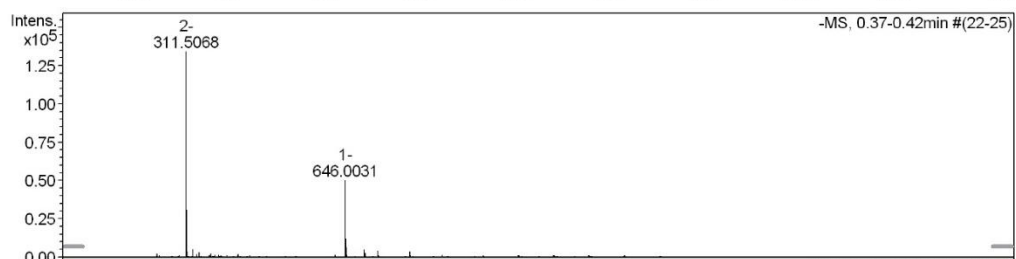
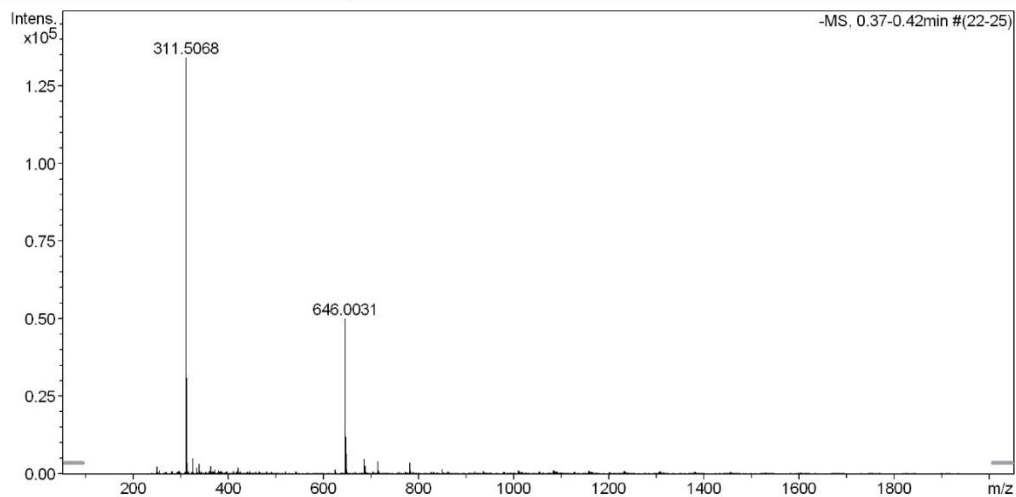
Acquisition Parameter

General	Fore Vacuum	2.40e+000 mBar	High Vacuum	1.15e-007 mBar	Source Type	ESI
	Scan Begin	75 m/z	Scan End	2000 m/z	Ion Polarity	Positive
Source	Set Nebulizer	2.0 Bar	Set Capillary	4500 V	Set Dry Gas	8.0 l/min
	Set Dry Heater	200 °C	Set End Plate Offset	-500 V		
Quadrupole	Set Ion Energy (MS only)	4.0 eV				
Coll. Cell	Collision Energy	8.0 eV	Set Collision Cell RF	600.0 Vpp	100.0 Vpp	
Ion Cooler	Set Ion Cooler Transfer Time	75.0 µs	Set Ion Cooler Pre Pulse Storage Time	10.0 µs		

High Resolution Mass Spectrometry Report

Sample Name **Laurent Jucker / JL-215P**
Comment 5 ug/mL in MeOH, analyzed in MeCN

Instrument maXis 4G
Method 33 Direct_neg_higher.m



High Resolution Mass Spectrometry Report

Measured m/z vs. theoretical m/z

Meas. m/z	#	Formula	Score	m/z	err [mDa]	err [ppm]	mSigma	rdb	e ⁻ Conf	z
311.5068	1	C 18 H 22 I N 7 O 6 S 2	100.00	311.5064	-0.4	-1.2	13.3	11.0	even	2-
646.0031	1	C 18 H 22 I N 7 Na O 6 S 2	100.00	646.0021	-1.0	-1.6	1.4	10.5	even	1-

Mass list

#	m/z	I %	I
1	248.9612	0.4	500
2	250.5046	1.6	2167
3	255.2325	0.8	1082
4	281.2489	0.4	585
5	283.2636	0.6	744
6	294.9532	0.4	583
7	297.0472	0.8	1015
8	297.1536	0.6	831
9	311.1684	2.5	3403
10	311.5068	100.0	134030
11	312.0079	23.0	30802
12	312.1712	0.6	791
13	312.5057	10.4	13897
14	313.0067	2.6	3487
15	313.0782	1.5	1975
16	313.5060	0.5	658
17	316.9484	0.4	561
18	323.2201	0.4	504
19	325.1841	3.7	4931
20	326.1874	0.7	899
21	334.0752	1.4	1881
22	339.1995	2.3	3111
23	340.2035	0.6	739
24	343.4750	0.5	653
25	360.4560	0.6	836
26	361.4549	0.5	622
27	362.9407	1.7	2340
28	367.3583	0.5	680
29	369.3006	0.4	531
30	371.0656	0.9	1244
31	380.1171	0.8	1126
32	381.3728	0.4	521
33	383.3162	0.4	600
34	384.9350	0.6	830
35	387.0965	0.5	611
36	396.8900	0.6	841
37	397.3324	0.5	706
38	411.3467	0.5	724
39	419.9749	0.7	981
40	420.9833	1.4	1830
41	425.3632	0.5	610
42	439.3790	0.4	505
43	445.0857	0.7	962
44	465.3043	0.5	684
45	480.5085	0.5	699
46	520.9093	0.4	599
47	541.5101	0.4	568
48	542.9858	0.4	488
49	624.0205	1.0	1286
50	646.0031	37.2	49920
51	647.0054	8.9	11891
52	648.0001	4.8	6373
53	649.0019	0.9	1269
54	685.9427	3.5	4652
55	686.9455	0.9	1141
56	687.9413	1.9	2483
57	688.9437	0.5	678
58	703.9619	0.5	688
59	713.9910	3.0	3972
60	714.9935	0.8	1054
61	715.9889	0.4	502

High Resolution Mass Spectrometry Report

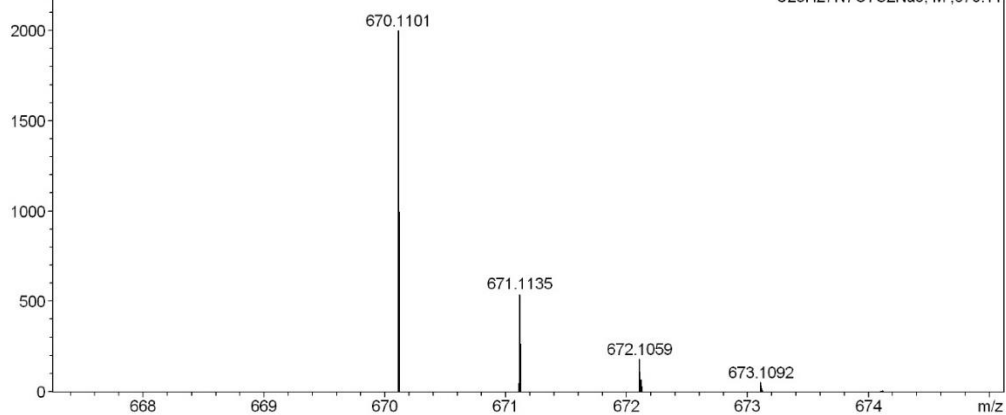
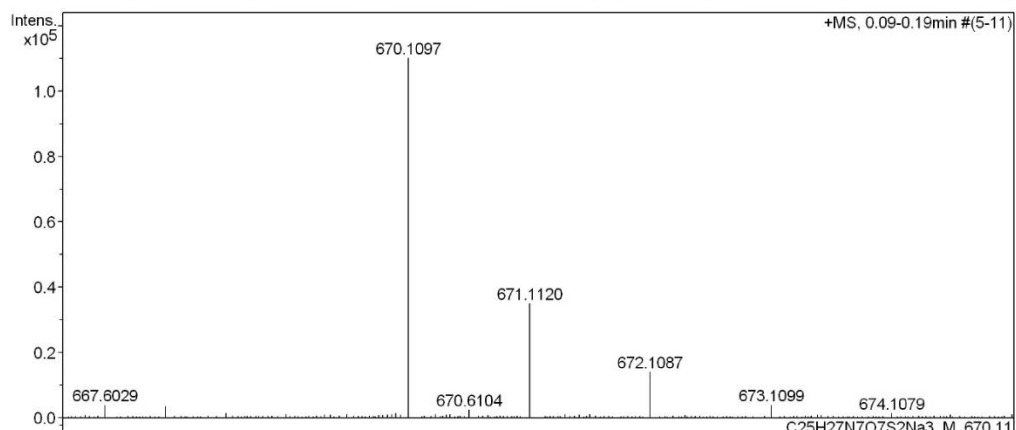
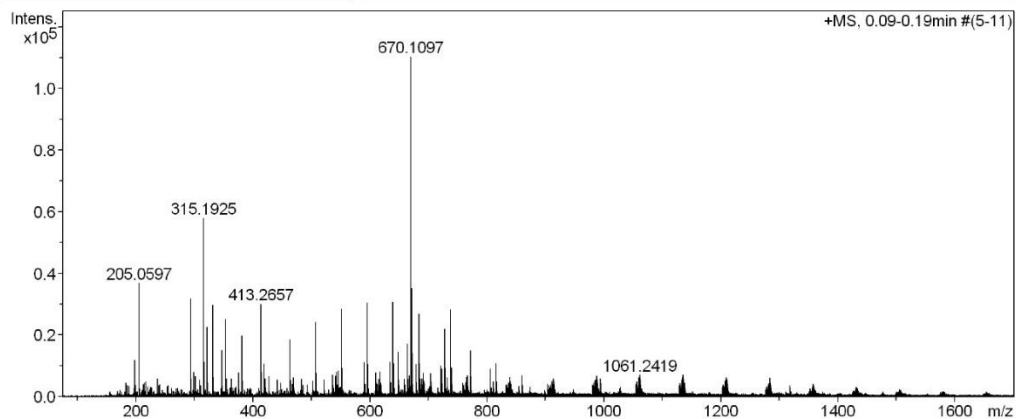
#	m/z	I %	I
62	771.9521	0.4	520
63	781.9802	2.6	3431
64	782.9831	0.7	883
65	787.1670	0.4	505
66	849.9681	1.0	1351
67	861.1896	0.4	565
68	917.9579	0.5	659
69	935.2079	0.6	855
70	936.2105	0.5	644
71	937.2085	0.5	681
72	1009.2333	0.7	905
73	1010.2325	0.7	880
74	1011.2312	0.6	850
75	1012.2288	0.5	612
76	1016.6873	0.4	497
77	1017.1883	0.4	490
78	1053.1992	0.4	493
79	1054.1956	0.4	563
80	1083.2548	0.8	1028
81	1084.2505	0.7	991
82	1085.2518	0.7	1005
83	1086.2524	0.5	641
84	1090.2157	0.4	521
85	1090.7117	0.4	552
86	1091.2080	0.4	542
87	1127.7256	0.4	532
88	1128.2228	0.4	520
89	1157.2744	0.6	821
90	1158.2749	0.7	944
91	1159.2756	0.7	940
92	1160.2741	0.5	703
93	1164.2337	0.4	516
94	1231.2964	0.4	543
95	1232.2960	0.5	731
96	1233.2965	0.6	836
97	1234.2952	0.4	572
98	1306.3209	0.5	605
99	1307.3211	0.5	613
100	1308.3187	0.4	499

Acquisition Parameter

Source Type	ESI	Ion Polarity	Negative	Set Nebulizer	0.4 Bar
Focus	Not active	Set Capillary	4500 V	Set Dry Heater	180 °C
Scan Begin	100 m/z	Set End Plate Offset	-500 V	Set Dry Gas	4.0 l/min
Scan End	2000 m/z	Set Collision Cell RF	100.0 Vpp	Set Ion Energy (MS only)	-8.0 eV

High Resolution Mass Spectrometry Report

Sample Name	Laurent Jucker / JL-225P	Instrument	maXis 4G
Comment	10 ug/mL in MeOH, analyzed in MeOH+0.1%HCOOH	Method	22 Direct_pos_mid.m



High Resolution Mass Spectrometry Report

Measured m/z vs. theoretical m/z

Meas. m/z	#	Formula	Score	m/z	err [mDa]	err [ppm]	mSigma	rdb	e ⁻ Conf	z
670.1097	1	C 25 H 27 N 7 Na 3 O 7 S 2	100.00	670.1101	0.4	0.7	12.7	14.5	even	1+

Mass list

#	m/z	I %	I
1	198.0908	10.7	11831
2	205.0597	33.3	36655
3	237.1466	5.3	5814
4	293.2445	28.8	31751
5	294.2477	5.3	5874
6	299.1607	7.2	7909
7	301.1403	5.9	6511
8	309.2045	4.8	5337
9	315.1925	52.5	57813
10	316.1955	10.2	11225
11	321.2756	20.5	22612
12	331.1872	26.9	29570
13	331.2234	11.9	13081
14	332.1908	5.8	6365
15	347.1821	13.7	15036
16	353.2657	22.7	25024
17	354.2690	5.3	5882
18	363.2133	5.3	5815
19	375.2495	7.0	7743
20	381.2969	17.9	19670
21	413.2657	27.2	29937
22	414.2692	7.3	8086
23	419.2755	9.6	10542
24	421.0883	5.3	5871
25	427.2842	5.8	6411
26	441.2968	4.8	5306
27	463.3022	16.8	18511
28	464.3058	4.8	5243
29	469.0809	5.6	6136
30	483.3111	5.1	5663
31	507.3285	21.9	24127
32	508.3315	6.9	7590
33	521.3806	4.9	5347
34	536.1650	6.3	6967
35	541.1199	6.0	6633
36	543.1005	7.4	8106
37	546.3991	7.5	8297
38	551.3548	25.8	28428
39	552.3581	8.4	9212
40	590.4255	10.0	11065
41	595.3808	27.6	30399
42	596.3846	9.4	10340
43	610.1835	7.0	7670
44	615.1391	5.1	5645
45	617.1193	7.4	8100
46	634.4513	10.1	11165
47	639.4070	27.7	30512
48	640.4108	9.7	10725
49	648.1232	13.0	14351
50	649.1253	4.8	5326
51	659.1157	5.1	5610
52	664.0926	15.5	17050
53	665.0951	5.2	5750
54	667.1008	6.1	6722
55	670.1097	100.0	110120
56	671.1120	31.7	34930
57	672.1087	12.7	13970
58	678.4779	9.4	10377
59	683.4334	24.4	26843
60	684.2015	4.9	5397
61	684.4364	9.8	10761
62	685.4375	5.3	5871

High Resolution Mass Spectrometry Report

#	m/z	I %	I
63	689.1573	5.3	5888
64	691.1395	6.9	7607
65	704.1039	6.7	7410
66	721.5763	9.0	9917
67	722.5037	8.1	8910
68	727.4590	19.9	21959
69	728.4628	8.3	9105
70	732.0793	5.5	6092
71	738.0965	25.6	28141
72	739.0990	8.4	9294
73	765.1578	5.8	6346
74	766.5303	6.2	6853
75	771.4848	13.5	14822
76	772.4886	5.8	6390
77	806.0833	8.2	9003
78	815.5108	9.7	10694
79	839.1779	5.7	6281
80	859.5376	6.1	6724
81	913.2010	5.3	5885
82	914.1975	4.6	5095
83	985.2311	4.7	5172
84	986.2331	4.8	5338
85	987.2216	6.0	6574
86	988.2179	5.0	5483
87	993.6683	5.2	5778
88	1059.2498	5.5	6077
89	1060.2490	5.6	6147
90	1061.2419	6.4	6996
91	1062.2379	5.1	5576
92	1133.2674	4.9	5408
93	1134.2669	5.7	6234
94	1135.2620	6.3	6939
95	1136.2590	5.1	5641
96	1207.2862	4.6	5107
97	1208.2843	4.8	5293
98	1209.2812	5.6	6119
99	1210.2760	4.9	5423
100	1283.2966	5.4	5924

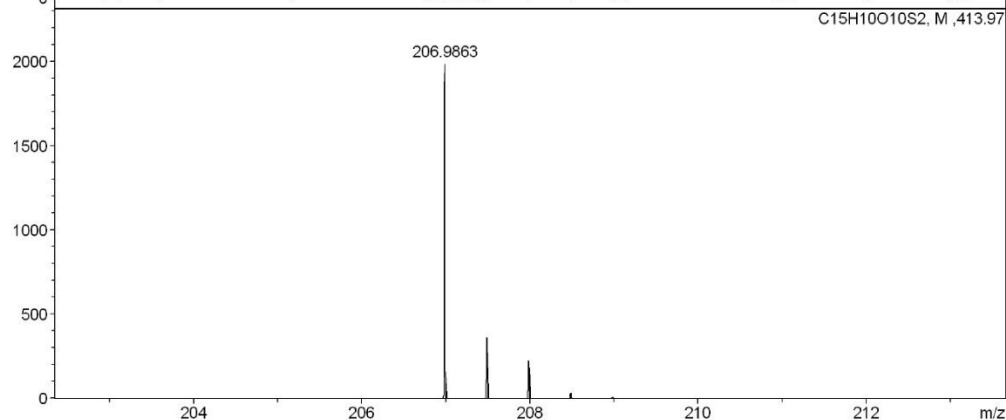
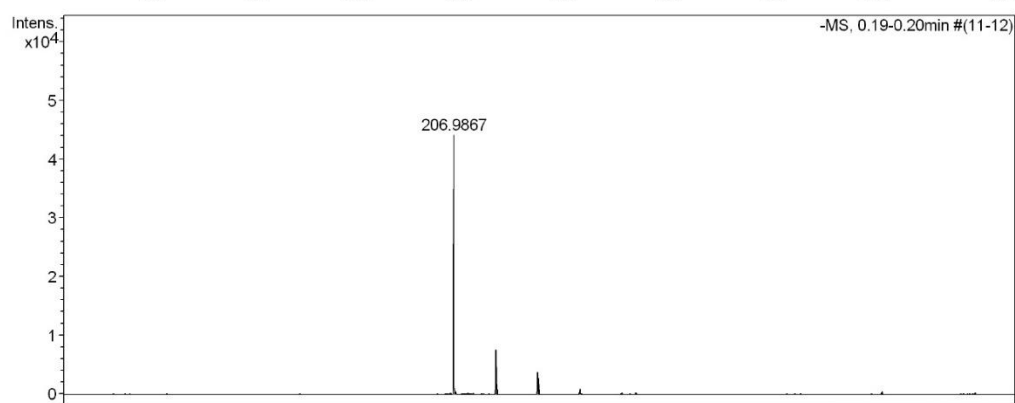
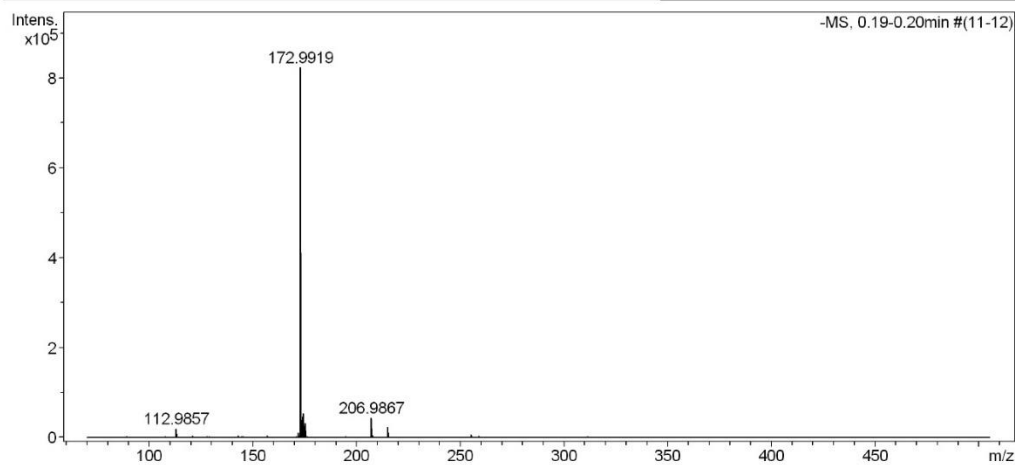
Acquisition Parameter

Source Type	ESI	Ion Polarity	Positive	Set Nebulizer	0.4 Bar
Focus	Not active	Set Capillary	3600 V	Set Dry Heater	180 °C
Scan Begin	75 m/z	Set End Plate Offset	-500 V	Set Dry Gas	4.0 l/min
Scan End	1700 m/z	Set Collision Cell RF	350.0 Vpp	Set Ion Energy (MS only)	4.0 eV

High Resolution Mass Spectrometry Report

Sample Name **JL-616**
 Comment analyzed in MeOH

Instrument maXis 4G
 Method 31 Direct_neg_low.m



High Resolution Mass Spectrometry Report

Measured m/z vs. theoretical m/z

Meas. m/z	#	Formula	Score	m/z	err [mDa]	err [ppm]	mSigma	rdb	e ⁻ Conf	z
206.9867	1	C 15 H 10 O 10 S 2	100.00	206.9863	-0.4	-1.9	22.4	11.0	even	2-

Mass list

#	m/z	I %	I
1	89.0247	0.3	2064
2	93.0352	0.1	1093
3	108.0217	0.4	3005
4	109.0293	0.2	1405
5	112.9857	2.5	20962
6	115.0404	0.2	1754
7	117.0196	0.1	1122
8	121.0295	0.7	5949
9	128.0353	0.4	2963
10	129.0558	0.3	2643
11	131.0349	0.1	1036
12	131.0715	0.1	1004
13	142.9814	0.2	1609
14	143.0718	0.1	1208
15	143.1077	0.7	5399
16	144.9644	0.2	2058
17	145.0508	0.4	3634
18	157.0871	0.2	1741
19	157.1234	0.6	4734
20	170.0044	0.1	1198
21	171.0666	0.2	1410
22	171.1030	0.2	1446
23	171.1395	0.3	2147
24	171.9838	1.5	12309
25	172.9919	100.0	823945
26	173.0825	0.1	1035
27	173.9946	6.6	54142
28	174.9875	4.1	34046
29	175.9909	0.3	2265
30	194.9734	0.4	3702
31	206.9867	5.4	44242
32	207.4882	0.9	7676
33	207.9855	0.5	3848
34	215.0020	2.9	23900
35	216.0055	0.2	2009
36	216.9986	0.1	1110
37	227.2019	0.1	1089
38	255.2328	0.8	6642
39	256.2364	0.2	1332
40	258.9919	0.7	5614
41	283.2639	0.2	2010
42	297.1529	0.2	1279
43	311.1691	0.3	2088
44	325.1848	0.2	1324

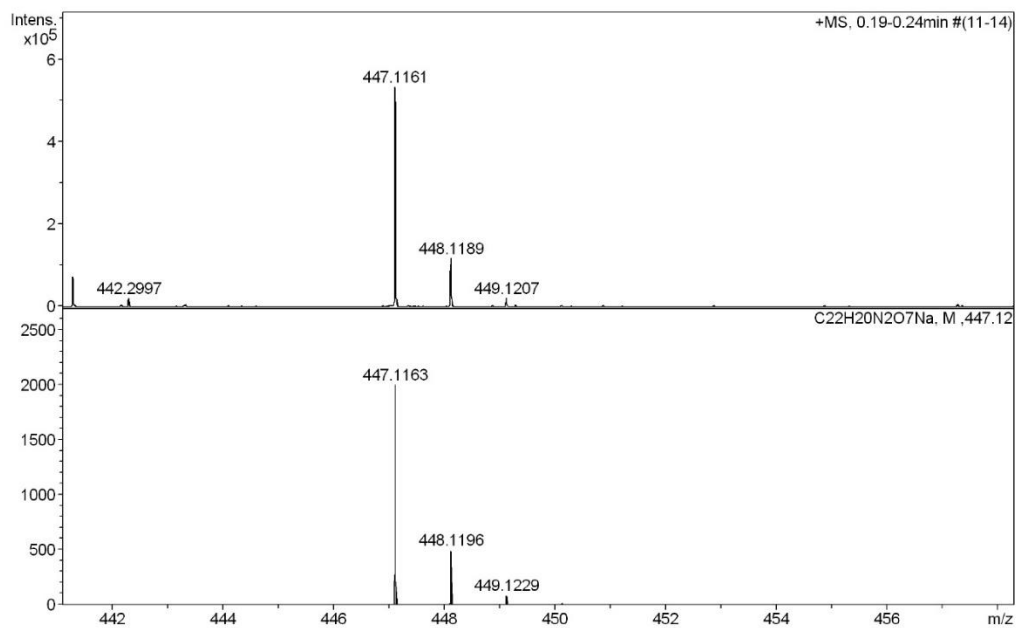
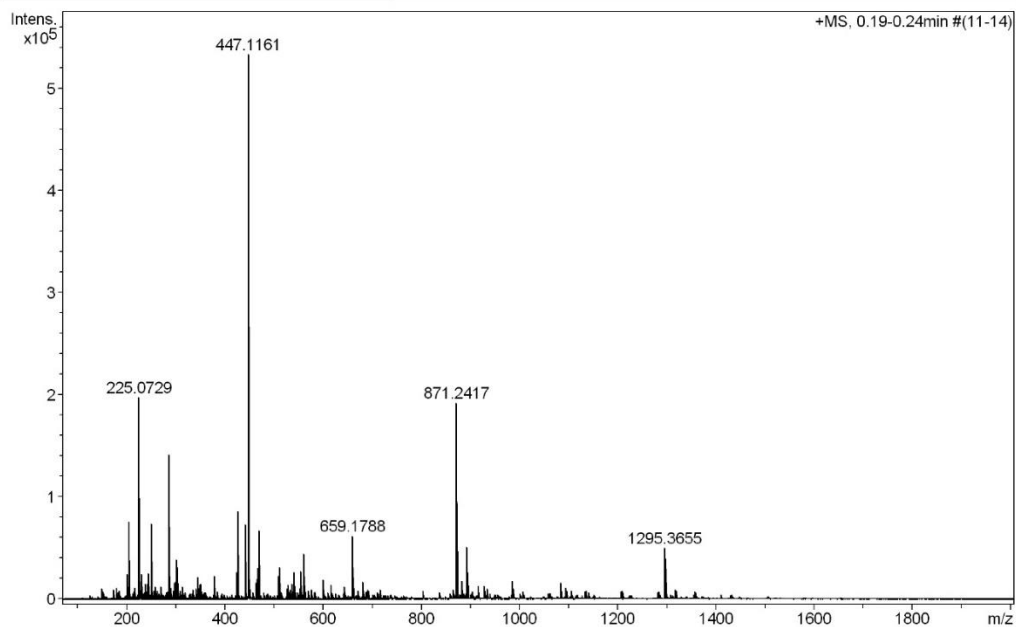
Acquisition Parameter

General	Fore Vacuum	2.60e+000 mBar	High Vacuum	1.19e-007 mBar	Source Type	ESI
	Scan Begin	75 m/z	Scan End	500 m/z	Ion Polarity	Negative
Source	Set Nebulizer	0.4 Bar	Set Capillary	4500 V	Set Dry Gas	4.0 l/min
	Set Dry Heater	180 °C	Set End Plate Offset	-500 V		
Quadrupole	Set Ion Energy (MS only)	-4.0 eV				
Coll. Cell	Collision Energy	-5.0 eV	Set Collision Cell RF	50.0 Vpp	50.0 Vpp	
Ion Cooler	Set Ion Cooler Transfer Time	25.0 µs	Set Ion Cooler Pre Pulse Storage Time	2.0 µs		

High Resolution Mass Spectrometry Report

Sample Name **JL-588**
Comment

Instrument maXis 4G
Method ms_nocolumn_mid_pos.m



High Resolution Mass Spectrometry Report

Measured m/z vs. theoretical m/z

Meas. m/z	#	Formula	Score	m/z	err [mDa]	err [ppm]	mSigma	rdb	e ⁻ Conf	z
447.1161	1	C 22 H 20 N 2 Na O 7	100.00	447.1163	0.2	0.4	14.8	13.5	even	1+

Mass list

#	m/z	I %	I
1	149.9529	1.9	10103
2	173.0781	1.7	8821
3	179.0311	2.0	10764
4	201.1093	4.5	24226
5	205.0595	14.2	75702
6	217.1040	2.2	11504
7	225.0729	37.0	197558
8	226.0760	3.4	18154
9	226.9509	3.1	16355
10	230.0781	4.6	24645
11	239.0882	2.7	14430
12	242.2834	2.7	14580
13	245.0776	4.8	25531
14	250.9918	13.8	73796
15	251.0520	3.4	18011
16	257.0987	2.2	11879
17	269.2077	2.3	12021
18	286.1408	26.5	141465
19	287.1440	4.3	22728
20	288.9214	2.1	11205
21	297.0936	3.0	16033
22	300.1196	3.2	16868
23	301.1401	7.2	38575
24	302.0991	3.8	20038
25	304.2600	5.8	30927
26	313.2339	2.2	11690
27	335.1669	1.8	9468
28	341.2654	2.0	10543
29	345.2026	4.0	21449
30	348.9893	2.6	13771
31	350.2658	1.9	10196
32	350.9862	2.7	14565
33	379.1254	4.2	22204
34	379.1929	3.1	16418
35	423.2192	4.9	25965
36	425.1335	16.1	86171
37	426.1364	4.0	21462
38	441.2965	13.7	73382
39	442.2997	3.8	20424
40	447.1161	100.0	533712
41	448.1189	22.0	117579
42	449.1207	3.8	20049
43	463.0890	2.9	15726
44	465.1258	3.7	19890
45	467.2451	5.7	30418
46	469.0973	12.5	66947
47	470.1004	2.8	15055
48	509.0854	4.2	22575
49	511.2713	5.7	30683
50	527.0961	1.8	9855
51	528.5101	2.5	13478
52	533.0521	1.7	8912
53	537.0839	2.2	11940
54	537.3933	2.8	14774
55	541.1193	5.0	26589
56	542.1201	2.5	13378
57	543.1176	1.7	8906
58	553.4575	2.1	11216
59	555.2976	5.0	26910
60	561.1466	8.3	44082
61	562.1497	2.6	13625
62	577.0729	1.7	9122

High Resolution Mass Spectrometry Report

#	m/z	I %	I
63	599.3236	3.6	19055
64	615.1382	2.7	14254
65	643.3497	2.3	12205
66	659.1788	11.6	61925
67	659.6803	9.3	49873
68	660.1814	4.1	21768
69	681.1604	3.2	16938
70	681.6618	2.3	12086
71	690.1605	1.7	9226
72	716.1939	1.7	9277
73	716.6944	1.7	8975
74	865.4213	1.8	9615
75	871.2417	36.0	192178
76	871.7428	7.7	41048
77	872.2444	17.6	93984
78	872.7455	1.9	10090
79	873.2463	4.6	24607
80	882.2319	3.1	16801
81	882.7329	3.3	17437
82	883.2349	1.8	9817
83	893.2227	9.5	50736
84	893.7241	2.8	15002
85	894.2260	4.9	26187
86	915.2035	2.4	12705
87	928.2560	2.1	11291
88	928.7574	2.4	12847
89	933.2106	1.9	10090
90	985.2709	3.4	18192
91	986.2735	1.9	10289
92	1083.3030	2.5	13185
93	1083.8058	3.0	16001
94	1084.3073	2.2	11723
95	1094.2932	1.7	9177
96	1094.7956	2.1	11160
97	1295.3655	9.3	49879
98	1296.3696	7.0	37176
99	1297.3709	3.0	16107
100	1317.3464	1.7	9331

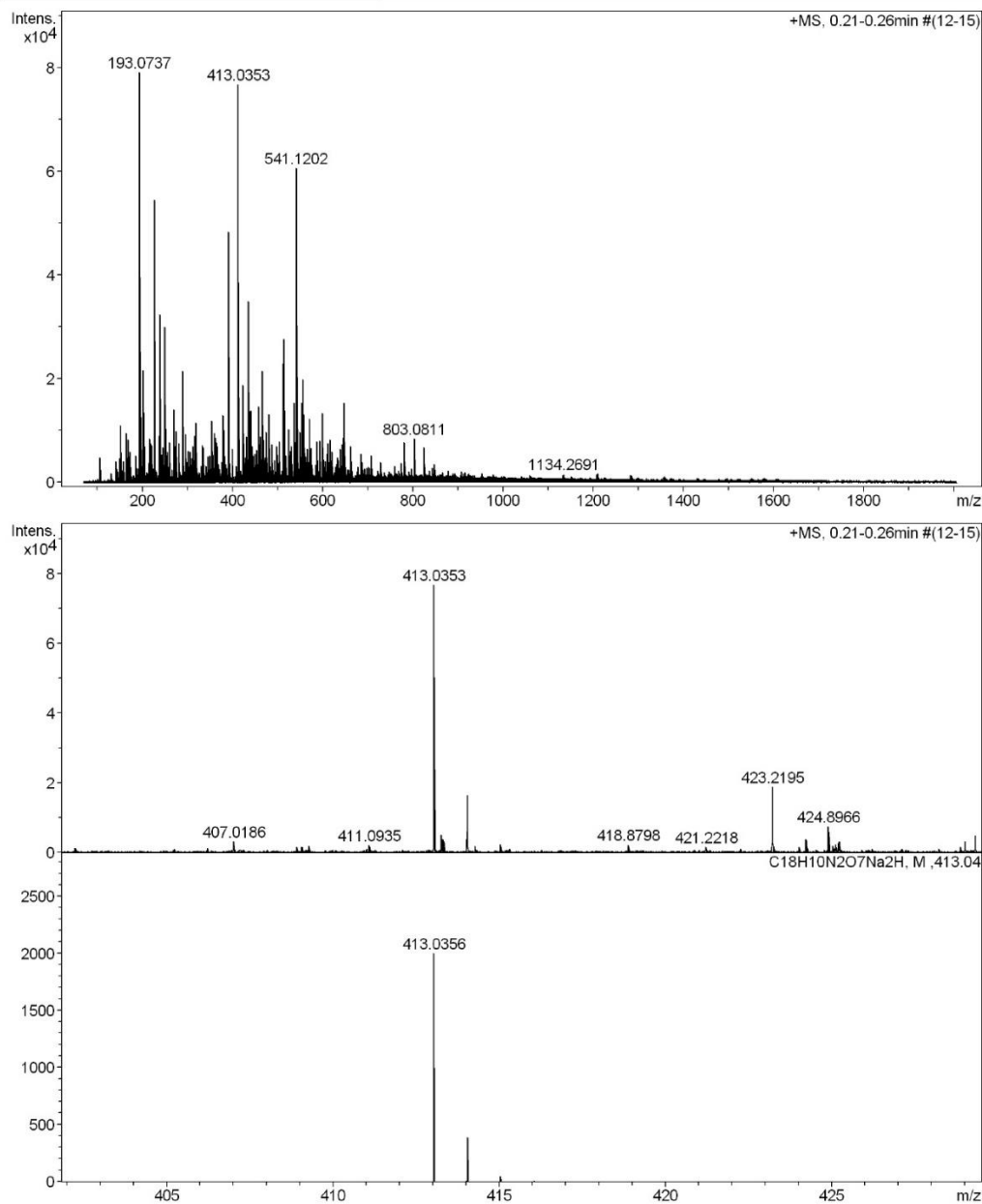
Acquisition Parameter

General	Fore Vacuum	2.40e+000 mBar	High Vacuum	1.11e-007 mBar	Source Type	ESI
	Scan Begin	75 m/z	Scan End	2000 m/z	Ion Polarity	Positive
Source	Set Nebulizer	2.0 Bar	Set Capillary	4500 V	Set Dry Gas	8.0 l/min
	Set Dry Heater	200 °C	Set End Plate Offset	-500 V		
Quadrupole	Set Ion Energy (MS only)	4.0 eV				
Coll. Cell	Collision Energy	8.0 eV	Set Collision Cell RF	600.0 Vpp	100.0 Vpp	
Ion Cooler	Set Ion Cooler Transfer Time	75.0 µs	Set Ion Cooler Pre Pulse Storage Time	10.0 µs		

High Resolution Mass Spectrometry Report

Sample Name **JL-747**
Comment

Instrument maXis 4G
Method ms_nocolumn_mid_pos.m



High Resolution Mass Spectrometry Report

Measured m/z vs. theoretical m/z

Meas. m/z	#	Formula	Score	m/z	err [mDa]	err [ppm]	mSigma	rdb	e ⁻ Conf	z
413.0353	1	C 18 H 11 N 2 Na 2 O 7	100.00	413.0356	0.3	0.8	7.4	13.5	even	1+

Mass list

#	m/z	I %	I
1	153.0339	13.9	10979
2	164.1070	12.2	9654
3	169.0111	10.4	8243
4	193.0737	100.0	79136
5	194.0767	7.9	6283
6	195.0707	32.0	25345
7	198.0524	8.2	6464
8	201.1095	27.6	21811
9	205.0597	17.2	13585
10	217.1042	10.7	8483
11	218.0810	9.5	7499
12	220.9341	9.2	7249
13	226.9513	69.0	54571
14	237.0846	11.4	9046
15	238.8838	10.2	8095
16	239.1614	9.2	7266
17	240.0628	40.9	32338
18	245.0779	8.7	6915
19	249.1361	38.0	30089
20	251.1330	13.2	10464
21	261.1306	9.8	7758
22	271.1178	17.8	14103
23	275.1613	12.6	9974
24	281.0480	9.6	7635
25	288.9217	27.1	21477
26	296.2192	11.9	9417
27	312.8881	8.8	6987
28	317.2447	11.5	9104
29	319.2602	14.7	11616
30	333.1695	9.1	7189
31	335.1673	8.6	6842
32	353.2655	15.2	12006
33	360.3229	12.1	9606
34	362.9261	10.9	8616
35	365.0900	8.6	6816
36	365.1050	9.9	7827
37	366.0881	8.8	6968
38	379.1935	16.4	12953
39	381.1005	12.8	10096
40	381.2969	12.3	9756
41	391.0534	61.1	48327
42	392.0565	13.1	10368
43	399.3074	8.2	6522
44	413.0353	97.0	76762
45	414.0385	20.8	16470
46	423.2195	23.8	18811
47	424.8966	9.6	7578
48	430.9132	11.3	8936
49	435.0172	44.1	34888
50	436.0197	8.6	6823
51	439.1236	17.5	13823
52	441.2969	17.6	13939
53	443.3337	8.9	7041
54	453.0243	8.0	6332
55	456.9988	18.5	14674
56	461.2884	11.2	8900
57	467.1015	25.7	20308
58	467.2458	27.3	21609
59	468.1021	10.6	8382
60	475.0057	12.3	9744
61	481.0220	16.8	13281
62	487.3599	9.3	7351

High Resolution Mass Spectrometry Report

#	m/z	I %	I
63	497.3955	8.8	7001
64	503.0039	10.0	7948
65	511.2719	28.9	22907
66	513.1432	34.9	27649
67	514.1443	14.9	11813
68	515.1415	9.8	7783
69	524.9862	13.0	10292
70	531.3861	9.0	7112
71	536.1649	19.5	15410
72	537.1653	10.2	8041
73	541.1202	76.7	60673
74	542.1211	38.3	30344
75	542.9926	11.9	9408
76	543.1190	25.9	20486
77	544.1185	9.5	7555
78	549.0098	12.4	9835
79	553.4584	19.4	15315
80	554.4615	8.0	6330
81	555.2982	25.0	19823
82	557.0938	16.7	13227
83	558.0947	7.9	6289
84	566.9599	8.1	6421
85	569.4322	15.6	12336
86	570.9913	11.3	8927
87	575.4123	8.5	6739
88	587.1619	10.1	7971
89	592.9732	10.2	8101
90	599.3245	17.0	13453
91	610.9802	9.6	7569
92	615.1388	10.5	8282
93	638.9783	8.2	6468
94	643.3505	9.4	7419
95	646.1548	10.9	8639
96	648.1536	19.3	15292
97	660.9612	8.9	7006
98	781.0990	9.7	7709
99	803.0811	10.7	8485
100	825.0627	8.6	6815

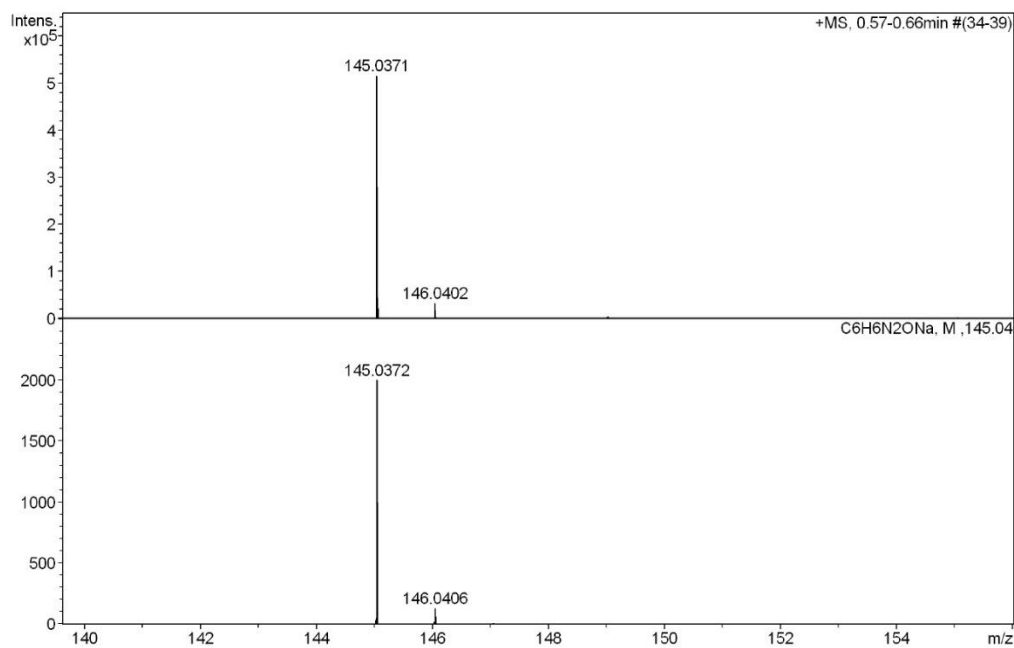
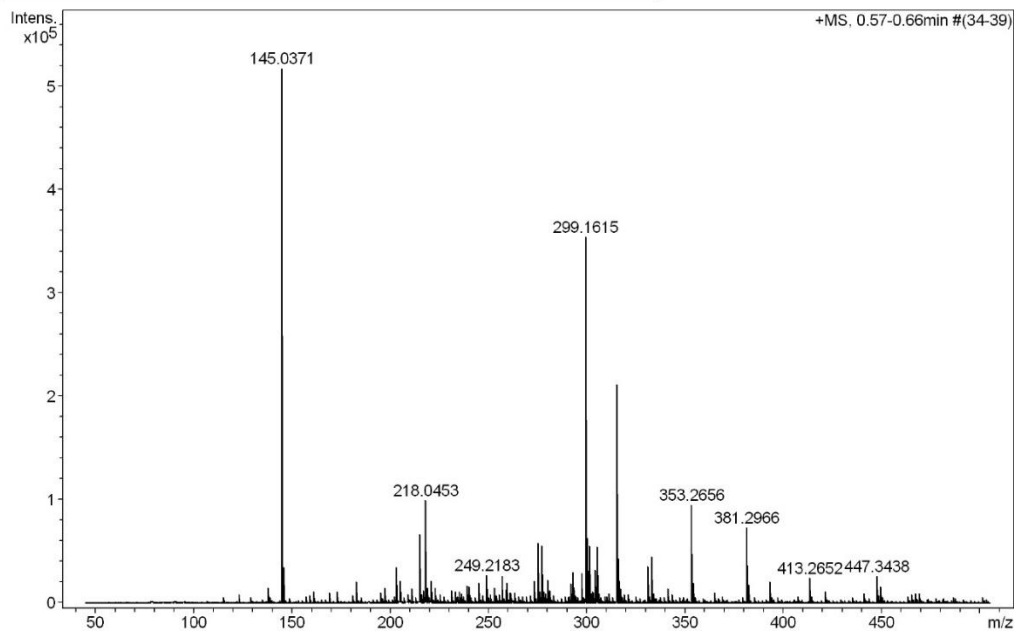
Acquisition Parameter

General	Fore Vacuum	2.48e+000 mBar	High Vacuum	9.43e-008 mBar	Source Type	ESI
	Scan Begin	75 m/z	Scan End	2000 m/z	Ion Polarity	Positive
Source	Set Nebulizer	2.0 Bar	Set Capillary	4500 V	Set Dry Gas	8.0 l/min
	Set Dry Heater	200 °C	Set End Plate Offset	-500 V		
Quadrupole	Set Ion Energy (MS only)	4.0 eV				
Coll. Cell	Collision Energy	8.0 eV	Set Collision Cell RF	600.0 Vpp	100.0 Vpp	
Ion Cooler	Set Ion Cooler Transfer Time	75.0 µs	Set Ion Cooler Pre Pulse Storage Time	10.0 µs		

High Resolution Mass Spectrometry Report

Sample Name **JL-717**
Comment analyzed in MeOH

Instrument maXis 4G
Method 21 Direct_pos_low.m



High Resolution Mass Spectrometry Report

Measured m/z vs. theoretical m/z

Meas. m/z	#	Formula	Score	m/z	err [mDa]	err [ppm]	mSigma	rdb	e ⁻ Conf	z
145.0371	1	C 6 H 6 N 2 Na O	100.00	145.0372	0.1	0.8	4.3	4.5	even	1+

Mass list

#	m/z	I %	I
1	138.0887	2.8	14635
2	145.0371	100.0	517375
3	146.0402	6.6	34402
4	161.0109	2.0	10352
5	161.0957	2.2	11146
6	169.0468	1.9	9937
7	173.0781	2.1	10643
8	183.0527	4.0	20865
9	195.0626	1.6	8300
10	195.0991	1.9	9736
11	197.0780	2.8	14687
12	203.0522	6.6	34304
13	205.0597	4.1	21130
14	209.1145	1.6	8446
15	211.0938	2.7	14166
16	215.0675	12.9	66664
17	217.1044	2.3	11983
18	218.0453	19.2	99125
19	219.1354	2.9	15043
20	221.1166	4.2	21488
21	223.0940	2.8	14551
22	225.1096	1.6	8287
23	231.1351	1.9	9674
24	231.1713	2.3	11869
25	233.0776	2.2	11393
26	235.1301	1.7	8982
27	235.1682	2.1	10739
28	236.0712	1.8	9371
29	239.0886	3.2	16798
30	240.0271	3.0	15519
31	245.0778	3.8	19589
32	245.1871	3.6	18405
33	249.1456	2.0	10238
34	249.2183	5.2	26680
35	253.2133	2.9	15234
36	255.2676	1.7	8638
37	257.1506	5.1	26166
38	259.1297	2.5	12686
39	259.2026	3.7	19213
40	261.1268	1.9	9868
41	263.1247	1.9	9750
42	273.2183	4.2	21738
43	275.1248	11.3	58482
44	275.1975	1.6	8415
45	276.1279	1.9	9784
46	276.1587	2.1	10997
47	277.1402	2.5	13172
48	277.1788	3.6	18459
49	277.2132	3.4	17464
50	277.2496	10.6	54859
51	278.1762	1.8	9357
52	278.2522	2.1	11055
53	279.2290	1.8	9410
54	280.1901	4.2	21950
55	281.1716	2.2	11546
56	292.1904	3.5	18325
57	293.1740	5.8	30125
58	293.2077	2.2	11224
59	293.2444	2.6	13371
60	297.2393	5.7	29387
61	299.1615	68.4	354124
62	300.1642	12.2	62910

High Resolution Mass Spectrometry Report

#	m/z	I %	I
63	301.1404	10.8	55730
64	301.1750	3.4	17367
65	302.1438	1.8	9220
66	303.0845	2.2	11419
67	303.2288	2.0	10421
68	304.2605	6.1	31510
69	305.1003	10.4	53923
70	305.2443	2.7	13787
71	305.2805	2.4	12332
72	306.1034	1.8	9064
73	311.1247	1.8	9118
74	315.1353	5.8	29922
75	315.1561	40.8	211004
76	315.2647	1.6	8353
77	316.1588	8.4	43279
78	317.1703	2.6	13688
79	317.2807	2.2	11345
80	321.2388	1.6	8209
81	331.1300	6.9	35612
82	331.1499	2.9	15045
83	333.1666	8.6	44632
84	334.1698	1.7	8768
85	341.2655	2.7	14124
86	353.2656	18.4	95229
87	354.2688	3.8	19744
88	365.2735	1.9	9957
89	381.2966	14.1	72830
90	382.3001	3.3	17282
91	393.2970	4.0	20726
92	413.2652	4.6	23975
93	421.2093	2.2	11515
94	421.3278	1.8	9118
95	441.2962	1.8	9112
96	447.3438	5.0	25694
97	449.3724	3.1	15818
98	465.3689	1.6	8479
99	467.3845	1.8	9253
100	469.3269	1.8	9241

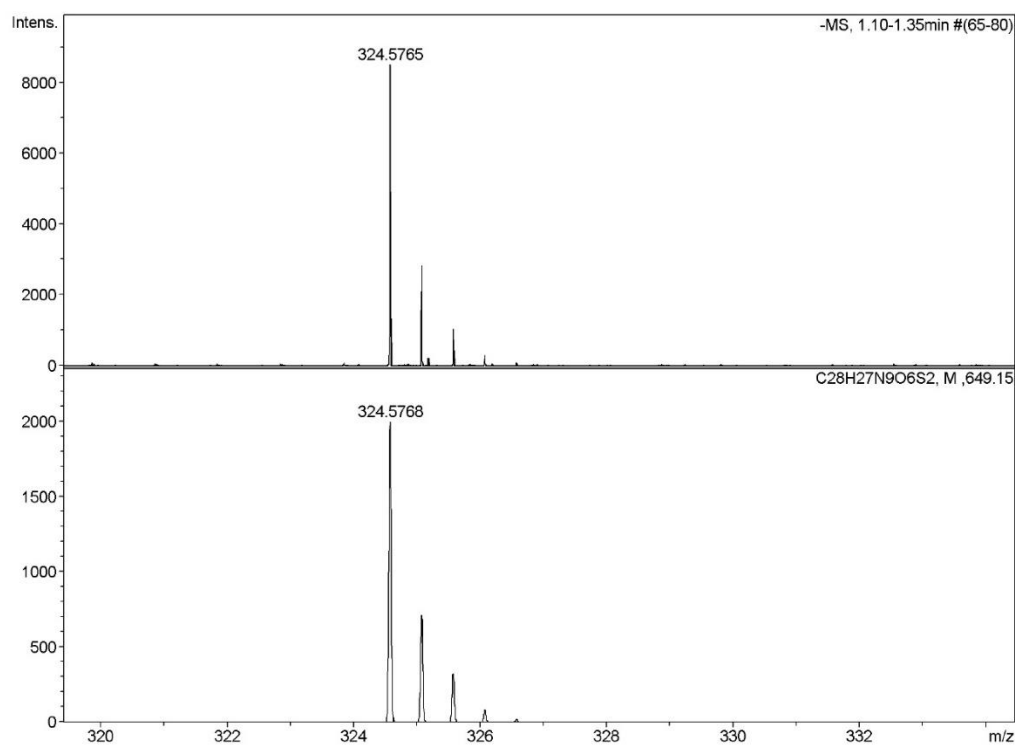
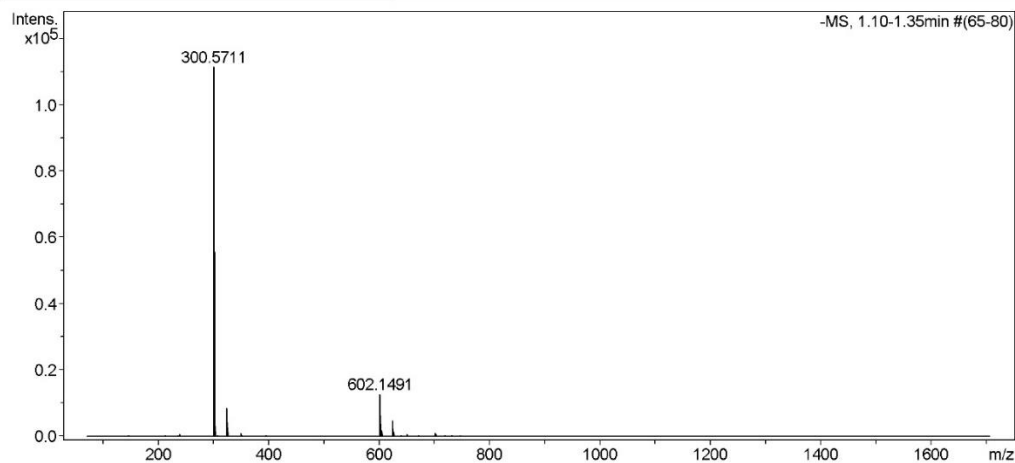
Acquisition Parameter

General	Fore Vacuum	2.48e+000 mBar	High Vacuum	9.56e-008 mBar	Source Type	ESI
	Scan Begin	50 m/z	Scan End	500 m/z	Ion Polarity	Positive
Source	Set Nebulizer	0.4 Bar	Set Capillary	3600 V	Set Dry Gas	3.0 l/min
	Set Dry Heater	180 °C	Set End Plate Offset	-500 V		
Quadrupole	Set Ion Energy (MS only)	4.0 eV				
Coll. Cell	Collision Energy	8.0 eV	Set Collision Cell RF	350.0 Vpp	55.0 Vpp	
Ion Cooler	Set Ion Cooler Transfer Time	55.0 µs	Set Ion Cooler Pre Pulse Storage Time	7.0 µs		

High Resolution Mass Spectrometry Report

Sample Name **JL-628**
Comment

Instrument maXis 4G
Method ms_c18_300-600_neg_2min.m



High Resolution Mass Spectrometry Report

Measured m/z vs. theoretical m/z

Meas. m/z	#	Formula	Score	m/z	err [mDa]	err [ppm]	mSigma	rdb	e ⁻ Conf	z
324.5765	1	C ₂₈ H ₂₇ N ₉ O ₆ S ₂	100.00	324.5768	0.4	1.1	26.9	20.0	even	2-

Mass list

#	m/z	I %	I
1	300.5711	100.0	111455
2	301.0724	29.2	32555
3	301.5706	11.8	13135
4	302.0711	3.1	3427
5	324.5765	7.6	8520
6	325.0778	2.5	2827
7	325.5764	1.0	1059
8	602.1491	11.5	12838
9	603.1517	3.6	4017
10	604.1481	1.5	1644
11	624.1309	4.4	4917
12	625.1336	1.3	1491
13	702.0742	1.0	1104

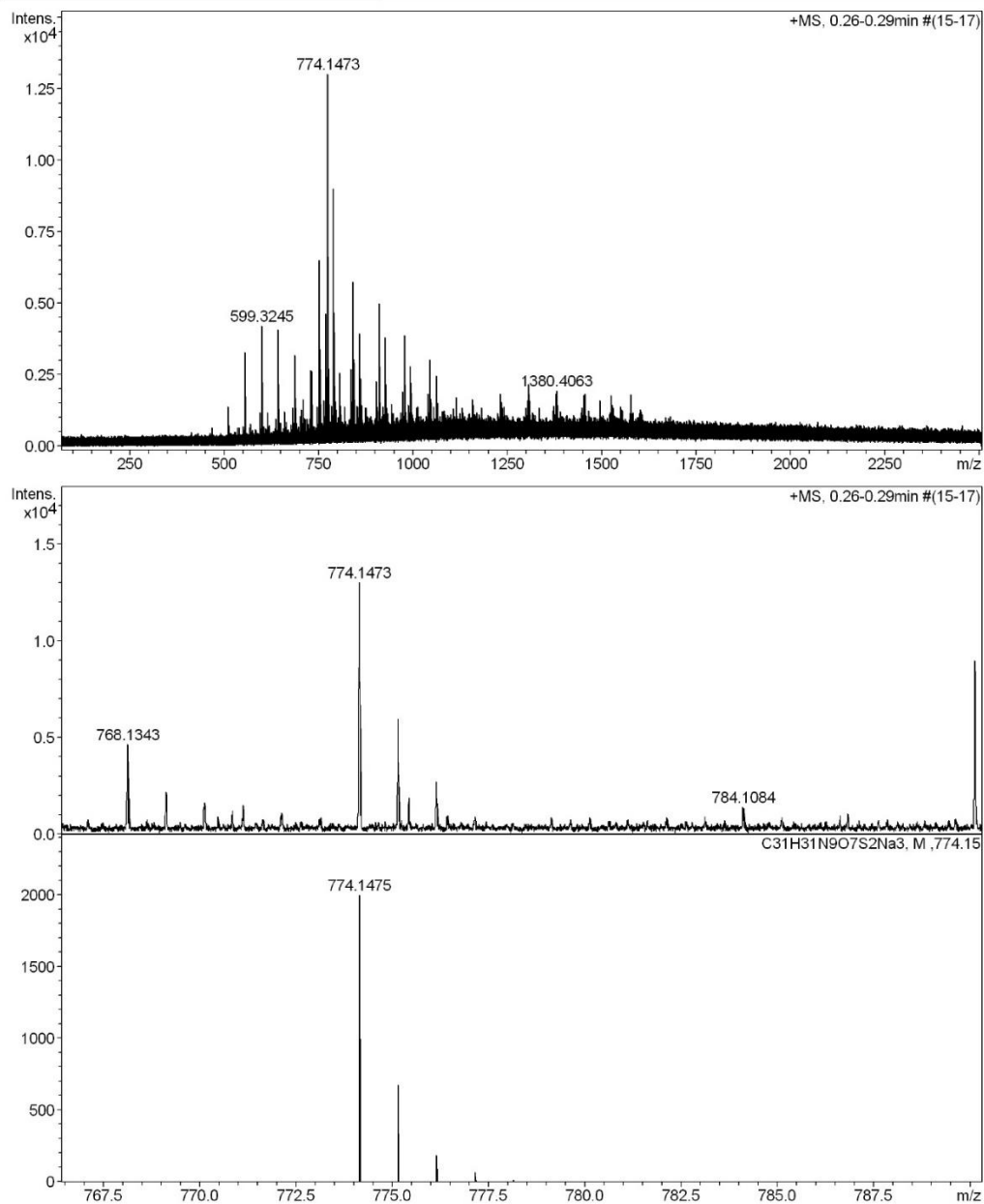
Acquisition Parameter

General	Fore Vacuum	2.29e+000 mBar	High Vacuum	9.97e-008 mBar	Source Type	ESI
	Scan Begin	75 m/z	Scan End	1700 m/z	Ion Polarity	Negative
Source	Set Nebulizer	2.0 Bar	Set Capillary	4500 V	Set Dry Gas	8.0 l/min
	Set Dry Heater	200 °C	Set End Plate Offset	-500 V		
Quadrupole	Set Ion Energy (MS only)	-4.0 eV				
Coll. Cell	Collision Energy	-10.0 eV	Set Collision Cell RF	350.0 Vpp	100.0 Vpp	
Ion Cooler	Set Ion Cooler Transfer Time	75.0 µs	Set Ion Cooler Pre Pulse Storage Time	10.0 µs		

High Resolution Mass Spectrometry Report

Sample Name **JL-732**
Comment

Instrument maXis 4G
Method ms_nocolumn_high_pos_use_acn.m



High Resolution Mass Spectrometry Report

Measured m/z vs. theoretical m/z

Meas. m/z	#	Formula	Score	m/z	err [mDa]	err [ppm]	mSigma	rdb	e ⁻ Conf	z
774.1473	1	C ₃₁ H ₃₁ N ₉ Na ₃ O ₇ S ₂	100.00	774.1475	0.3	0.3	41.2	19.5	even	1+

Mass list

#	m/z	I %	I
1	511.2726	10.6	1380
2	555.2983	25.3	3290
3	599.3245	32.4	4218
4	600.3289	11.2	1457
5	643.3517	31.3	4081
6	644.3542	10.2	1328
7	682.4238	10.3	1345
8	687.3776	24.7	3212
9	688.3818	10.5	1363
10	703.3511	9.8	1283
11	708.5098	12.6	1641
12	730.1839	20.5	2677
13	731.4043	20.3	2642
14	746.1521	10.6	1375
15	752.1651	50.0	6517
16	753.1675	19.6	2558
17	754.1617	11.5	1499
18	764.6412	12.3	1607
19	768.1343	35.7	4656
20	769.1354	16.8	2183
21	770.1281	12.9	1675
22	771.1310	11.8	1534
23	774.1473	100.0	13030
24	775.1513	46.0	5989
25	775.4316	14.6	1897
26	776.1489	20.9	2721
27	784.1084	10.6	1382
28	790.1204	69.1	9009
29	791.1246	30.7	4003
30	792.1128	19.9	2597
31	793.1080	12.3	1597
32	794.0967	12.1	1571
33	806.0956	19.8	2584
34	807.0970	11.5	1494
35	836.1173	18.9	2466
36	837.1213	10.6	1388
37	838.8399	10.9	1421
38	842.1353	44.2	5762
39	843.1376	21.3	2772
40	844.1379	13.6	1778
41	852.0932	10.9	1421
42	854.0717	10.7	1389
43	858.1090	30.3	3954
44	859.1119	17.4	2267
45	860.0875	18.2	2370
46	861.0932	11.2	1463
47	862.0830	12.4	1615
48	864.0804	11.1	1444
49	904.1064	17.5	2274
50	910.1228	38.3	4995
51	911.1249	18.7	2442
52	912.1242	11.8	1540
53	926.0952	25.2	3285
54	927.1025	16.4	2131
55	928.0812	16.7	2172
56	942.0684	11.5	1503
57	972.0912	14.8	1927
58	978.1104	29.8	3876
59	979.1133	16.0	2083
60	988.0654	11.3	1467
61	994.0850	21.5	2796
62	995.0858	14.4	1877

High Resolution Mass Spectrometry Report

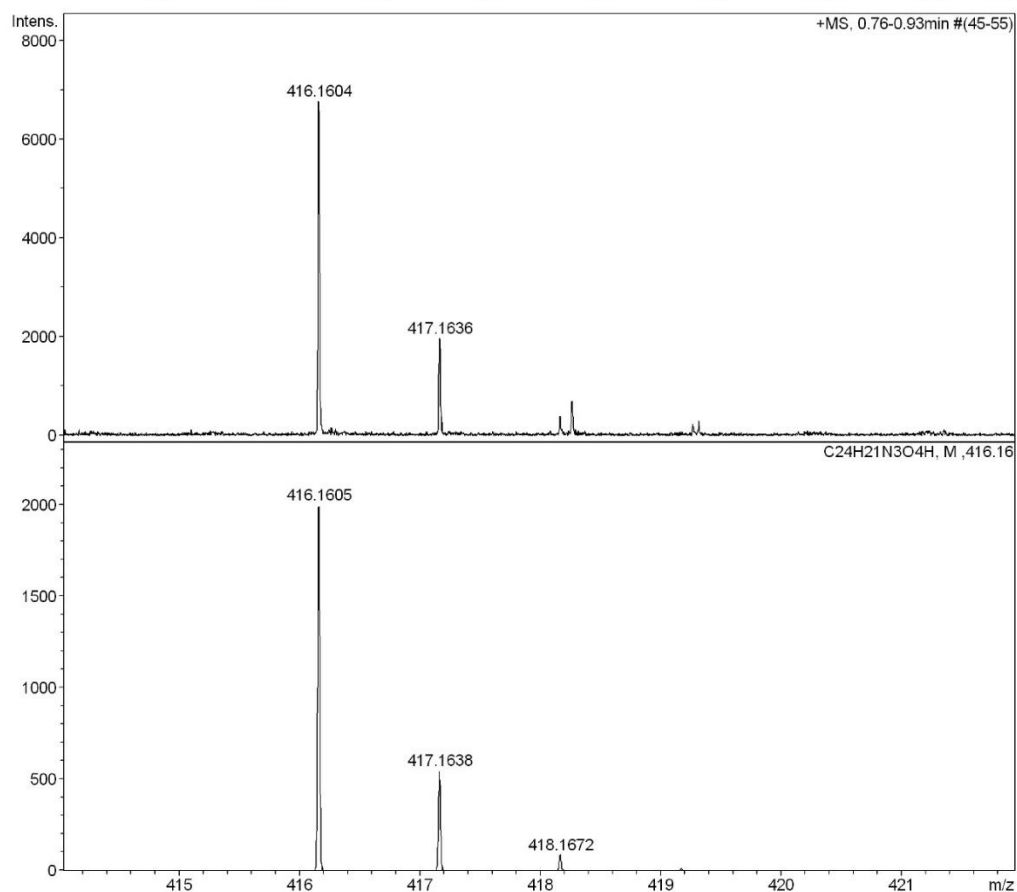
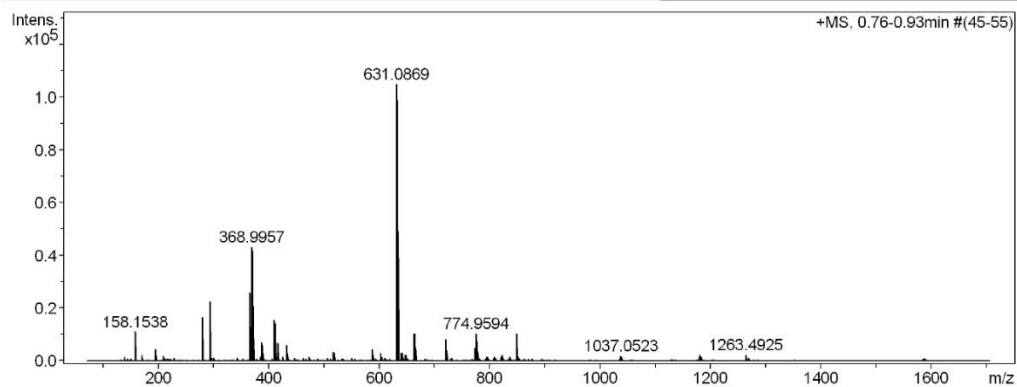
#	m/z	I %	I
63	996.0684	12.6	1636
64	1040.0786	14.2	1853
65	1046.0990	23.2	3028
66	1062.0695	18.9	2465
67	1063.0758	12.7	1650
68	1064.0696	11.6	1518
69	1114.0850	13.1	1712
70	1156.3474	12.6	1643
71	1157.3484	12.1	1577
72	1230.3685	12.4	1611
73	1231.3665	14.1	1834
74	1232.3674	12.4	1611
75	1304.3873	12.3	1605
76	1305.3874	13.7	1786
77	1306.3804	12.6	1646
78	1307.3827	12.4	1612
79	1379.4055	14.3	1864
80	1380.4063	15.0	1954
81	1381.4037	14.4	1875
82	1453.4243	13.6	1770
83	1454.4319	14.3	1865
84	1455.4235	13.2	1721
85	1494.9403	12.3	1605
86	1523.8931	12.8	1666
87	1577.8078	13.8	1803

Acquisition Parameter

General	Fore Vacuum	2.40e+000 mBar	High Vacuum	1.06e-007 mBar	Source Type	ESI
	Scan Begin	75 m/z	Scan End	2500 m/z	Ion Polarity	Positive
Source	Set Nebulizer	2.0 Bar	Set Capillary	4500 V	Set Dry Gas	8.0 l/min
	Set Dry Heater	200 °C	Set End Plate Offset	-500 V		
Quadrupole	Set Ion Energy (MS only)	4.0 eV				
Coll. Cell	Collision Energy	12.0 eV	Set Collision Cell RF	2000.0 Vpp	800.0 Vpp	
Ion Cooler	Set Ion Cooler Transfer Time	120.0 µs	Set Ion Cooler Pre Pulse Storage Time	18.0 µs		

High Resolution Mass Spectrometry Report

Sample Name **JL-707** Instrument **maXis 4G**
 Comment **dissolved in acetone, analyzed in MeCN** Method **22 Direct_pos_mid.m**



High Resolution Mass Spectrometry Report

Measured m/z vs. theoretical m/z

Meas. m/z	#	Formula	Score	m/z	err [mDa]	err [ppm]	mSigma	rdb	e ⁻ Conf	z
416.1604	1	C ₂₄ H ₂₂ N ₃ O ₄	100.00	416.1605	0.1	0.2	27.8	15.5	even	1+

Mass list

#	m/z	I %	I
1	139.0729	1.5	1622
2	158.1538	10.6	11154
3	159.1572	1.1	1130
4	170.1174	2.4	2504
5	196.0636	4.3	4535
6	210.1486	1.7	1797
7	228.1595	1.1	1141
8	279.0933	15.8	16666
9	280.0969	3.1	3293
10	293.1090	21.3	22447
11	294.1122	4.3	4522
12	297.0594	1.3	1400
13	301.0754	1.3	1347
14	343.0304	1.1	1208
15	366.0467	24.8	26051
16	367.0498	5.9	6160
17	368.0450	10.6	11163
18	368.9957	41.2	43277
19	369.0480	2.3	2413
20	369.9990	8.1	8528
21	370.9954	39.8	41830
22	371.9986	8.3	8762
23	386.0217	1.4	1442
24	387.0060	6.7	6992
25	388.0133	1.3	1321
26	389.0060	5.7	5971
27	390.0093	1.3	1346
28	410.0221	14.7	15500
29	411.0256	3.4	3621
30	412.0220	13.8	14541
31	413.0251	3.1	3269
32	416.1604	6.4	6780
33	417.1636	1.9	1976
34	425.3627	1.7	1780
35	433.1869	5.7	5984
36	434.1904	1.9	1994
37	462.2913	1.1	1131
38	473.3202	1.6	1640
39	506.3172	1.2	1228
40	517.2955	3.1	3306
41	519.2950	3.1	3262
42	550.3435	1.2	1214
43	587.1112	4.3	4532
44	588.1143	1.6	1694
45	589.1097	2.1	2185
46	603.1058	2.9	3074
47	604.1090	1.3	1368
48	605.1053	1.4	1428
49	610.1833	1.3	1364
50	631.0869	100.0	105149
51	632.0901	37.2	39132
52	633.0869	94.1	98962
53	634.0898	37.1	39035
54	635.0929	6.9	7280
55	640.7639	3.0	3134
56	641.2658	2.9	3062
57	641.7666	1.4	1450
58	643.2414	1.2	1287
59	647.0808	2.1	2230
60	649.0810	2.1	2221
61	663.0584	9.8	10303
62	664.0618	3.7	3916

High Resolution Mass Spectrometry Report

#	m/z	I %	I
63	665.0583	9.9	10406
64	666.0620	3.9	4059
65	667.0622	1.1	1122
66	721.1477	7.8	8206
67	722.1508	3.1	3232
68	730.9835	1.0	1101
69	772.9603	4.8	5066
70	773.9636	2.0	2067
71	774.9594	10.1	10602
72	775.9632	4.1	4301
73	776.9589	7.1	7462
74	777.9629	2.6	2727
75	778.9591	1.7	1738
76	794.7218	1.5	1603
77	796.7376	1.6	1641
78	808.7376	1.5	1580
79	810.7524	1.1	1173
80	820.7383	1.6	1634
81	822.7529	2.3	2390
82	823.7566	1.3	1325
83	824.7672	1.1	1194
84	836.7680	1.5	1586
85	848.3400	9.9	10459
86	848.7692	1.6	1633
87	849.3432	5.7	5996
88	850.3461	1.8	1923
89	850.7844	1.3	1348
90	853.2958	1.3	1317
91	1037.0523	2.1	2160
92	1038.0532	1.2	1280
93	1039.0512	1.4	1464
94	1178.9254	1.6	1667
95	1180.9244	2.1	2175
96	1181.9277	1.1	1199
97	1182.9245	1.5	1582
98	1263.4925	2.3	2392
99	1264.4960	2.2	2293
100	1268.4492	1.1	1155

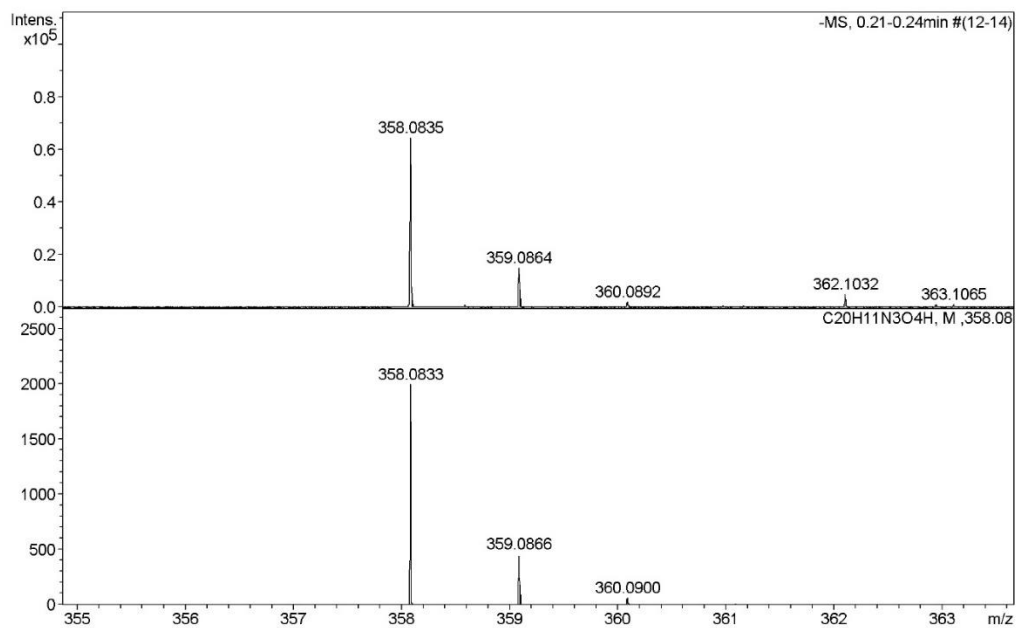
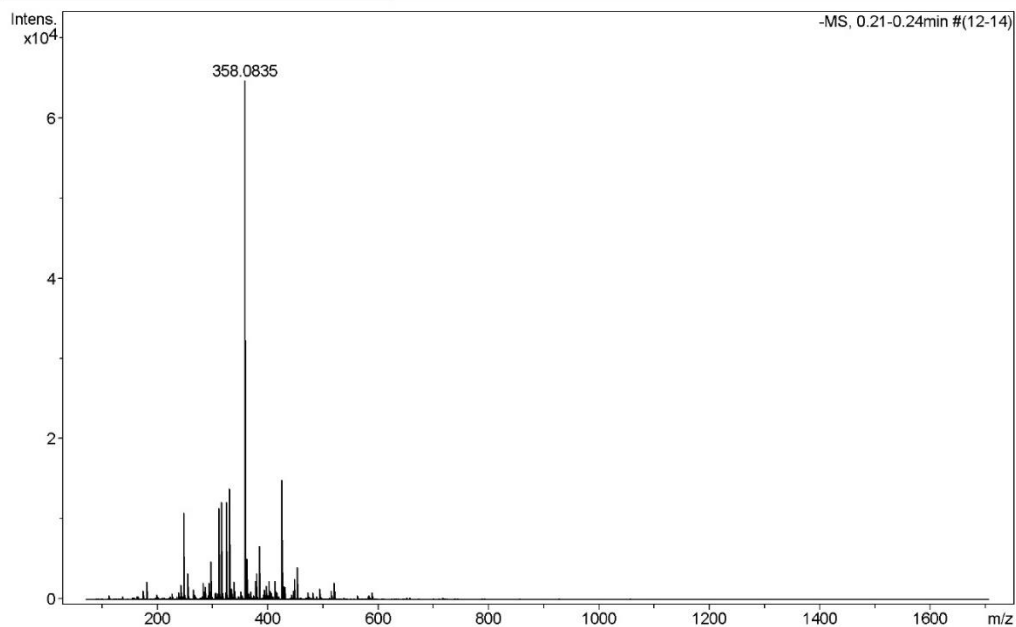
Acquisition Parameter

General	Fore Vacuum	2.48e+000 mBar	High Vacuum	1.11e-007 mBar	Source Type	ESI
	Scan Begin	75 m/z	Scan End	1700 m/z	Ion Polarity	Positive
Source	Set Nebulizer	0.4 Bar	Set Capillary	3600 V	Set Dry Gas	4.0 l/min
	Set Dry Heater	180 °C	Set End Plate Offset	-500 V		
Quadrupole	Set Ion Energy (MS only)	4.0 eV				
Coll. Cell	Collision Energy	8.0 eV	Set Collision Cell RF	350.0 Vpp	100.0 Vpp	
Ion Cooler	Set Ion Cooler Transfer Time	75.0 µs	Set Ion Cooler Pre Pulse Storage Time	10.0 µs		

High Resolution Mass Spectrometry Report

Sample Name **JL-710**
Comment

Instrument maXis 4G
Method ms_nocolumn_mid_neg.m



High Resolution Mass Spectrometry Report

Measured m/z vs. theoretical m/z

Meas. m/z	#	Formula	Score	m/z	err [mDa]	err [ppm]	mSigma	rdB	e ⁻ Conf	z
358.0835	1	C ₂₀ H ₁₂ N ₃ O ₄	100.00	358.0833	-0.2	-0.4	2.6	16.5	even	1-

Mass list

#	m/z	I %	I
1	174.9561	1.7	1109
2	180.9731	3.4	2220
3	242.9436	2.9	1863
4	248.9605	16.7	10774
5	255.2329	5.0	3222
6	265.1476	1.9	1258
7	283.2644	3.2	2092
8	286.0870	2.2	1414
9	293.1767	3.1	1988
10	297.1530	7.2	4674
11	310.9308	2.7	1763
12	311.1685	17.6	11412
13	312.1718	3.7	2421
14	316.9482	18.8	12153
15	325.1841	18.8	12155
16	326.1871	4.6	2991
17	330.0770	21.4	13810
18	331.0807	4.7	3060
19	333.0769	1.8	1151
20	334.8972	2.1	1327
21	339.1997	3.4	2181
22	358.0835	100.0	64682
23	359.0864	23.2	15003
24	360.0892	3.3	2135
25	362.1032	7.8	5034
26	363.1065	1.9	1199
27	378.9184	3.5	2257
28	379.1562	1.8	1135
29	380.0651	5.0	3240
30	384.9354	10.2	6625
31	393.1715	1.8	1195
32	398.0647	2.7	1718
33	402.8851	3.5	2262
34	404.8821	1.6	1060
35	414.0590	3.6	2338
36	426.0708	23.1	14935
37	427.0736	5.2	3365
38	430.0904	2.4	1544
39	446.9060	1.7	1104
40	448.0525	3.9	2509
41	452.9229	6.2	4015
42	494.0586	2.0	1311
43	516.0404	1.8	1135
44	520.9103	3.2	2038

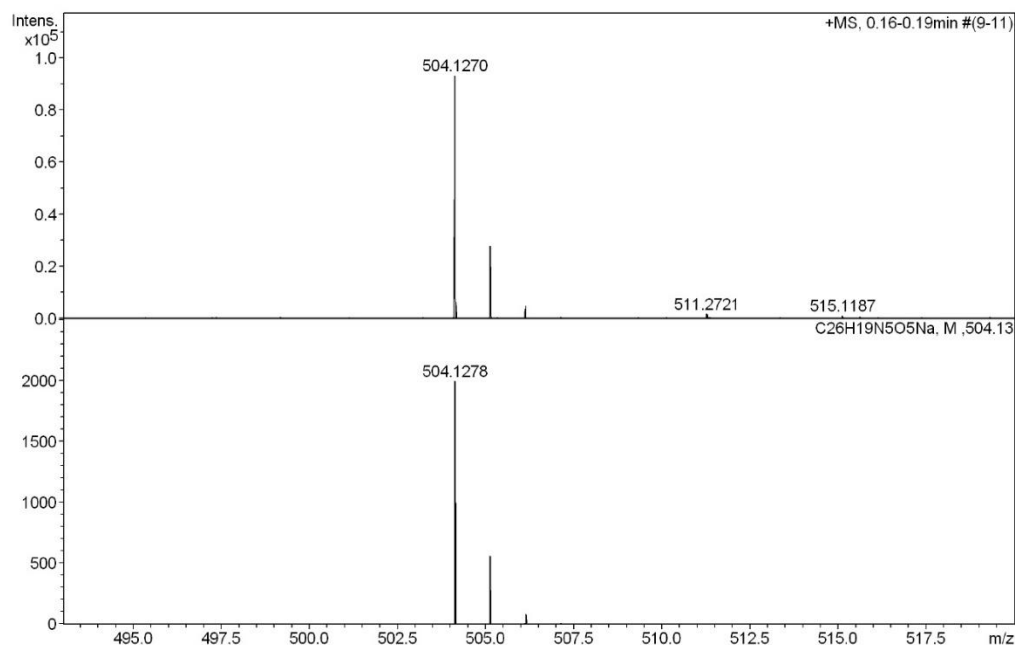
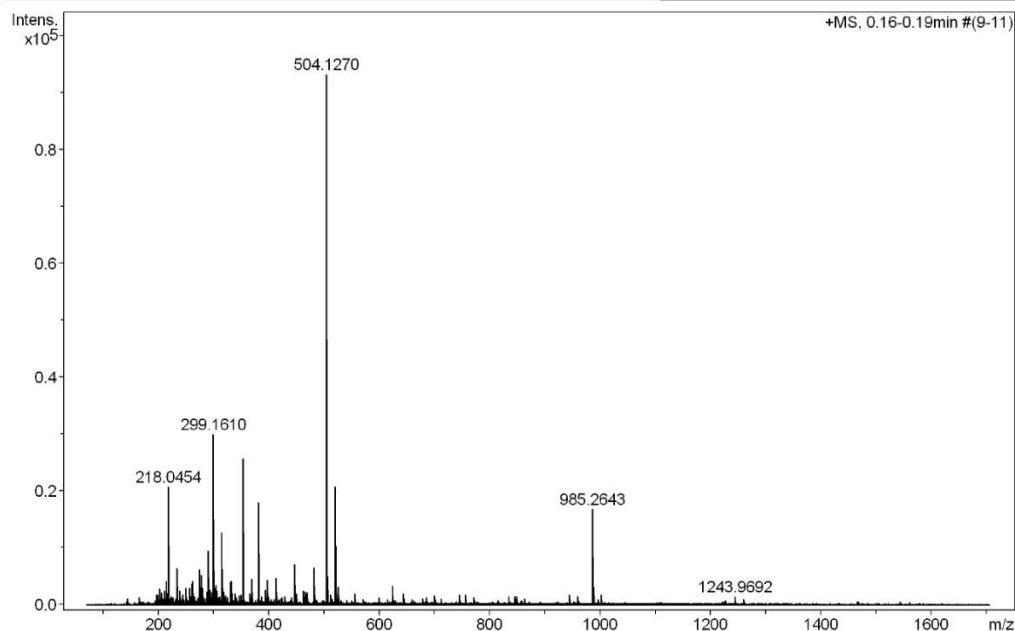
Acquisition Parameter

General	Fore Vacuum	2.60e+000 mBar	High Vacuum	1.01e-007 mBar	Source Type	ESI
	Scan Begin	75 m/z	Scan End	1700 m/z	Ion Polarity	Negative
Source	Set Nebulizer	0.4 Bar	Set Capillary	4500 V	Set Dry Gas	4.0 l/min
	Set Dry Heater	180 °C	Set End Plate Offset	-500 V		
Quadrupole	Set Ion Energy (MS only)	-4.0 eV				
Coll. Cell	Collision Energy	-10.0 eV	Set Collision Cell RF	100.0 Vpp	100.0 Vpp	
Ion Cooler	Set Ion Cooler Transfer Time	75.0 µs	Set Ion Cooler Pre Pulse Storage Time	10.0 µs		

High Resolution Mass Spectrometry Report

Sample Name **JL-720**
 Comment analyzed in MeOH

Instrument maXis 4G
 Method 22 Direct_pos_mid.m



High Resolution Mass Spectrometry Report

Measured m/z vs. theoretical m/z

Meas. m/z	#	Formula	Score	m/z	err [mDa]	err [ppm]	mSigma	rdb	e ⁻ Conf	z
504.1270	1	C ₂₆ H ₁₉ N ₅ NaO ₅	100.00	504.1278	0.9	1.7	0.2	19.5	even	1+

Mass list

#	m/z	I %	I
1	197.0779	2.0	1873
2	198.0842	1.9	1762
3	203.0520	3.1	2931
4	205.0600	2.3	2184
5	211.0938	2.8	2573
6	215.0678	4.5	4227
7	217.1045	2.1	1961
8	218.0454	22.3	20777
9	218.2109	2.1	1934
10	219.0484	2.0	1845
11	234.0194	4.7	4394
12	234.2057	6.9	6455
13	239.0887	1.7	1559
14	240.0270	2.8	2574
15	245.0778	1.9	1817
16	249.2183	3.3	3057
17	257.1505	3.2	2995
18	261.1299	3.9	3683
19	262.2372	4.6	4311
20	274.2732	3.2	2972
21	275.1243	6.7	6291
22	277.1776	1.9	1734
23	277.2130	3.6	3328
24	277.2494	5.6	5183
25	279.2290	3.2	3027
26	288.2888	2.5	2313
27	290.2682	10.2	9489
28	291.1926	1.8	1706
29	291.2706	2.2	2072
30	293.1735	2.9	2661
31	293.2078	2.7	2491
32	293.2447	2.2	2063
33	297.2391	2.4	2264
34	299.1610	32.1	29975
35	300.1642	6.3	5897
36	301.1402	6.5	6088
37	303.2285	1.7	1610
38	304.2602	3.8	3533
39	304.2834	1.8	1698
40	305.1560	2.3	2183
41	305.2444	2.7	2486
42	315.1350	4.6	4271
43	315.1559	13.7	12734
44	315.1919	1.9	1763
45	316.1590	3.2	2983
46	317.1706	1.8	1719
47	319.2235	2.5	2332
48	321.2390	1.8	1642
49	331.1300	3.9	3642
50	331.1873	4.3	4024
51	333.1670	4.5	4163
52	339.1776	2.2	2062
53	347.1822	1.8	1650
54	349.1826	2.0	1903
55	353.2654	27.6	25783
56	354.2688	6.0	5561
57	365.2757	2.1	1971
58	369.2389	5.0	4646
59	381.2966	19.3	17980
60	382.3001	4.3	3968
61	386.2236	1.7	1550
62	393.2975	2.9	2691

High Resolution Mass Spectrometry Report

#	m/z	I %	I
63	397.2152	4.8	4465
64	397.2699	3.5	3248
65	397.7164	1.7	1600
66	399.1757	1.7	1564
67	413.2651	5.1	4712
68	414.2684	1.6	1532
69	447.3431	7.6	7122
70	448.3475	2.1	1943
71	449.3724	2.1	1976
72	463.3180	2.8	2603
73	465.3686	2.5	2352
74	467.2454	2.0	1893
75	469.3261	2.3	2107
76	482.1446	7.1	6645
77	483.1487	1.8	1659
78	504.1270	100.0	93259
79	505.1300	30.0	27960
80	506.1325	5.4	5020
81	511.2721	2.0	1844
82	520.1007	22.2	20749
83	521.1038	6.6	6153
84	522.1019	2.4	2226
85	526.1079	3.4	3126
86	555.2981	2.1	1967
87	624.0852	3.5	3295
88	644.0107	2.1	1958
89	699.1829	1.8	1718
90	744.6960	2.0	1833
91	745.1963	1.9	1737
92	755.6867	1.9	1742
93	756.1899	1.9	1780
94	848.3023	1.7	1554
95	943.9900	1.9	1774
96	959.9641	1.7	1566
97	985.2643	18.0	16815
98	986.2679	11.5	10737
99	987.2702	3.5	3220
100	1001.2398	2.0	1845

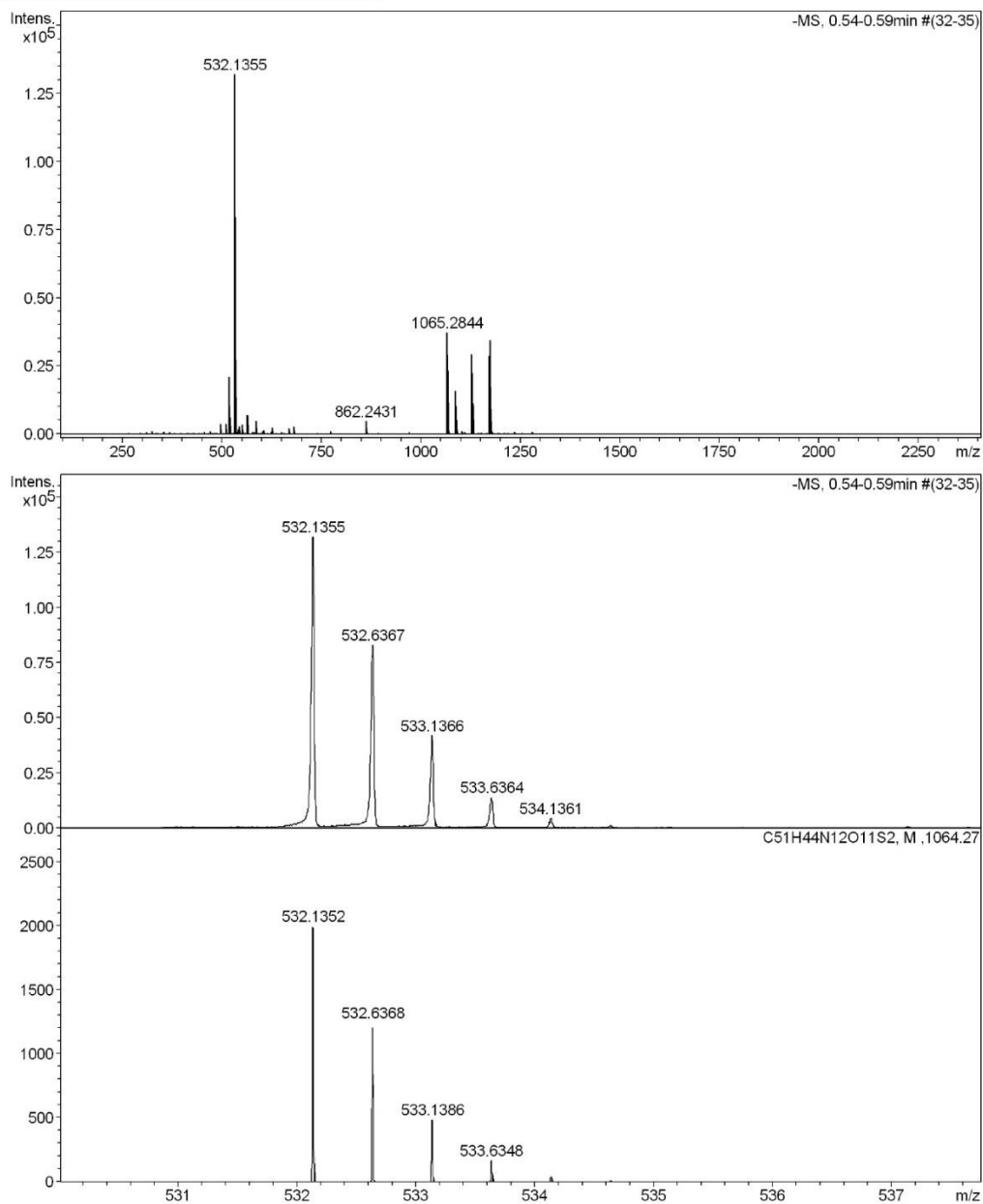
Acquisition Parameter

General	Fore Vacuum	2.53e+000 mBar	High Vacuum	9.56e-008 mBar	Source Type	ESI
	Scan Begin	75 m/z	Scan End	1700 m/z	Ion Polarity	Positive
Source	Set Nebulizer	0.4 Bar	Set Capillary	3600 V	Set Dry Gas	4.0 l/min
	Set Dry Heater	180 °C	Set End Plate Offset	-500 V		
Quadrupole	Set Ion Energy (MS only)	4.0 eV				
Coll. Cell	Collision Energy	8.0 eV	Set Collision Cell RF	350.0 Vpp	100.0 Vpp	
Ion Cooler	Set Ion Cooler Transfer Time	75.0 µs	Set Ion Cooler Pre Pulse Storage Time	10.0 µs		

High Resolution Mass Spectrometry Report

Sample Name **JL-745**
Comment

Instrument maXis 4G
Method 34 Direct_neg_high.m



High Resolution Mass Spectrometry Report

Measured m/z vs. theoretical m/z

Meas. m/z	#	Formula	Score	m/z	err [mDa]	err [ppm]	mSigma	rdb	e ⁻ Conf	z
532.1355	1	C 51 H 44 N 12 O 11 S 2	100.00	532.1352	-0.2	-0.4	10.0	36.0	even	2-

Mass list

#	m/z	I %	I
1	325.1843	0.8	1055
2	471.1320	0.8	995
3	496.1374	2.9	3803
4	496.6371	2.3	3080
5	497.1368	1.0	1305
6	510.1390	2.8	3759
7	510.6418	1.9	2550
8	511.1425	0.9	1197
9	518.1320	16.0	21094
10	518.6338	9.5	12592
11	519.1331	4.7	6224
12	519.6341	1.9	2539
13	531.9220	1.1	1450
14	531.9477	1.5	1926
15	531.9853	1.6	2067
16	532.1355	100.0	132093
17	532.2132	0.8	1089
18	532.2333	0.8	1060
19	532.2528	0.9	1127
20	532.2677	0.8	1118
21	532.3016	1.1	1392
22	532.3519	1.1	1486
23	532.3656	1.3	1749
24	532.4041	1.3	1674
25	532.4075	1.3	1705
26	532.4178	1.2	1542
27	532.4658	1.6	2120
28	532.4898	1.5	2023
29	532.5078	1.7	2202
30	532.6367	63.0	83190
31	532.7819	0.8	1075
32	532.8087	0.8	997
33	532.8363	0.8	1083
34	532.8613	1.0	1262
35	532.8740	0.8	1047
36	532.8998	0.9	1171
37	532.9191	0.9	1123
38	532.9430	0.9	1233
39	532.9493	0.9	1212
40	532.9695	1.0	1292
41	532.9929	1.0	1363
42	533.0064	1.0	1305
43	533.0309	1.0	1352
44	533.1366	31.9	42148
45	533.5701	0.8	1050
46	533.6364	10.8	14232
47	534.1361	3.6	4747
48	534.6382	1.1	1431
49	541.0995	1.5	2020
50	541.5996	0.9	1162
51	542.0981	1.2	1581
52	543.1246	2.1	2750
53	543.6279	1.2	1648
54	551.1415	2.8	3737
55	551.6429	1.5	1959
56	552.1448	0.9	1214
57	563.0918	5.3	7048
58	563.5942	3.6	4699
59	564.0925	5.4	7078
60	564.5909	2.9	3820
61	565.0903	1.3	1716
62	585.0830	3.5	4560

High Resolution Mass Spectrometry Report

#	m/z	I %	I
63	585.5854	2.3	2984
64	586.0836	3.7	4884
65	586.5848	2.3	3007
66	587.0830	0.9	1243
67	603.0713	0.8	1119
68	604.0711	1.1	1502
69	625.1655	1.9	2488
70	668.1698	1.6	2059
71	680.1705	2.2	2885
72	681.1711	1.0	1371
73	772.7077	0.9	1177
74	773.2081	1.0	1263
75	862.2431	3.7	4837
76	863.2452	2.1	2783
77	1065.2844	28.3	37417
78	1066.2877	17.9	23652
79	1067.2877	8.7	11526
80	1068.2884	3.3	4301
81	1069.2875	1.1	1489
82	1087.2672	12.1	15940
83	1088.2700	7.9	10396
84	1089.2698	3.8	4966
85	1090.2751	1.4	1810
86	1103.2410	0.8	1017
87	1126.2010	9.4	12461
88	1127.2085	22.4	29567
89	1128.2076	17.0	22492
90	1129.2082	15.7	20675
91	1130.2092	8.1	10678
92	1131.2093	3.4	4553
93	1132.2065	1.4	1788
94	1171.1876	21.8	28852
95	1172.1885	13.9	18345
96	1173.1869	26.1	34536
97	1174.1898	15.0	19860
98	1175.1891	7.2	9490
99	1176.1886	2.8	3678
100	1177.1943	0.8	1101

Acquisition Parameter

General	Fore Vacuum	2.61e+000 mBar	High Vacuum	9.49e-008 mBar	Source Type	ESI
	Scan Begin	100 m/z	Scan End	2400 m/z	Ion Polarity	Negative
Source	Set Nebulizer	0.4 Bar	Set Capillary	4500 V	Set Dry Gas	4.0 l/min
	Set Dry Heater	180 °C	Set End Plate Offset	-500 V		
Quadrupole	Set Ion Energy (MS only)	-10.0 eV				
Coll. Cell	Collision Energy	-20.0 eV	Set Collision Cell RF	500.0 Vpp	120.0 Vpp	
Ion Cooler	Set Ion Cooler Transfer Time	140.0 µs	Set Ion Cooler Pre Pulse Storage Time	22.0 µs		

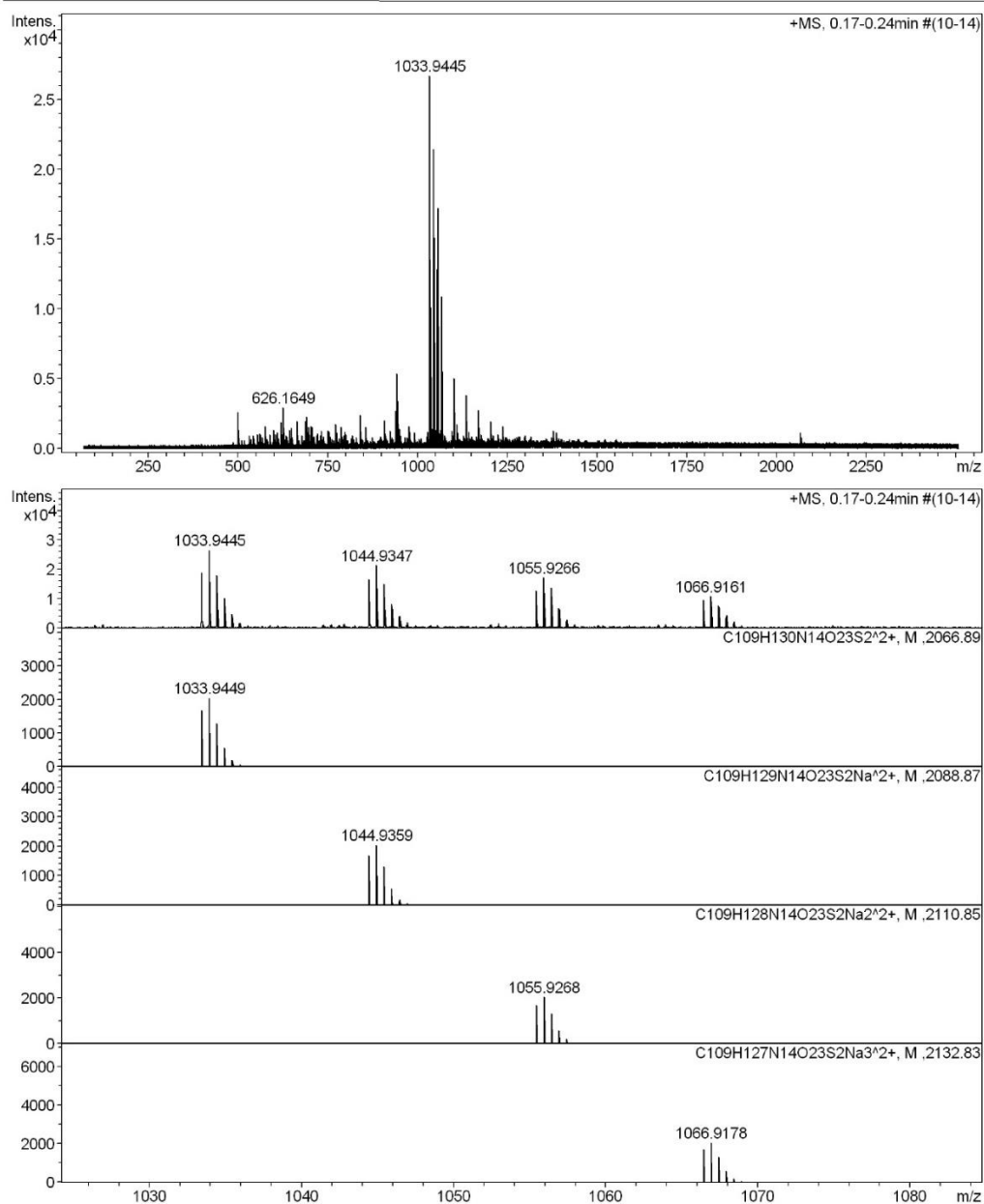
High Resolution Mass Spectrometry Report

Sample Name **JL-736 F3**

Instrument maXis 4G

Comment

Method ms_nocolumn_high_pos_use_acn.m



High Resolution Mass Spectrometry Report

Measured m/z vs. theoretical m/z

Meas. m/z	#	Formula	Score	m/z	err [mDa]	err [ppm]	mSigma	rdb	e ⁻ Conf	z
1033.4423	1	C 109 H 130 N 14 O 23 S 2	100.00	1033.4432	0.9	0.8	37.1	52.0	even	2+
1044.4337	1	C 109 H 129 N 14 Na O 23 S 2	100.00	1044.4342	0.5	0.5	19.2	52.0	even	
1055.4252	1	C 109 H 128 N 14 Na 2 O 23 S 2	100.00	1055.4251	-0.0	-0.0	29.5	52.0	even	
1066.4152	1	C 109 H 127 N 14 Na 3 O 23 S 2	100.00	1066.4161	0.9	0.8	50.1	52.0	even	

Mass list

#	m/z	I %	I
1	500.3006	9.8	2625
2	500.8020	6.7	1788
3	575.4121	6.2	1660
4	599.3246	5.0	1332
5	610.1836	4.3	1149
6	619.4375	7.0	1859
7	626.1649	11.1	2970
8	643.3518	5.2	1378
9	648.1459	4.3	1138
10	649.4489	5.5	1467
11	663.4644	7.3	1947
12	687.3772	5.1	1361
13	689.2982	7.4	1969
14	689.6319	8.6	2305
15	689.9655	7.9	2109
16	690.2987	4.6	1221
17	696.6248	4.6	1234
18	696.9577	5.9	1586
19	702.8626	6.0	1616
20	707.4898	6.0	1592
21	751.5148	4.4	1175
22	752.1647	4.8	1279
23	770.8495	6.6	1754
24	774.1461	4.4	1174
25	787.8413	5.9	1590
26	797.5937	4.7	1245
27	838.8357	9.2	2460
28	855.8276	5.7	1533
29	906.8236	7.5	2008
30	923.8141	5.0	1327
31	940.2554	10.0	2683
32	941.2570	10.2	2713
33	942.2529	20.2	5385
34	943.2548	12.8	3424
35	944.2533	12.5	3339
36	945.2519	5.3	1419
37	949.5597	5.2	1398
38	974.8116	6.2	1651
39	1033.4423	71.5	19112
40	1033.9445	100.0	26723
41	1034.4455	67.6	18053
42	1034.9455	38.1	10176
43	1035.4467	17.9	4791
44	1035.9463	6.5	1737
45	1041.9393	5.5	1459
46	1042.7996	5.5	1475
47	1044.4337	63.1	16851
48	1044.5062	6.0	1601
49	1044.9347	80.3	21465
50	1045.4362	56.8	15170
51	1045.5073	4.7	1249
52	1045.9359	31.6	8442
53	1046.4368	15.4	4114
54	1046.5086	6.3	1672
55	1046.9372	7.1	1901
56	1052.4292	5.1	1371
57	1052.9277	6.9	1833
58	1055.4252	48.0	12833
59	1055.9266	64.4	17215

High Resolution Mass Spectrometry Report

#	m/z	I %	I
60	1056.4267	51.3	13697
61	1056.9272	25.6	6834
62	1057.4296	11.6	3111
63	1057.9295	5.3	1418
64	1063.9188	5.0	1333
65	1066.4152	36.1	9653
66	1066.9161	40.9	10924
67	1067.4179	28.9	7714
68	1067.9190	17.1	4568
69	1068.4184	9.2	2465
70	1095.8981	4.9	1304
71	1100.4101	14.8	3952
72	1100.9108	18.9	5049
73	1101.4111	12.7	3406
74	1101.9136	8.8	2359
75	1108.9028	6.0	1613
76	1109.4034	6.5	1734
77	1109.9046	5.6	1493
78	1134.4044	11.9	3186
79	1134.9047	14.4	3852
80	1135.4048	10.5	2795
81	1135.9081	7.1	1887
82	1168.3980	7.2	1928
83	1168.8983	10.4	2777
84	1169.3981	7.8	2091
85	1169.8987	5.6	1502
86	1202.3899	5.2	1388
87	1202.8911	7.3	1963
88	1236.8864	6.1	1626
89	1378.5910	4.8	1286

Acquisition Parameter

General	Fore Vacuum	2.48e+000 mBar	High Vacuum	1.03e-007 mBar	Source Type	ESI
	Scan Begin	75 m/z	Scan End	2500 m/z	Ion Polarity	Positive
Source	Set Nebulizer	2.0 Bar	Set Capillary	4500 V	Set Dry Gas	8.0 l/min
	Set Dry Heater	200 °C	Set End Plate Offset	-500 V		
Quadrupole	Set Ion Energy (MS only)	4.0 eV				
Coll. Cell	Collision Energy	12.0 eV	Set Collision Cell RF	2000.0 Vpp	800.0 Vpp	
Ion Cooler	Set Ion Cooler Transfer Time	120.0 µs	Set Ion Cooler Pre Pulse Storage Time	18.0 µs		